1888 Role of von Willebrand Factor Sequestration and Glycoprotein 1b Expression in Wilms Tumor-Associated Acquired von Willebrand Syndrome: An Immunohistochemical Study

Alexander Thurman, Jamal Benhamida, Scott Kogan. University of California, San Francisco Medical Center, San Francisco, CA.

Background: Acquired von Willebrand syndrome (AvWS) represents an acquired quantitative or qualitative defect in von Willebrand factor (vWF) that may result in clinical bleeding. AvWS is known to be associated with various disease states, including myeloproliferative disorders, paraproteinemias, solid tumors, autoimmune disorders, and hormonal alterations. Specifically, AvWS has been well-described in pediatric patients with Wilms tumor (WT). The incidence of this complication is high, with estimates of laboratory-confirmed AvWS ranging from 8 to 30 percent. The pathogenesis underlying this association is unknown, although mechanisms involving secreted hyaluronic acid and/or sequestration of vWF by tumor cells have been proposed. We herein present (1) the largest immunohistochemical study to date of surface vWF labeling in WT and (2) to our knowledge, the first study to explore a potential etiologic link between WT and AvWS—namely, the expression of glycoprotein 1b (GP1b), a component of the canonical vWF-binding GP1b-9-5 surface receptor complex, by WT cells.

Design: We retrospectively collected 28 cases of WT and 26 control cases from the archived clinical specimens of the Department of Pathology at the University of California, San Francisco Medical Center. Control cases consisted of 16 clear cell renal cell carcinomas (RCCs), 5 papillary RCCs, 2 chromophobe RCCs, 2 clear cell papillary RCCs, and 1 rhabdoid tumor of kidney. AvWS-related clinical and laboratory data were obtained for all patients. Immunohistochemical (IHC) staining for both vWF and GP1b were performed on all cases at ARUP Laboratories (Salt Lake City, Utah).

Results: 7 of 28 patients with WT (25%) experienced clinical bleeding episodes which were suspicious for a bleeding diathesis. AvWS laboratory parameters were available in only 1 WT patient with clinical bleeding but were not diagnostic for AvWS. Tumor cells from WT and control cases did not exhibit membranous staining with either vWF or GP1b. Patchy, nonspecific cytoplasmic staining for vWF was noted in a minority of cases, predominantly occurring in stromal cells.

Conclusions: Our results are consistent with prior immunohistochemical and indirect immunofluorescence studies of vWF labeling performed on clinical samples from patients with WT and AvWS. Lack of staining with both vWF and GP1b provides compelling evidence against a role for vWF sequestration or aberrant GP1b expression in the pathogenesis of WT-associated AvWS.

1889 Histologic Features of Intestinal Thrombotic Microangiopathy (iTMA) After Hematopoietic Stem Cell Transplant (HSCT)

Mikako Warren, Javier El-Bietar, Christopher Dandoy, Kasiani Myers, Adam Lane, Stella Devies, Sonata Jodele. Cincinnati Children's Hospital, Cincinnati, OH.

Background: We showed post-transplant TMA can be systemic and has poor outcome with <20% 1-year survival (Jodele S et al. Blood 2014). These patients with severe bleeding were reported to have gastrointestinal (GI) vascular injuries. We reviewed 108 post-HSCT endoscopic biopsies from 50 patients and newly identified statistically significant histological features of iTMA.

Design: Biopsies from patients with suspected intestinal graft vs. host disease (iGVHD) were used. In addition to histological evaluation of iGVHD, we evaluated 8 criteria for iTMA (table). Patients were divided into 3 groups using current clinical criteria of iGVHD and TMA: iGVHD/TMA, iGVHD alone, and no iGVHD/no TMA. Histologic markers were scored as present or absent in a blind fashion. Statistical analysis was performed using Fisher exact test.

Results: Fifteen patients (30%) had iGVHD and TMA. Out of 35 patients without TMA, 21 had iGVHD and 14 did not. Incidence of clinically severe iGVHD (stage 3-4) was similar in TMA/iGVHD and iGVHD alone groups (79% vs 64%). Histologic signs of iTMA except for mucosal hemorrhages and endothelial swelling were statistically significant in patients with TMA. Intravascular thrombi were only seen in TMA group.

HSCT patients with diarrea (n=50)				
	TMA/iGVHD (n=15)	iGVHD alone (n=21)	No TMA/no iGVHD (n=14)	p=value
Mucosal hemorrhages	12 (80%)	11 (52.4%)	5 (36%)	0.057
Loss of glands	11 (73.3%)	8 (38%)	0 (0%)	
Intravascular schistocytes	10 (66.7%)	5 (23.8%)	3 (21.4%)	0.016
Intravascular fibrin	8 (53.3%)	2 (9.55%)	2 (14%)	0.008
Intravascular microthrombi	4 (26.6%)	0 (0%)	0 (0%)	0.010
Endothelial swelling	13 (86.6%)	13 (61.9%)	7 (50%)	0.086
Endothelial separation	8 (53.3%)	3 (14.3%)	1 (7%)	0.007
Mucosal denudation	7 (46.7%)	3 (14.3%)	0 (0%)	0.005

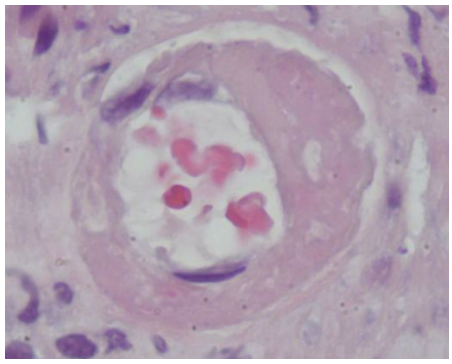

Conclusions: We identified histologic features of iTMA that are useful to delineate GI vascular injuries in post-HSCT patients. Recognition of these histological signs in patients with GI symptoms may guide early treatments for iTMA.

Pulmonary Pathology (including Mediastinal)

1890 Yield of EGFR and ALK Testing in Poorly Differentiated Non-Small Cell Lung Carcinomas

Charles Allen, Bin Yang, Carol Farver, Sanjay Mukhopadhyay. Cleveland Clinic, Cleveland, OH.

Background: Current IASLC/ATS/ERS guidelines recommend testing all non-squamous non-small cell lung carcinomas (NSCLC) for EGFR mutations and ALK translocations, including adenocarcinomas that require immunohistochemistry for subtyping and NSCLC that are unclassifiable after immunohistochemistry (NSCLC, NOS). There is no data comparing the yield of molecular testing in these groups to adenocarcinomas that are easily subtyped on H&E. The aim of this study was to compare the yield of molecular testing in adenocarcinomas that are easily classifiable on H&E to adenocarcinomas that require immunohistochemistry for subclassification, and NSCLC, NOS.

Design: Ninety-one (91) lung specimens (61 biopsies, 30 resections) with NSCLC were reviewed by a pulmonary pathologist blinded to the original diagnosis, results of immunohistochemical stains (if used) and EGFR/ALK status. Cases were separated into 3 categories: adenocarcinoma, easily classifiable on H&E, poorly differentiated adenocarcinoma (unclassifiable on H&E, but TTF-1-positive) and NSCLC, NOS (unclassifiable on H&E, and negative for TTF-1 and p63/p40). The incidence of EGFR mutations and ALK translocations in the 3 groups was compared. An additional 22 cases (18 biopsies, 4 resections) of NSCLC, NOS were retrieved from our pathology archives. Results of molecular testing in each group were reviewed.

Results: Of 91 NSCLC,13 were classified as squamous cell carcinoma on H&E and excluded.Of the remaining 78, 61 were readily subtyped as adenocarcinoma on H&E, 10 were unclassifiable on H&E but TTF-1-positive (poorly differentiated adenocarcinoma), and 7 were NSCLC, NOS. An additional 22 random NSCLC, NOS cases were added, bringing the NSCLC, NOS cases to 29. EGFR mutations were detected in 11/61 adenocarcinomas easily classifiable on H&E (18%), 1/10 poorly differentiated adenocarcinomas (10%) and 0/29 NSCLC, NOS (0%). ALK translocations were found in 2/61 easily classifiable adenocarcinomas (3%), 0/10 poorly differentiated adenocarcinomas (0%) and 2/29 NSCLC, NOS (7%). EGFR mutations were significantly less likely to be found in NSCLC, NOS than in adenocarcinomas (p=0.0168, Fisher's exact test, 2-tailed).

Conclusions: Oncogenic driver mutations (EGFR or ALK) do occur in poorly differentiated adenocarcinomas and NSCLC, NOS, although the yield of EGFR mutations is significantly lower in NSCLC, NOS when compared to adenocarcinomas. These findings support molecular testing of all non-squamous NSCLC, including poorly differentiated adenocarcinomas that require immunohistochemistry for subtyping, and NSCLC, NOS.

1891 A Novel High-Speed Droplet-Polymerase Chain Reaction Can Detect Epidermal Growth Factor Receptor Gene Mutation in Non-Small Cell Lung Cancer in Less Than 10 Minutes

Shiho Asaka, Akihiko Yoshizawa, Kazuyuki Matsuda, Akemi Yamaguchi, Yukihiro Kobayashi, Rie Nakata, Zhang Meng, Mitsutoshi Sugano, Takayuki Honda. Shinshu University Hospital, Matsumoto, Nagano, Japan; Seiko Epson Corporation, Shiojiri, Nagano, Japan.

Background: Somatic mutations in the epidermal growth factor receptor (*EGFR*) gene are associated with the response to tyrosine kinase inhibitors in patients with non-small-cell lung cancer (NSCLC). Cases of clinical urgency require the use of a rapid assay for detecting *EGFR* gene mutations. The purpose of this study was to develop a novel rapid assay for detecting *EGFR* gene mutations by using a real-time droplet-polymerase chain reaction (d-PCR) system (Seiko Epson Corporation) with formalin-fixed paraffin-embedded (FFPE) fresh bronchial lavage fluid (BLF) and fresh pleural effusion (PE) specimens.

Design: First, we selected 14 specimens from NSCLC patients with L858R mutation in exon 21, which is the most common mutation of the *EGFR* gene. Next, we attempted to confirm the mutation by direct sequencing (for seven FFPE specimens) and real-time

PCR using Therascreen EGFR RGO PCR kit (QIAGEN) (for six BLF and one PE specimens). Finally, we determined reaction time and evaluated amplification efficiency by using the d-PCR system for all 14 specimens.

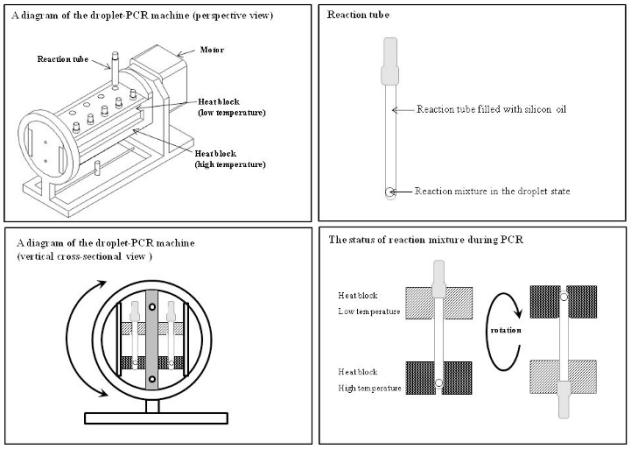

Results: We confirmed L858R mutation in all specimens by conventional methods (direct sequencing and real-time PCR). Using d-PCR, we detected the mutation in all 14 specimens within 40 cycles. The reaction time for 40 cycles in d-PCR was less than 10 minutes, while it took about over two hours with the conventional methods.
Conclusions: The d-PCR method markedly reduced the reaction time for detecting *EGFR* mutation, compared with direct sequencing and conventional real-time PCR, and showed the same accuracy as direct sequencing in FFPE specimens and similar reactivity as real-time PCR using Therascreen EGFR RGO PCR kit in BLF and PE specimens. Although this study is preliminary, our novel rapid assay can contribute to shortening the turnaround time for reporting the mutational status of the *EGFR* gene in NSCLC patients. Currently, we are developing methods for detecting *EGFR* gene mutations other than L858R.

1892 Aberrant Expression of NHERF1 Is Common in Pulmonary Squamous Cell Carcinoma and Unrelated To PTEN Expression

Deborah Belchis, Rajni Sharma, Nathan Cuka, Neeraj Sharma, Christopher Gocke. Johns Hopkins University, Baltimore, MD.

Background: Na/H exchange regulator factor 1 (NHERF1/EBP50), an adaptor/scaffolding protein that interacts with growth factors and regulatory proteins through its PDZ domains, relocalizes from its normal apical position to membranous, cytoplasmic, or nuclear positions in tumors. NHERF1 interacts with the pleckstrin-homology domain leucine rich repeat protein phosphatases and PTEN to form an inhibitory network on the PI3K-AKT pathway. This study explored the expression of NHERF1 in lung cancers and the expression of NHERF1 and PTEN in squamous cell carcinoma where PI3K and PTEN have been implicated in pathogenesis and prognosis.
Design: The study was divided into two stages. Stage 1 examined the expression of NHERF1 in lung cancer using a lung cancer microarray consisting of 10 squamous cell, 18 adeno, 2 mucinous, 10 predominantly lepidic adeno, and 10 small cell carcinomas, 5 atypical carcinoids, 9 metastatic squamous cell carcinomas, and 10 benign lung tissues. The slides were read independently by 2 pathologists and scored based on the combined intensity and percentage positive.
Stage 2: 21 squamous cell carcinomas were stained with NHERF1 and PTEN. PTEN was considered absent if <10% of cells stained. Clinical information was retrieved from the medical records. Next Gen Sequencing (NGS) was performed on FFPE tissue.
Results: Stage 1: In the array, statistical analysis revealed a strong correlation between the histologic subtype and NHERF1 staining. Most of the squamous cell carcinomas showed strong cytoplasmic staining compared to weak or negative staining in the adenocarcinomas (all types) and predominantly negative staining in the small cell carcinomas ($p < 0.001$). Stage, sex, and age did not differ.
Stage 2: 19 of 21 squamous cell carcinomas expressed NHERF1: all 19 showed cytoplasmic staining, 8 showed nuclear staining, 7 showed membranous staining. None showed apical staining. PTEN was lost in 7 cases and retained in 14, 2 with weak staining. Both the original and the recurrent tumors available in one patient expressed PTEN and NHERF1 (80% cytoplasmic only). In the 2 cases without NHERF1 staining, one expressed PTEN and one did not. NGS showed no mutations, including in *AKT, PTEN, PIK3CA, MET.*
Conclusions: 1) Aberrant expression of NHERF1 is common in squamous cell carcinoma of the lung.
2) NHERF1 and PTEN expression are independent.
3) Loss of PTEN expression does not correlate with an underlying genetic mutation; therefore an indirect mechanism is postulated.

1893 Pulmonary Pathology of Substance Abuse: An Autopsy Study

Melissa Blessing, Eunhee Yi, Loralie Langman, Anja Roden. Mayo Clinic, Rochester, MN.

Background: Recreational drug use is known to cause select histopathologic findings in the lungs. Systemic changes from drug abuse may also be seen in the lungs, and may support a prolonged history of substance abuse. While studies have correlated histology with specific drugs of abuse, to our knowledge, a comprehensive autopsy study describing and systematically comparing histologic pulmonary findings across a large spectrum of common drugs of abuse has not been performed.
Design: Institutional autopsy files (1998-2014) were queried for cases with a history of substance abuse and positive post-mortem toxicological studies. All lung slides from each case were re-reviewed blinded to clinical findings and toxicologic studies. Histologic findings of interstitium, vasculature, airways and pleura were noted. Autopsy reports and available clinical records were reviewed and salient history, other autopsy findings, and postmortem toxicology results were recorded.
Results: Forty two autopsy cases (29 men) from patients with a mean age of 44.4 (range, 18-71) were reviewed. Patients died most commonly of drug toxicity (n= 16), other toxic substances (n=6) including carbon monoxide, ethylene or isopropyl glycol, methanol or huffing, and blunt force trauma (n=6). Postmortem toxicology was most commonly positive for ethanol (28.6%) followed by citalopram (16.7%) and opiates (14.3%). Most common pulmonary findings included respiratory bronchiolitis (n=23); polarizable perivascular material in patients with known (33.3%), unknown (14.8%) and no (10.0%) intravenous drug abuse; pulmonary artery and venous changes in 66.7 % of patients with positive amphetamine toxicology; pigmented macrophages (other than smoker's macrophages or hemosiderin) in 18.8 % of patients with a history of cannabis smoking, and mild, often only focal, chronic interstitial inflammation in 26.1 % of patients with ethanol abuse. Two (of 2) cases of aspiration pneumonia had recent use of cocaine.
Conclusions: Our study shows that the systematic morphologic review of lungs at autopsy in patients with a history of substance abuse or positive postmortem toxicologic studies might help to identify previously unknown drug abuse and/or support a known clinical history of abuse. Moreover, this knowledge constitutes part of a complete medicolegal death investigation and provides important epidemiologic data.

1894 ALK Positivity Rate Is Highly Dependent on Patient Age

Kenneth Bloom, Sucha Sudarsanam. Clarient Diagnostic Services, Aliso Viejo, CA.

Background: The anaplastic lymphoma kinase (ALK) gene codes for a transmembrane receptor tyrosine kinase (RTK) in the insulin receptor superfamily. It has been identified as the fusion partner and driver oncogene in non-small cell lung cancer as well as a number of different malignancies. The reported frequency of ALK translocations in NSCLC ranges from 2-7%. Crizotinib was approved for the treatment of ALK positive NSCLC patients as determined by the presence of an ALK gene rearrangement based on a companion diagnostic FISH assay. We assessed a large series of patients to determine the positivity rate of this assay in a US based population.
Design: 20810 consecutive formalin fixed paraffin embedded non-small cell lung cancer samples sent to our laboratory for determination of ALK rearrangement status were assessed using the Abbott LSI ALK break apart rearrangement FISH probe. Fifty tumor cells were enumerated for the presence of a break apart signal which was considered as present when at least one set of orange and green signals were 2 or more signal diameters apart or when a single orange signal without a corresponding green signal was observed in more than 15% of the tumor cells.
Results: Of the 20810 samples tested, 1774 did not contain sufficient tumor content to conduct testing or demonstrated suboptimal hybridization. 474 (2.49%) samples demonstrated an ALK rearrangement. The positivity rate was highly variable by age, ranging from 15.9% in patients less than 40 to 3.72% in patients between 40 and 65 to 1.73% in patients older than 65.

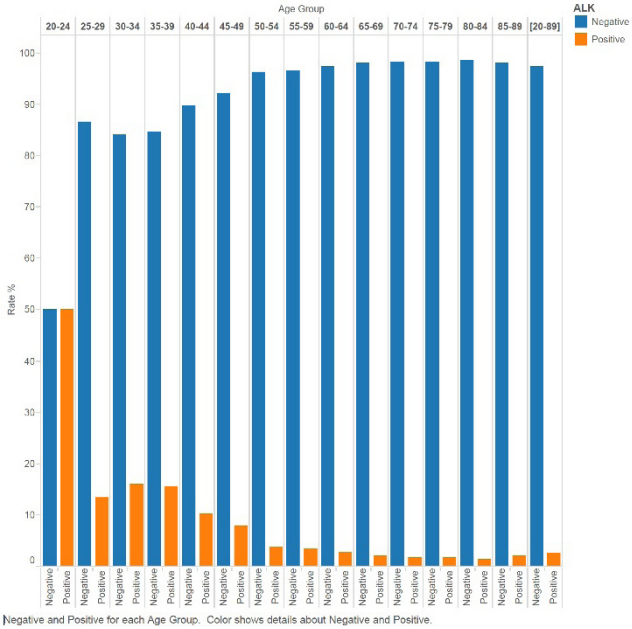

Conclusions: The frequency of ALK rearrangements was 2.49% in our series of NSCLC patients. This number is in line with the expected rates based on previous studies and helps define the positivity rate in a US based population. Interestingly, the rate of positivity was highly dependent on the age of the patient with younger patients demonstrating a much higher rate of ALK rearrangements.

1895 c-Met Expression and MET Amplification in Malignant Pleural Mesothelioma

Melanie Bois, Aaron Mansfield, William Sukov, Sarah Jenkins, Julian Molina, Tobias Peikert, Anja Roden. Mayo Clinic, Rochester, MN.

Background: Inhibition of c-Met, a receptor tyrosine kinase (RTK), may aid in the treatment of malignant pleural mesothelioma (MPM). c-Met has been found to be overexpressed in MPM. *MET* mutations were identified in 3-16% of MPM, however *MET* amplification has not been reported. We studied c-Met expression and *MET* amplification in MPM and examined associations with morphologic and clinical features and outcome.

Design: MPMs, identified from Mayo Clinic Rochester files (1987-2014) were re-reviewed. Slides were stained with antibodies to c-Met (clone 3D4). Staining intensity (0-3) and distribution (0-100%) were recorded and multiplied (H-score). Staining localization (cytoplasmic and/or membranous) was noted. Fluorescence in situ hybridization (FISH) was performed using probes for *MET* and centromere 7 (Abbott Laboratories). Medical records were reviewed. A p-value <0.05 was considered significant.

Results: 42 patients (pts) (31 men, 25 with known asbestos exposure) at a median age of 69.5 yrs (range, 41-87) had epithelioid (n=21) or sarcomatoid (n=21) MPM. Median follow up of all pts was 0.6 yrs (range, 7 days-1.9 yrs). 40 pts died, 38 of disease (2 lost to follow up). Results of c-Met staining are summarized in Table1.

MPM	Epithelioid (n=21)	Sarcomatoid (n=21)	p-Value
c-Met Staining Intensity (% cases) None/ WeakModerateStrong	028.671.4	23.847.628.6	0.002
c-Met H-score Median (range)	270 (100-300)	180 (70-285)	0.002
c-Met Staining Pattern (% cases)* Cytoplasmic onlyMembranous and cytoplasmic	9.590.5	4060	0.03
6-month Survival	75.0	42.9	

**21/21 epithelioid and 20/21 sarcomatoid MPM stained with c-Met*

Staining localization or H-score were not associated with survival or clinical features (age, gender, smoking). Stronger staining intensity only correlated with increased survival among pts without chemotherapy (n=26; p=0.02). Pts without known asbestos exposure had a greater % c-Met-positive tumor cells (p=0.02). While *MET* amplification was not identified in any MPM (9 epithelioid, 8 sarcomatoid), *MET* duplication was seen in 1 epithelioid MPM, which also demonstrated distinct Golgi staining. Chromosome 7 aneusomy was observed in 11/17 MPM. A trend toward decreased survival in pts with *MET* aneusomy was noted (p=0.08).

Conclusions: We found that strong c-Met expression correlated with epithelioid MPM, but was not predictive of survival. *MET* aneusomy may be associated with decreased survival. Studies to correlate c-Met expression with treatment response to RTK inhibitors are needed.

1896 Pattern-Based Grading of Pulmonary Adenocarcinoma – Analysis of 534 Cases With Comparison Between Observers

Jennifer Boland, Jason Wampfler, Ping Yang, Eunhee Yi. Mayo Clinic, Rochester, MN.

Background: The 2011 consensus classification of pulmonary adenocarcinoma (pADCA) recommends recording invasive patterns in 5% increments and determining predominant pattern (PP), which may be prognostic. There is debate over the best way to implement pattern-based grading, and whether such systems are reproducible.

Design: 534 resected pADCA were reviewed by 2 pulmonary pathologists to determine PP and percentages of all observed patterns. Three different grading schemes were applied based on predicted prognosis scores: score 1 (lepidic), score 2 (acinar/papillary), and score 3 (solid/micropapillary/cribriform). Mucinous tumors were separately evaluated with scores 2 and 3 since their prognosis is ambiguous. The first grading scheme used PP score; the second used worst observed pattern score; and the third categorized tumors with ³20% of any score 3 pattern(s) as score 3, tumors with ≥80% lepidic growth as score 1, and all remaining as score 2.

Results: The PP assigned by each observer was an exact match in 51.7% of cases, a "close match" in 27.3% (same prognosis score), and a mismatch in 21%. PP determined by both observers showed significant stratification of overall and progression-free survival (OS and PFS).

Figure 1. Kaplan-Meyer curves of overall survival based on predominant growth pattern determined by observer 1 (A) and observer 2 (B).

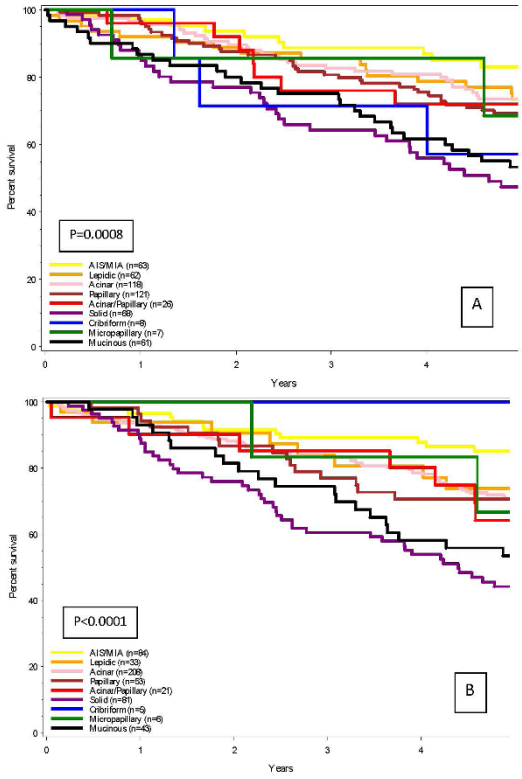

All 3 grading schemes showed a significant difference in OS and PFS determined by both observers, but the worst score scheme provided suboptimal separation and did not always provide expected risk stratification (survival of score 1 > 2 > 3), likely due to a very small score 1 group.

Figure 2. Kaplan-Meyer curves of overall survival for observer 1 (left column, A, C, and E) and observer 2 (right column, B, D and F) based on predominant pattern score (A and B), worst pattern score (C and D), and lepidic growth/high grade patterns (E and F).

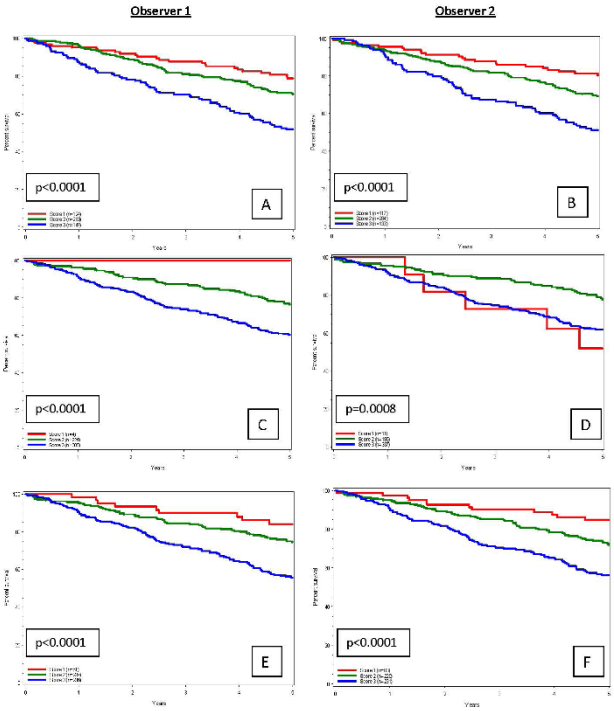

Survival differences for all grading schemes maintained significance whether mucinous tumors were considered score 2 or 3.

Conclusions: Pattern-based grading has prognostic significance in pADCA. Interobserver variation is present, but 2 observers were able to predict significant differences in OS and PFS using various pattern-based grading schemes. Multivariate and stage I specific analyses will further evaluate if any independent predictive power exists.

1897 Comparison of Programmed Cell Death Ligand 1 (PD-L1) Expression in Main Tumor and Lymph Node Metastasis of Stage II and III Lung Adenocarcinomas

Emine Bozkurtlar, Hironori Uruga, Tiffany Huynh, Michael Lanuti, Eugene Mark, Mari Mino-Kenudson. Massachusetts General Hospital, Boston, MA.

Background: PD-L1 is an important immunoregulatory molecule in suppressing cytotoxic immune response in a variety of physiologic and pathologic pathways. Thus inhibition of PD-L1 can lead to reactivating tumor immunity and assist to cancer therapy. PD-L1 overexpression in the tumor cells has been correlated to a lessened immune response and consequent worse prognosis in a variety of cancers. However, it has not been well investigated whether PD-L1 expression is altered along with tumor progression and/or is different between various organs in a given tumor. Thus, we sought to compare PD-L1 expression in the main tumor and lymph node metastases of surgically resected stage II and III lung adenocarcinomas (ADCs).

Design: Immuhistochemistry for PD-L1 (clone:E1L3N, Cell Signaling Technology) was performed on sections of the main tumor and metastatic lymph nodes from 74 surgically resected stage II and III ADCs. Only membranous staining of tumor cells was evaluated, and the percentage of tumor cells with PD-L1 staining was recorded. We also scored the intensity of the membranous staining using a four-tiered grading system (grade 0-3). Overall, membranous staining of any intensity present in ≥ 5% of the tumor cells was deemed positive for PD-L1 overexpression.

Results: Of the 74 cases of ADCs analyzed, N1 node metastasis was present in 64(86.6%), N2 node metastasis in 34(45.3%) and N3 node metastasis in only 1(1%). No PD-L1 expression was seen in either the main tumor or lymph node metastases of 22(29.7%) cases. The main tumor, N1 lymph node, N2 lymph node and N3 lymph node was positive for PD-L1 overexpression in 39%(29/74), 23.4%(15/64), 23.5%(8/34) and 100% (1/1), respectively. The main tumor and lymph node metastases exhibited the same extent of the tumor cells with PD-L1 membranous staining in 20(26.6%) cases. The main tumor showed a larger fraction of the tumor cells with PD-L1 staining in 23(30.6%) cases while they were more prevalent in lymph nodes in 9(12.1%). Overall the intensity of PD-L1 membranous staining in the main tumor correlated well with that in lymph node metastases.

Conclusions: The results of our study indicate that there is no increase in PD-L1 expression when the tumor cells metastasize to lymph nodes in the vast majority of lung adenocarcinomas. Further studies, including the evaluation of PD-L1 expression in other organ metastases, are required to identify mechanisms for this somewhat counter institutive finding.

1898 Idiopathic Tracheal Stenosis

Emine Bozkurtlar, Hironori Uruga, Lida Hariri, Mari Mino-Kenudson, Eugene Mark. Marmara University, Istanbul, Turkey; Toranomon Hospital, Tokyo, Japan; Massachusetts General Hospital, Boston, MA.

Background: Tracheal stenosis causing respiratory difficulty that prompts surgical correction in adults commonly is due to prior intubation or trauma. A subset of patients with tracheal stenosis have no such underlying cause. The great majority of patients are female. Familial disease has been reported.

Design: We previously reported on idiopathic tracheal stenosis not related to trauma in 63 cases. Here we report an additional one hundred and twenty-two cases with a clinical diagnosis of idiopathic tracheal stenosis seen over the last six years by the Thoracic Surgery Service at our hospital. We analyzed histopathology, principally with hematoxylin and eosin staining, stressing the location and character of the scarring. We excluded cases that might have been associated with Wegener's granulomatosis, relapsing ploychondritis, amyloid, or other. We principally studied whole cross sections of resected trachea. Because the disease is virtually limited to women, we studied estrogen and progesterone receptors. ANCA had been measured in some cases.

Results: Our prior report emphasized the character of dense fibrosis and preserved inner perichondrium of tracheal cartilage. In this reprot we concentrate on dilatation of mucus glands and ducts, which were observed in 30% or more of cases. The dilatation ranged from two or more times normal diameter of the duct. The larger dilatation lesions were filled with mucus or proteinaceous material. Many smaller ducts which had dilatation lesions were surrounded by circumferential myxoid fibrosis. A lymphoplasmacytic infiltrate was observed in many cases. In our cohort seventy-two cases were evaluated for estrogen and progesterone receptors. 78% of cases were positive for estrogen receptor and 80% for progesterone receptor. We established three grades for lymphoplasmacytic infiltrate, with the infiltrate from none to marked. Only one patient had even borderline elevation of ANCA. All but four patients were females.

Conclusions: Idiopathic tracheal stenosis, also termed idiopathic laryngotracheal stenosis, has distinctive pathology, both in terms of the character of the fibrosis and in terms of ductular dilatation and periductal fibrosis, which has some aspects are reminiscent of bronchiolitis as can be seen in collagen-vascular diseases.

1899 SOX-2 Expression and Its Prognostic Value in Stage II and III Lung Adenocarcinomas

Emine Bozkurtlar, Hironori Uruga, Tiffany Huynh, Michael Lanuti, Eugene Mark, Mari Mino-Kenudson. Massachusetts General Hospital, Boston, MA.

Background: SOX-2 is a transcription factor that has been found overexpressed in some types of poorly differentiated carcinomas. It is associated with better prognosis in lung squamous cell carcinoma (SCC) but its expression and prognostic significance in lung adenocarcinoma (ADC) are controversial. In particular, little is known about the role of SOX-2 expression in predicting response to therapies. The aim of this study was to examine SOX-2 expression in advanced stage ADC and correlate it with clinicopathological parameters and patient outcomes with respect to adjuvant therapy status.

Design: Immunohistochemistry for SOX-2 was performed in 112 surgically resected stage II and III ADCs consisting of 61 and 51 cases with and without adjuvant therapies, respectively. Nuclear expression of SOX-2 was evaluated using H score (calculated based on the intensity of nuclear staining and the percentage of positive tumor cells: maximum 300). H score ≥10 was used as a cut-off for positive SOX-2 expression. SOX-2 expression was correlated with clinicopathological features and patient outcomes.

Results: Positive SOX-2 expression was seen in 55% (62) of the entire cohort, 57.5% (35) of the adjuvant therapy group and 43.5% (27) of the non-adjuvant therapy group. There was a trend toward higher stage tumors exhibiting SOX-2 expression (p=0.08). Histologically, there was correlation between SOX-2 positivity and predominant micropapillary pattern (p=0.02). Whereas solid predominant pattern was not associated with SOX-2 positivity, SOX-2 was often expressed in regions with solid pattern in tumors with heterogeneous histology, and SOX-2 expression was associated with the presence of solid pattern in ≥10% of the tumor cells (p=0.03). No other clinicopathological features including smoking history were associated with SOX-2 expression in stage II and III ADCs. Among the patients who underwent adjuvant therapies, five-year recurrence free survival was 31.7% and 51.9% in the SOX-2 positive and negative groups, respectively. Conversely, there was no difference in survival between the 2 groups among those without adjuvant therapies.

Conclusions: SOX-2 expression is associated with high-grade histologic patterns and likely dictates unfavorable outcomes after adjuvant therapy in advanced stage ADCs. The finding suggests the possibility of SOX-2 to be a marker for resistance to adjuvant therapy in ADC opposed to a lineage specific marker predicting favorable outcomes in SCC.

1900 P40 and GATA-3 Are Useful To Distinguish Between Lung Squamous Cell Carcinoma and Triple Negative Breast Cancer

Elena Brachtel, Tiffany Huynh, Mari Mino-Kenudson. Massachusetts General Hospital, Boston, MA.

Background: Patients with lung nodules or mediastinal lymphadenopathy often undergo fine needle aspiration biopsy to confirm malignancy and primary site. To distinguish between non-small cell lung cancer with squamous differentiation (LSCC) and triple-negative breast cancer (TNBC), a heterogenous subtype which also includes spindle cell carcinomas, is particularly difficult in small samples. This study evaluates commonly used immunohistochemical markers in diagnostically validated lung and breast cancers.

Design: Diagnostically confirmed formalin-fixed paraffin-embedded tissue samples from 90 patients with LSCC, 67 TNBC of various morphologies and 45 estrogen-receptor positive (ER+) breast cancers were selected. Tissue microarrays were prepared and immunohistochemically stained by routine procedures with an automated stainer and reagents. Cytoplasmic staining for napsin A, GCDFP-15 and mammaglobin (MG), and nuclear staining for TTF-1, p40, and GATA-3 was assessed semiquantitatively. Stain intensity was scored as 0 (negative), 1 (faint) and 2 (strong), extent as 0 (negative), 1 (<10%), 2 (10-50%), and 3 (>50% positive).

Results: As expected, all LSCC showed strong p40 expression, and were negative for napsin A and TTF-1; no significant staining was seen with mammary markers (GATA-3, GCDFP-15 and MG). Most TNBC showed GATA-3 expression (68%), with a few cases expressing p40 (5%) and several cases with faint TTF-1. All ER+ breast cancers expressed GATA-3 and no p40.

	Average Scores and %	p40	TTF-1	Napsin A	GATA-3	GCDFP-15	MG
Lung SCC	Intensity (0-2)	2	0	0	0.3	0	0
N=90	Extent (0-3)	3	0	0	0.5	0	0
	% Positive Cases	100	0	0	10	0	0
Breast TNBC	Intensity (0-2)	0.3	0.4	0	1	0.2	0.1
N=67	Extent (0-3)	0.3	0.6	0	3	0.2	0.1
	% Positive Cases	5	17	0	68	6	2
Breast ER+	Score Intensity (0-2)	0.1	0	0	2	0.4	0.7
N=45	Score Extent (0-3)	0	0	0	3	0.4	0.9
	% Positive Cases	0	0	0	100	15	32

Conclusions: This side-by-side comparison of several lung and breast diagnostic markers on diagnostically validated cases shows p40 and GATA-3 as the most useful immunomarkers to differentiate between TNBC and LSCC. LSCC consistently express p40 but none of the other lung and breast markers tested in this study. Most TNBC express GATA-3 with only few positive for p40. Small tissue samples obtained at lung and mediastinal biopsies determine treatment and effective diagnostic markers are of utmost importance.

1901 BAP1 Is a Highly Specific Marker for the Differential Diagnosis Between Mesothelioma and Reactive Mesothelial Proliferations

Marta Cigognetti, Silvia Lonardi, Andrea Tironi, Luisa Bercich, Mattia Bugatti, Giulio Rossi, Bruno Murer, Mattia Barbareschi, Silvia Giuliani, Alberto Cavazza, Simona Fisogni, Piera Balzarini, Vilma Pellegrini, William Vermi, Fabio Facchetti. University Hospital of Brescia, Brescia, Italy; Policlinico, Modena, Italy; Hospital, Mestre, Italy; S. Chiara Hospital, Trento, Italy; IRRCCS, Reggio Emilia, Italy.

Background: The distinction between malignant mesothelioma (MM) and reactive mesothelial proliferation (RMP) can be challenging and immunohistochemistry is of limited support. *BAP1* gene germline loss-of-function mutations are responsible for an inherited cancer syndrome which includes MM; moreover, somatic *BAP1* gene

anomalies resulting in protein loss have been reported in sporadic MM. We evaluated the usefulness of BAP1 expression in the differential diagnosis between MM and RMP in tissue and cytological samples.
Design: Mouse monoclonal antibody anti-BAP1 (clone C-4) was applied on biopsies from MM (208 cases), benign mesothelial tumors (BMT)(12) and RMP (39, 12 with atypical features [AMP]); RMP included 29 pleural and 1 peritoneal samples obtained during evaluation of recurrent effusion and/or thoracoscopic anomalies; this group was followed clinically and/or radiologically for variable periods of time (up to 9 years). BAP1 stain was also performed in 63 cytological samples (40 MM, 23 RMP, including 6 AMP). BAP1 expression was evaluated in cell nuclei.
Results: BAP1 was positive in all BMT; 137/208 MM were BAP1-, with higher frequency in epithelioid/biphasic subtype (135/195, 69.2%). BAP1 loss was easily recognizable since all tumor cells lacked protein expression; in BAP1- MM superficial mesothelium was also negative, independently from the degree of atypia. Thirty-six RMP (11 AMP) were BAP1+; 3 of them (2 AMP) developed BAP1+ MM. BAP1 loss was found in 3 patients with RMP (1 AMP), 2 developed BAP1- MM within two years, one (AMP) died of intra-abdominal metastasis after 4 years. BAP1 reactivity on cytological samples was also easily assessed; tumor cells in 25/40 (62.5%) MM were BAP1-; 4/23 RMP were BAP1-, all were AMP and later diagnosed as BAP1- MM.
Conclusions: BAP1 loss is frequently found in epithelioid/biphasic MM; it has an absolute specificity (100%) in the differential with RMP both in tissue and cytological samples and, in contrast to other markers, its evaluation is straightforward (present/absent). RPM cases with BAP1 loss should be carefully re-evaluated, likely representing non invasive MM. BAP1 stain might also be useful in the study of tumor extent in resectable BAP1- MM.

1903 Histological Difference Between Idiopathic Interstitial Pneumonias and Connective Tissue Disease-Associated Interstitial Pneumonias

Mutsumi Dairiki, Hiromi Ichikawa, Tomonori Tanaka, Hiroyuki Taniguchi, Takeshi Johkoh, Kensuke Kataoka, Yasuhiro Kondoh, Junya Fukuoka. Nagasaki University School of Medicine, Nagasaki, Japan; Nagasaki University Graduate School of Biomedical Sciences, Nagasaki, Japan; Nagasaki University Hospital, Nagasaki, Japan; Tosei General Hospital, Seto, Aichi, Japan; Kinki Central Hospital of Mutual Aid Association of Public School Teachers, Itami, Hyogo, Japan.
Background: Idiopathic interstitial pneumonias (IIPs) and connective tissue disease (CTD)-associated interstitial pneumonias (IPs) are the two most common types of IPs. CTD-IPs and IIPs share common histological features, yet the clinical managements are different. Separation of the two conditions solely by histology is challenging, and there are no established criteria.
Design: We selected consecutive 106 IIPs (80 IPF-UIP and 26 idiopathic NSIP) and 56 cases of CTD-IPs (21 RA, 12 SSc, 13 PM/DM, 7 SjS, and 3 MCTD). Whole slide images of all specimens in 200x magnification were prepared. Eighteen histological factors were evaluated by 2 observers independently and graded semi-quantitatively into score of 0 to 3. The consensus scores were obtained afterwards by the discussion which also includes another pulmonary pathologist. Association between the score of each markers and diagnosis of CTD was investigated using qui square and Fisher's exact test.
Results: Histological markers positively suggestive for IIPs were dense fibrosis ($p<0.01$), microscopic honeycomb ($p<0.01$), fibroblastic focus ($p<0.01$), smooth muscle hyperplasia ($p<0.01$), and interstitial giant cells ($p=0.02$). Markers positively suggestive for CTD-IPs were extensive pleuritis ($p<0.01$), lymphoid aggregates with germinal center ($p<0.01$), prominent plasmacytic infiltration ($p<0.01$), and airspace fibrin ($p=0.02$).
When histological pattern was limited to UIP, histological markers suggestive for IPF-UIP were fibroblastic focus ($p=0.02$) and smooth muscle hyperplasia ($p=0.04$). On the other hand, markers suggestive for CTD-UIP were extensive pleuritis ($p=0.04$), lymphoid aggregates with germinal center ($p<0.01$), prominent plasmacytic infiltration ($p<0.01$), and fat metaplasia ($p=0.04$).
When NSIP was considered, dense fibrosis ($p=0.04$), smooth muscle hyperplasia ($p<0.01$), and dense perivascular collagen ($p=0.04$) associated with idiopathic-NSIP, however, none associated positively with CTD-NSIP.
Conclusions: We identified the histological markers distinguishing CTD-IPs from IIPs: extensive pleuritis, lymphoid aggregates with germinal center, prominent plasmacytic infiltration. The value of these histological markers as diagnostic criteria for CTD-IPs should be further confirmed.

1904 Comprehensive Genomic Profiling (CGP) of 44 RET-Fused Lung Adenocarcinomas (LADCA) With Histologic and Clinical Correlates

Julia Elvin, Sanjay Mukhopadhyay, Siraj Ali, Kai Wang, Mark Bailey, Vamsidhar Velcheti, Yuan Li, Norma Palma, Rachel Erlich, Doron Lipson, Roman Yelensky, Juliann Chmielecki, Philip Stephens, Vincent Miller, Jeffrey Ross. Foundation Medicine Inc, Cambridge, MA; Cleveland Clinic, Cleveland, OH; Shanghai Cancer Hospital, Shanghai, China; Albany Medical College, Albany, NY.
Background: Clinical responses of LADCA with *RET*-fusions to RET inhibitors were reported recently. We present CGP of the largest series to date of *RET*-fused LADCA to delineate the clinical, histologic and molecular features of tumors with this unusual oncogenic driver.
Design: Hybridization captured libraries for 236 cancer-related genes and 19 genes commonly rearranged in cancer were applied to ≥ 50ng of DNA extracted from 1905 LADCA FFPE specimens and sequenced to high, uniform coverage. Patient samples were analyzed for all classes of genomic alterations (GA), including base subs, small insertions/deletions, rearrangements, and copy number alterations. 3 pathologists independently reviewed 44 LADCA (2.3%) harboring *RET*-fusions (19 primary, 25 recurrence/mets) and assigned consensus patterns.
Results: *RET*-fused LADCA patients were relatively young (48.8y) and more often women (27F, 17M). Advanced stage (85% III/IV, 16% ≤ II/unk), lymphatic involvement (50% primary), pleural spread (23%), and symptomatic effusion (11.4%) were noted, despite small primary tumor size (reported in 10 cases; pT1a 80%; pT1b 20%). *RET* was most commonly fused to *KIF5B* (64%) and *CCDC6* (18%), but one fusion to each of *NCOA4, TRIM33, ZNF477P, ERCC1, HTR4, CLIP1*, and 2 intragenic *RET* rearrangements was identified. The most common predominant histologic pattern was solid (55%), with cribriform (18%), micropapillary (14%) and papillary (7%) patterns accounting for the remainder. Histologic pattern did not correlate with fusion partner. At least a small micropapillary component was present in 47%. Co-occurring homozygous deletion of *CDKN2A/B* (p14/p16; 25%) was present almost exclusively in the cases lacking a micropapillary component. At least one additional GA occurred in 90% including *p53, MDM2, SETD2, CTNNB1, MYC* alterations. However, there were no cases with concurrent *ALK* or *RAS* alterations. Of note, the *NCOA4-RET* case was originally called negative by *RET* break-apart FISH assay and had no other co-occurring known driver mutations detected.
Conclusions: *RET*-fused LADCA show a predilection for women and occur at a relatively young mean age. Most are solid-pattern predominant, but a micropapillary component is common. *KIF5B* and *CCDC6* are the most common, but not the only, oncogenic fusion partners. Since there are no pathognomonic clinical or morphologic features, CGP is required for detection of this potentially actionable oncogenic driver.

1905 Amplification of c-MET in Malignant Mesothelioma

Franco Fedeli, Serena Varesano, Sandra Salvi, Simona Boccardo, Mauro Truini, Paola Ferro, Pier Aldo Canessa, Maria Pia Pistillo, Silvio Roncella. ASL5, La Spezia, Italy; IRCCS A.O.U. San Martino–IST, Genova, Italy.
Background: Malignant mesothelioma is an aggressive tumour, with poor prognosis and limited possibility of treatment.
c-MET tyrosine-kinase was recently proposed for a targeted therapy and clinical trials with specific drugs, such as monoclonal antibodies or small-molecule tyrosine-kinase inhibitors, are in progress in tumours characterized by the presence of *c-MET* deregulation.
C-MET amplification leads to over-expression of its receptor expressed on the tumour cell membranes and identifies a subgroup of patients potentially able to respond to c-MET inhibitors. In contrast, it has been reported that *c-MET* amplification can represent an element of resistance for anti-EGFR inhibitor therapy.
The aim of this study was to analyze *c-MET* amplification and expression in mesothelioma.
Design: We analyzed paraffin-embedded tissues from 60 mesotheliomas (40 males and 20 females) in different stages and organ locations. FISH to evaluate *c-MET* gene amplification was performed by "Vysis MET Spectrum Red FISH Probe Kit" (Abbott Molecular Inc.). The samples with more than two *c-MET* gene hybridization spots in >10% of cell nucleos were considered amplified.
Immunohistochemistry was performed using the "PATHWAY kit" by Benchmark XT system (Ventana Medical Systems Inc.) with "Met (C-12): sc-10" monoclonal antibody (Santa Cruz Biotechnology Inc.).
Results: By previously described FISH methods, we evaluated the status of *c-MET* in 60 mesotheliomas (36 epithelioid, 12 sarcomatoid, 8 biphasic, 2 papillary and 2 desmoplastic types). We identified 4/60 (6.7 %) mesotheliomas with *c-MET*

amplification. All amplified specimens were of epithelioid type and showed a high number (about ten) of specific hybridization spots in more than 80% of nucleos. Over-expression of c-MET receptor was found on the tumour cell membranes of all the amplified specimens.
Conclusions: We report for the first time that, in a small proportion (about 7 %) of mesotheliomas, the amplification of *c-MET* was present and this amplification was associated with c-MET receptor over-expression. These preliminary observations may represent the basis for designing new clinical trials assessing c-MET targeting agents in mesotheliomas. Moreover, the possibility of c-*MET* amplification should be considered before starting treatments with the EGFR targeted inhibitors.

1906 Usefulness of Histomolecular Profiling of Sarcomatoid Carcinoma of the Lung for Targeted Therapies

Fabien Forest, Violaine Yvorel, Olivier Tiffet, Jean-Michel Vergnon, Pierre Fournel, Michel Peoc'h. Saint Etienne University Hospital, Saint Etienne, France; Oncology Institute Lucien Neuwirth, Saint Etienne, France.
Background: Sarcomatoid carcinoma of the lung (SCL) is a rare primary lung neoplasm. Its treatment relies mainly on surgical excision. This lung carcinoma subtype is often resistant to chemotherapy and radiotherapy. We wondered if a morphological, immunophenotypic and molecular sub-typing would be able to distinguish prognosis factor or targetable molecular features.
Design: Clinical records of all patients undergoing surgical resection for SCL at our institution from 1997 to 2014 and all corresponding slides were reviewed. Slides were immunostained with TTF-1, napsin A, p40, p63, CK5/6 for immunophenotypic differentiation and c-MET, ROS1, ALK. EGFR, KRAS, HER2, BRAF and PIK3CA genes sequencing was performed on 23 cases.
Results: Among 36 SCL (2 spindle cell carcinomas, 3 giant cell carcinomas, 30 pleomorphic carcinomas and 1 pulmonary blastoma), the prognosis was independent of morphological or immunophenotypic sub-typing whereas classic prognostic factors (stage, pleural invasion) influenced the prognosis.
Among the 23 cases with complete mutational profile, results show that 8/17 SCL with a adenocarcinomatous or "undifferentiated" carcinomas differentiation harbored a EGFR (n=1), KRAS (n=2), BRAF (n=1), HER2 (n=3) and PIK3CA (n=1) mutation. Within SCL expressing TTF-1 and/or napsin A, 5/8 were mutated for KRAS (n=2), BRAF (n=1) and HER2 (n=2). None (0/4) SCL with only squamous cell differentiation or p40 positive harbored a EGFR, KRAS, BRAF, HER2 and PIK3CA mutation. c-MET over-expression (H-score>200) only concerned SCL with adenocarcinomatous of undifferentiated component (n=6) without squamous cell component, whereas lack of c-MET over-expression (H-score<200) concerns SCL with adenosquamous (n=2), adenocarcinomatous (n=9), squamous cell carcinoma (n=6) and undifferenciated carcinoma component (n=13). Overall, no immunoexpression of ROS 1 and ALK was detected within all our SCL.
Conclusions: Our results suggest that morphological or immunophenotypic identification of an adenocarcinomatous component in SCL might be associated with the presence of targetable gene mutations and might be suitable for molecular targeted therapies.

1907 Vascular Neoplasia in Germ Cell Tumors: The Role of Dysplastic Angioblastic Mesenchyme (DAM) in Their Histogenesis

Samuel Franks, Narasimhan Agaram, Liang Cheng, Thomas Ulbright. Indiana University School of Medicine, Indianapolis, IN; Memorial Sloan Kettering Cancer Center, New York, NY.
Background: Vascular neoplasms, including angiosarcoma (AS), are a rare complication of germ cell tumors (GCT) in male patients and disproportionately affect mediastinal primaries. We have identified a vasoformative tissue derived from yolk sac tumor (YST), termed DAM, as the likely source for vascular neoplasia in this context.
Design: A natural language search of pathology cases from 1999-2010 was performed to include GCT and vascular lesions. One additional case from 1988 was also included. All available material was reviewed to confirm the diagnosis and categorize the vascular lesion as AS, DAM or hemangioma (H). Immunohistochemical (IHC) studies for AE1/AE3 keratin, CD31, CD34 and ERG, and FISH for i(12p) were performed in some cases.
Results: 19 patients 19-55 years old (median 27.5) were identified. 15 (79%) had mediastinal GCTs, 3 (15%) testicular, and in 1 the primary site was unknown. The vascular tumor occurred 0-40 months (median, 5) after the primary. 7 cases (37%) were classified as AS; 11 (58%) as DAM and 1 (5%) as H. AS showed anastomosing vascular channels lined by a single layer of atypical, enlarged cells with hyperchromatic nuclei. DAM consisted mostly of non-anastomosing, thin-walled vessels lined by a single layer of cells that varied from flat and cytologically bland to plump and hyperchromatic. One DAM had muscular arterioles with atypical smooth muscle and endothelium. Both AS and DAM were associated with a fibromyxoid stroma that had dysplastic stellate cells displaying vasoformative properties, including intracytoplasmic lumens and linear fusion that produced vessel-like structures. Stromal cells of AS and DAM were widely reactive with AE1/AE3 and occasionally positive for CD34 (8/8) and ERG (6/8) but not CD31 (0/4). Vascular lining cells were positive for all 3 markers. i(12p) was present in both the vascular lining cells and stromal cells of AS and DAM (4/7). 1 patient with DAM was known to have progressed to metastatic AS 25 months later.
Conclusions: GCTs, mostly of mediastinal origin, may show a spectrum of vascular neoplasia. We provide evidence that the source for these lesions is a distinctive neoplastic stroma with vasoformative properties that derives from YST (sometimes designated "magma reticulare"). Recognition of DAM is important because it may lead to metastatic AS.

1908 Necrosis and Solid Growth Pattern Augment Nuclear Grading in Predicting Survival in Epithelioid Malignant Mesothelioma: An International, Multi-Institutional Study

Alexander Gallan, Vijayalakshmi Ananthanarayanan, Kenzo Hiroshima, Alberto Marchevsky, Stephanie McGregor, MAngeles Montero, Kazuki Nabeshima, Wickii Vigneswaran, Ann Walts, Thomas Krausz, Aliya Husain. University of Chicago, Chicago, IL; Loyola University, Maywood, IL; Tokyo Women's Medical University, Tokyo, Japan; Cedars-Sinai Medical Center, Los Angeles, CA; Royal Brompton and Harefield Hospitals, London, United Kingdom; Fukuoka University, Fukuoka, Japan.
Background: A recently described nuclear grading system has been shown to predict survival in patients with epithelioid diffuse malignant pleural mesothelioma (EMM). The current study was undertaken to identify additional prognostic characteristics to augment the nuclear grading system and more accurately predict survival.
Design: We analyzed cases of EMM from five institutions across the United States, England, and Japan from 1998-2013. Nuclear grade was computed combining nuclear pleomorphism and mitoses into a grade of I-III using the published system. The presence or absence of necrosis and patterns of growth were also evaluated. Overall survival (OS) was used as the primary endpoint. Data were examined using Student's t-test.
Results: A total of 117 cases of EMM were analyzed. Of these, 53 (45%) were Grade I, 47 (40%) were Grade II, and 17 (15%) were Grade III. The mean OS was 28 months. Our multi-institutional data confirmed that higher nuclear grades are associated with worse OS (Grade I - 40 months, Grade II – 20 months, Grade III – 13 months, I vs II $p<0.001$, II vs. III $p=0.05$, I vs. III $p<0.001$). Importantly, Grade II tumors with associated necrosis behave similarly to Grade III tumors (10 vs 13 months, $p=0.37$), and significantly worse than Grade IIs without necrosis (10 vs. 24 months, $p=0.003$). Additionally, a solid growth pattern was associated with worse OS (22 vs. 33 months, $p=0.02$).
Conclusions: This study confirms that nuclear grade predicts survival in EMM, and identifies the presence of necrosis as a predictor of especially aggressive behavior in Grade II tumors. Therefore, we recommend that Grade II tumors with necrosis be regarded as equivalent to Grade III tumors in behavior. Additionally, a solid growth pattern, regardless of the nuclear grade, is associated with a worse overall survival. In conclusion the assessment of non-nuclear features such as necrosis and the architectural pattern serve to augment nuclear grading in predicting survival in patients with EMM.

1909 microRNA Sequencing Identified Frequent Shutdown of Chromosome 14q32 miRNA Cluster in Neuroendocrine Lung Carcinomas

Paula Ginter, Theresa Scognamiglio, Nicole Panarelli, Zhengming Chen, Thomas Tuschl, Neil Renwick, Yao-Tseng Chen. Weill Cornell Medical College, New York, NY; Rockefeller University, New York, NY.
Background: Neuroendocrine tumors (NET) of the lung comprise a heterogeneous group of neoplasms that exhibit a wide variation in clinical behavior. MicroRNAs (miRNAs) are short noncoding RNAs that bind to mRNAs and target them for downregulation/degradation. Aberrant expression of miRNAs has been shown to contribute to oncogenesis in many malignancies, but data on their expression in NETs of the lung were limited. In this study, we used small RNA sequencing to comprehensively examine miRNA expression profiles in these neoplasms.
Design: Total RNA was extracted from formalin-fixed, paraffin-embedded tissue from typical carcinoids (TC, N=4), atypical carcinoids (AC, N=9), large cell neuroendocrine carcinomas (LCNEC, N=5) and small cell lung carcinomas (SCLC, N=5), and subjected to small RNA sequencing. NETs from other organs (N=52), i.e. pancreas, GI tract, adrenal and thyroid, were also profiled. Unsupervised clustering was performed using normalized data and mean miRNA expression levels were compared.
Results: Unsupervised hierarchical clustering showed clean separation of carcinoids from SCLC based on their miRNA profiles. In contrast, TC and AC could not be clearly separated. LCNEC were more heterogeneous, and 4 of 5 cases clustered with SCLC but one with the carcinoid group.
Comparisons between carcinoids and NECs showed the most significant difference to be the expression of 18 miRNAs clustered on chromosome 14q32. All 18 miRNAs showed lower expression in most (4/5) SCLC vs. carcinoids ($p<0.001$), 9 of them also downregulated in 4/5 LCNEC. Chr.14q32 contains the largest human miRNA cluster, and its downregulation has been described in various tumors but not in lung NECs. Of the non-pulmonary NETs that we profiled, pheochromocytoma also formed two subgroups that were separated by the differential expression of Chr14q32 miRNA cluster. Besides this cluster, putative tumor suppressor miR-129 (-3p and -5p) also showed lower expression in all 10 NEC (vs. carcinoids, $p<0.001$). Conversely, three miRNAs (miR-17, miR-20a, miR-21) were overexpressed in NECs ($p<0.001$), including miR-21 that has been shown to be overexpressed in multiple malignancies.
Conclusions: Benign and malignant lung NETs can be separated based on their miRNA profiles, most significant differences being the downregulation of tumor suppressor miR-129 and the Chr14q32 miRNA cluster in most NECs but not in carcinoids. Chr14q32 miRNA status appears to separate lung NECs into two molecular subgroups, similar to our findings in pheochromocytomas.

1910 EGFR Pathway Activation Via KRAS Mutation Leads To Cyclin D1 Expression and Decreased Proliferation in Lung Adenocarcinomas

Cora Hallas, Mia-Maria Warnke, Markus Tiemann. Institute for Haematopathology Hamburg, Hamburg, Germany; Semmelweis Universität Medizinische Fakultät, Hamburg, Germany.
Background: The EGFR/RAS/RAF-pathway is implicated as a pathogenetic driver in at least a proportion of adenocarcinomas of the lung. Activation of this pathway may lead to transcriptional overexpression of Cyclin D1 via NFkB, but expression and functional role of this cell cycle regulator in lung adenocarcinomas has not been sufficiently evaluated.

Design: Proliferation (MIB-1, % positive cells), vascularization (CD34, number of blood vessels) and Cyclin D1 expression (positive or negative) was determined immunohistochemically in 141 adenocarcinomas of the lung and counted in in three representative high power fields (HPF) each. Mutation status of EGFR (exons 18-21) and KRAS (exons 2 and 3) was analyzed by direct sequencing.
Results: On average 20% of tumor cells/HPF were proliferating and each HPF contained an average of 30 small blood vessels. 70% of adenocarcinomas displayed Cyclin D1 expression and a further 10% showed partial expression. No correlation between MIB-1, CD34, and Cyclin D1 expression, resp., and age of the patient and tumor stage was found. However, cases expressing Cyclin D1 demonstrated significantly lower proliferation than cases lacking Cyclin D1 ($p<0.0012$). Furthermore, significantly more Cyclin D1 expressing tumors carried a KRAS mutation as Cyclin D1 negative Tumors did (45% vs. 18.5%; $p<0.015$). KRAS mutation status was not linked with CD34 and MIB-1 expression or tumor stage. EGFR mutations were found in 10 cases, but mutation status did not correlate with any of the other parameters investigated, possibly because EGFR mutated carcinomas were sparse in this set of tumors.
Conclusions: Cyclin D1 expression correlated with KRAS mutation in this set of 141 lung adenocarcinomas, indicating that an constitutive activation of the EGFR-RAS-RAF pathway by an activating KRAS mutation may lead to a transcriptional activation of Cyclin D1. Surprisingly, this activation was linked to a decreased proliferation rate of the tumor. The cell cycle activating function of Cyclin D1 seems to be inhibited, although not completely blocked, by as yet unknown factors in these tumors. Nevertheless, inhibition of Cyclin D1 may be a therapeutic option in KRAS mutated adenocarcinomas of the lung.

1911 Clinicopathologic and Molecular Analysis of Explanted Lung of Patients With Lymphangioleiomyomatosis: Identification of Destruction of Airway Walls and Lack of Hypoxia Inducible Factor 1 Alpha Expression

Takuo Hayashi, Toshio Kumasaka, Keiko Mitani, Tsuyoshi Saito, Kieko Hara, Katsutoshi Ando, Kuniaki Seyama, Takashi Yao. Juntendo University School of Medicine, Tokyo, Japan; Japanese Red Cross Medical Center, Tokyo, Japan.
Background: Lymphangioleiomyomatosis (LAM), a rare progressive disease affecting almost exclusively women, is characterized by neoplastic proliferation of smooth muscle-like cells (LAM cells) that was caused by a functional loss of *tuberous sclerosis complex (TSC)* genes and consequent hyperactivation of the mammalian target of rapamycin complex 1 (mTORC1) signaling, which lead to formation of pulmonary cysts. Clinically, the most common abnormalities of pulmonary function tests in LAM patients are airflow obstruction. Also, activation of mTORC1 in tumor cells results in the accumulation of hypoxia inducible factor 1 alpha (HIF-1α), and increases expression of HIF-responsive genes including *vascular endothelial growth factor (VEGF)*. However, neither histopathology of airways nor expression of HIF-1α has not to be fully characterized in LAM patient's tissues.
Design: We examined histological analysis of explanted lung tissues in 30 LAM patients with special emphasis on airways. We further examined immunohistochemistry, RT-PCR, and western blot analyses focusing on mTORC1 signaling, HIF-1α, and vascular endothelial growth factor (VEGF)-D expression in LAM tissues.
Results: The results showed that destruction of airway walls caused by proliferation of LAM cells or lymphatic vessels was identified in all patients examined. Additionally, chronic inflammation in airways at a moderate level or higher was identified in 22 patients. Expression of phospho-p70S6K, phospho-S6, phospho-4E-BP1, and VEGF-D was found in all patients examined; when stratified according to staining grade (scale 0-3), average score in LAM lesions was 2.9 for phospho-p70S6K, 2.7 for phospho-S6, 2.2 for phospho-4E-BP1, and 2.5 for VEGF-D. In contrast, no expression of HIF-1α was detected in any patients.
Conclusions: These results indicate that destruction of airways caused by proliferation of LAM cells or lymphatics, accompanied by chronic inflammation is a common manifestation of patients with advanced stage of LAM. Furthermore, activation of mTORC1 does not result in upregulation of HIF-1α in LAM cells; this feature may distinguish LAM from other common tumors that have constitutive activation of mTORC1 signaling.

1912 Analysis of Expected Versus Actual Frequency of KRAS Mutation Subtypes Can Identify Mutations With Stronger Positive Selection

Dov Hershkovitz, Einav Simon, Sheli Ostrow, Elad Prinz, Tova Bick, Talia Shentzer, Edmond Sabo, Ruth Hershberg, Ofer Ben-Izhak. Rambam Health Care Campus, Haifa, Israel; Rappaport Faculty of Medicine, Technion, Haifa, Israel.
Background: *KRAS* is an oncogene that is commonly mutated in cancer. Different tumors show different distributions of *KRAS* mutation subtypes. These could be the result of factors such as exposure to different carcinogens or, on the other hand, the result of differences in natural selection. Recent studies suggest that different *KRAS* mutations have different downstream effects, which may affect their natural selection in different tumor types. The purpose of this work was to determine the relative contribution of mutational biases and natural selection to the distribution of *KRAS* mutations in colon, lung and pancreatic adenocarcinomas.
Design: We examined the distribution of *KRAS* mutation subtypes using the Catalogue Of Somatic Mutations In Cancer (COSMIC) database for colon, lung and pancreatic adenocarcinomas. To determine the contribution of mutational biases for each tumor type, we used data of synonymous mutations occurring within tumors of these types within the Cancer Genome Atlas (TCGA) database. Using these data we were able to normalize the actual *KRAS* mutation subtype distribution to the expected base pair changes and determine the relative selective power of each mutation. We then examined a sample set of 100 *KRAS* positive lung adenocarcinoma cases and correlated mutation subtype with clinico-pathological information.
Results: *KRAS* mutation subtype distribution was significantly different between the tumor types with c.35G>A presenting 35%, 17% and 51% of *KRAS* mutations in colon, lung and pancreatic adenocarcinoma, respectively ($p<0.0001$). Following normalization to the TCGA data, p.G12A and p.G12V were the most positively selected mutations in colon carcinoma and p.G12C was the most positively selected mutation in lung adenocarcinoma. In our lung adenocarcinoma data set the evolutionary selected, p.G12C mutation, was significantly associated with higher tumor stage (62.5%, 27.5% and 10% in stages 1, 2 and 3, respectively, in the p.G12C group compared to 83.3%, 14.8% and 1.9% in stages 1, 2 and 3 in the other mutations, $p=0.01$) and grade (18.4%, 57.9% and 23.7% in grades 1, 2 and 3, respectively, in the p.G12C group compared to 40.4%, 48.9% and 10.6% in grades 1, 2 and 3 in the other mutations, $p=0.01$).
Conclusions: Analysis of the expected and actual distribution of mutation subtypes can determine the relative selective strength of different mutations in each tumor type and may provide higher resolution for personalized anti-cancer therapy.

1913 p16 FISH Deletion Status in Effusion Smear Preparations Correlates With That in Underlying Malignant Pleural Mesothelioma

Tomoyuki Hida, Shinji Matsumoto, Makoto Hamasaki, Sohsei Abe, Tohru Tsujimura, Kenzo Hiroshima, Kazuki Nabeshima. Fukuoka University School of Medicine and Hospital, Fukuoka, Japan; Hyogo College of Medicine, Nishinomiya, Hyogo, Japan; Tokyo Women's Medical University Yachiyo Medical Center, Yachiyo, Chiba, Japan.
Background: As malignant pleural mesothelioma (MPM) starts with pleural effusions in over 80% of cases, the detection of mesothelioma cells in effusion smears is important for its early diagnosis. Unfortunately, differentiating MPM cells from reactive mesothelial hyperplasia (RMH) cells can be problematic. A homozygous deletion (HD) of p16 (CDKN2A), detected by fluorescence in situ hybridization (FISH), is a good marker of malignancy and is useful for differentiating between MPM and RMH cells. However, the correlation of p16 status between effusion smears and underlying MPM tissues has not been fully described.
Design: We performed p16-specific FISH to investigate 20 cases of MPM between 2007 and 2013, from which both effusion cytological smear and histological specimens were available. In five cases, histological specimens included both an invasive component and surface mesothelial proliferation. All cases exhibited epithelioid mesothelioma.
Results: In 14 cases (70%), both MPM tissue and atypical mesothelial cells in effusion smears were p16 HD-positive [%HD-positive cells (mean±SE) = 54.5±9.1 (tissues) vs. 58.1±9.9 (smears); coefficient of correlation (c.c.) value=0.974]. Conversely, the remaining six tumors (30%) were p16 HD-negative in both MPM tissues and effusion smears. Moreover, all five MPM cases with surface mesothelial proliferations and invasive components showed the p16 deletion in each of the effusion smears, surface mesothelial proliferations, and invasive MPM components [%HD-positive cells: 43.5±21.4 (smears), 66.3±16.5 (tissue-surface), 68±14.7 (tissue-invasive); c.c. values = 0.982 (smear vs. tissue-surface) and 0.987 (smear vs. tissue-invasive)].
Conclusions: Results by FISH to detect p16 deletions were the same for both cytologic smears and histological specimens. In addition, MPM cells in smears showed the same FISH pattern of p16 as tissue surface proliferations and invasive components. Thus, p16 deletion in smear cytologic samples may allow for diagnosis of MPM without additional tissue examination in cases with clinical and radiologic evidence of a diffuse pleural tumor, although the absence of p16 deletion in cytologic smear samples does not preclude MPM.

1914 STAT6 Immunohistochemistry and NAB2-STAT6 Gene Fusion Detection in 50 Thoracic Solitary Fibrous Tumors

Shih-Chiang Huang, Tse-Ching Chen, Chien-Feng Li, Jui Lan, Hui-Chun Tai, Yu-Chien Kao, Jen-Wei Tsai, Shih-Ming Jung, Hsuan-Ying Huang. Chang Gung Memorial Hospital, Taoyuan, Taiwan; Chi Mei Medical Center, Tainan, Taiwan; Kaohsiung Chang Gung Memorial Hospital and Chang Gung University College of Medicine, Kaohsiung, Taiwan; Changhua Christian Hospital, Changhua, Taiwan; Wan Fang Hospital and Taipei Medical University, Taipei, Taiwan; E-Da Hospital, Kaohsiung, Taiwan.
Background: *NAB2-STAT6* gene fusion was recently identified as the pathogonomic hallmark of SFT, which drives nuclear expression of STAT6. In thoracic SFTs, a robust study to compare clincopathological features, STAT6 immunoexpression status, and fusion variants of *NAB2-STAT6* is lacking.
Design: Fifty thoracic SFTs were retrieved to appraise histopathology, assess the immunoexpression of STAT6, and determine *NAB2-STAT6* fusion variants by RT-PCR, with location-relevant histologic mimics serving as controls.
Results: Twenty-nine female and 21 male patients, aged from 31 to 85 (median, 56) years, had 30 pleura-based, 11 mediastinal, and 9 pulmonary SFTs. Histologically, these were categorized into 9 malignant, 6 atypical, and 35 benign SFTs, including 1 fat-forming and 2 giant cell angiofibroma-like benign tumors. STAT6 distinctively labeled the tumoral nuclei in all but one (98%) SFTs, including 2 CD34-negative tumors. *NAB2-STAT6* fusion was detected in 32 SFTs (formalin-fixed, 30; fresh, 2), exhibiting the predominant *NAB2*ex4-*STAT6*ex2 variant in 27 (84%) and minor *NAB2*ex6-*STAT6*ex16/17 in 5. The predominant variant showed a trend toward older age ($p=0.077$) and hypocellularity ($p=0.059$). After a median follow-up of 29.9 (range, 1~175) months, 1 atypical and 5 malignant SFTs developed adverse outcomes, including local relapse in 1, intrapulmonary metastasis in 2, and extrathoracic dissemination in 3. Inferior disease-free survival was univariately associated with the mitosis ≥4/10 HPFs ($p=0.0019$) but neither related to fusion variants nor STAT6 immunostaining extent or intensity.
Conclusions: The vast majority of intrathoracic SFTs exhibit STAT6 nuclear staining, with *NAB2*ex4-*STAT6*ex2 being the predominant fusion variant. However, the variability in fusion types ad STAT6 immunostain is not related to clinical aggressiveness, which is only significantly associated with increased mitotic rate.

1915 Comprehensive Genomic Profiling of Pulmonary Atypical Carcinoid Tumors Reveals Potential New Routes To Targeted Therapies

Albert Huho, Kai Wang, Aseeb Rehman, Dion Middleton, Christine Sheehan, Llewellyn Foulke, Siraj Ali, Julia Elvin, Roman Yelensky, Doron Lipson, Juliann Chmielecki, Vincent Miller, Philip Stephens, Jeffrey Ross. Albany Medical College, Albany, NY; Foundation Medicine Inc, Cambridge, MA.

Background: Pulmonary atypical carcinoids (PAC) have distinct clinicopathologic features when compared to the extremes of typical carcinoids and small cell lung undifferentiated carcinomas (SCLC). We queried whether PAC also feature distinctive clinically relevant genomic alterations that could lead to targeted therapies for patients with advanced disease.

Design: DNA was extracted from 40 microns of FFPE sections from 26 PAC. Comprehensive genomic profiling was performed on hybridization-captured, adaptor ligation based libraries to a mean coverage depth of 647X for 3,769 exons of 236 cancer-related genes plus 47 introns from 19 genes frequently rearranged in cancer. The results were evaluated for all classes of genomic alterations (GA). Clinically relevant alterations were defined as those linked to targeted drugs on the market or under evaluation in mechanism driven clinical trials.

Results: There were 14 male and 12 female PAC patients with a median age of 58 years (range 20-72). There were 10 (38%) stage III and 16(62%) IV PAC. A total of 55 alterations were identified (mean 2.1; range 0-8 per PAC), with 21 (81%) samples containing at least one alteration. Clinically relevant alterations were identified in 14 (54%) patients including: *CCND1* (12%); *NF1* (8%); *HGF* (8%); *FGFR4* (8%); *CDK6* (8%); *ATM* (8%) and STK11, *RICTOR*, *RET*, *RAF1*, *MTOR*, *MET*, *EGFR*, *CDKN2A*, *BRAF*, *ATR* (each in a single patient). Other alterations identified included *MEN1* (27%); *TP53* (12%); *FGF19* (12%) and *ARID1A* (8%). In contrast with previously studied SCLC, which showed clinically relevant alterations of KIT (7%); *PIK3CA* (6%); *PTEN* (5%); *KRAS* (5%); *MCL1* (4%); *FGFR1* (4%); *BCRA2* (4%); *TSC1* (3%) and *EPHA3* (3%), PAC did not reveal alterations in any of these genes. Clinically relevant alterations common to both SCLC and PAC, though in different proportions, included *RICTOR* (10% in SCLC versus 4% in PAC); *EGFR* (5% versus 4%); *NF1* (3% versus 8%) and*CCND1* (3% versus 12%). Other alterations common to both SCLC and PAC in significantly different proportions, included *TP53* (86% in SCLC versus 12% in PAC); *RB1* (4% versus 54%) and *MLL2* (4% versus 17%).

Conclusions: Genomic profiling of PAC reveals a multiplex of clinically relevant alterations distinct from SCLC. Analogous to SCLC, however, a variety of potential therapy targets for patients with relapsed and metastatic PAC can be identified by comprehensive profiling that show potential to improve outcomes for patients with this aggressive form of malignancy.

1916 Clinicopatholgical and Molecular Features Associated With Programmed Cell Death Ligand 1 (PD-L1) Expression in Resected Lung Squamous Cell Carcinomas

Tiffany Huynh, Anthony Chi, Hironori Uruga, Emine Bozkurtlar, Eugene Mark, Mari Mino-Kenudson. Massachusetts General Hospital, Boston, MA.

Background: Recent strategies targeting PD-L1 with its receptor, PD-1, resulted in promising activity in early phase clinical trials. Preliminary results of the clinical trials indicate that tumor overexpression of PD-L1 by immunohistochemistry (IHC) could serve as a predictor of clinical response to PD-1/PD-L1 therapies. However, little is known about clinicopathological and molecular features of lung squamous cell carcinomas with PD-L1 overexpression.

Design: PD-L1 IHC (clone E1L3N, Cell Signaling Technology) was performed on tissue microarrays constructed of resected lung squamous cell carcinomas. The majority of those underwent clinical molecular testing (SNaPshot and FGFR and/or PDGFR FISH). Membranous staining of any intensity present in ≥5% of the tumor cells was deemed positive. Tumor infiltrating lymphocytes (TIL), more specifically T cells, were evaluated with a 2-tiered grading system using CD3 IHC. PD-L1 expression was correlated with clinicopathological and molecular features and patient outcomes.

Results: The study cohort consisted of 159 patients (M:F=90:69, mean age: 68 years), with 94 cases of stage I , 40 cases of stage II, 22 cases of stage III and 3 cases of stage IV. Of the 153 cases which were examined with SNaPshot, *PIK3CA*, *TP53* and other mutations were identified in 11, 11 and 2 cases, respectively. *FGFR* amplifications were found in 15 of the149 cases examined, and *PDGFR* amplifications in 4 of the 139 cases examined. PD-L1 overexpression was seen in 42 (26%) of the 159 cases, and was associated with significant TIL (p=0.0070) and advanced pathologic stage (stage I vs. stage II – IV, p=0.0058), but there was no association of PD-L1 overexpression with gender, age, or smoking history. Of the 11 *PIK3CA* mutants, 7 exhibited PD-L1 overexpression, and the association was statistically significant (p=0.012). In the entire cohort, 5-year recurrent free survival was 38% and 62% in those with and without PD-L1 overexpression (p=0.15), respectively, but there was no difference in survival between these 2 groups in the Stage I cohort.

Conclusions: PD-L1 overexpression by IHC is associated with significant TIL and advanced stage in resected lung squamous cell carcinomas. Interestingly, it is also associated with *PIK3CA* mutations. Further studies are required to determine the value of PD-L1 IHC in prognosis and prediction of response to PD-1/PD-L1 therapies especially in those with *PIK3CA* mutations for which no established targeted therapies are currently available.

1917 Clinicopathological and Molecular Features Associated With Programmed Cell Death Ligand 1 (PD-L1) Expression in Resected Lung Adenocarcinomas

Tiffany Huynh, Hironori Uruga, Emine Bozkurtlar, Eugene Mark, Mari Mino-Kenudson. Massachusetts General Hospital, Boston, MA.

Background: Recent strategies targeting PD-L1 with its receptor, PD-1, resulted in promising activity in early phase clinical trials. It has been reported that overexpression of PD-L1 by immunohistochemistry (IHC) could serve as a predictor of patient response to PD-1/PD-L1 therapies. However, little is known about clinicopathological and molecular features of lung adenocarcinomas with PD-L1 overexpression.

Design: PD-L1 IHC (clone E1L3N, Cell Signaling Technology) was performed on tissue microarrays constructed of resected lung adenocarcinomas that underwent clinical molecular testing (SNaPshot) and detailed histological analysis. Membranous staining of any intensity in ≥5% of the tumor cells was deemed positive. Tumor infiltrating lymphocytes (TIL), more specifically T cells, were evaluated with a 2-tiered grading system using CD3 IHC. PD-L1 expression was correlated with clinicopathological and molecular features and prognosis.

Results: The study cohort consisted of 141 patients (M:F=57:84, mean age: 67 years) with pathologic stages of 0 in 2 cases, I in 93, II in 23, III in 11 and IV in 12. The predominant histologic pattern was lepidic in 48 (including 3 AIS and 16 MIA), acinar in 49 (including 27 high-grade morphology), papillary in 16, micropapillary in 6, solid in 18, and variants in 4 cases. *KRAS*, *EGFR* and other mutations were identified in 56, 34 and 5 cases, respectively, and 46 cases harbored no mutations. Of the 141 cases, 19 (13.5%) exhibited PD-L1 overexpression which was associated with smoking history (>10 pack-year, p=0.0019), solid (p=0.018) or high-grade acinar (p=0.0024) predominant pattern and significant TIL (p=0.014), but there was no difference in PD-L1 expression between pathologic stages. PD-L1 overexpression was also associated with *KRAS* mutations (27%, p=0.0003). In the entire cohort, 5-year recurrent free survival was 92% and 63% in those with and without PD-L1 overexpression (p=0.16), respectively, but there was no difference in survival between these 2 groups in the Stage I cohort.

Conclusions: PD-L1 overexpression by IHC is associated with significant TIL and appears to predict better outcomes in resected lung adenocarcinomas. It is also associated with *KRAS* mutations and their clinicopathological signatures. Further studies are required to determine the value of PD-L1 IHC in prognosis and prediction of response to PD-1/PD-L1 therapies especially in those with *KRAS* mutations for which no effective targeted therapies are currently available.

1918 NKX2-1 Loss of Function Mutations in Mucinous Lung Adenocarcinoma

David Hwang, Lynette Sholl, Priyanka Shivdasani, Fei Dong. Brigham & Women's Hospital, Boston, MA.

Background: NKX2-1 (TTF-1) is a transcription factor with physiologic roles in lung development and function. Although NKX2-1 immunohistochemistry is used to distinguish cancers of pulmonary origin, a minority of lung adenocarcinomas lacks NKX2-1 expression and has been associated with KRAS mutations and mucinous differentiation. These neoplasms may be difficult to distinguish histologically from metastatic carcinomas of gastrointestinal sites. The molecular basis of the loss of NKX2-1 expression is unknown.

Design: We applied a targeted next generation sequencing platform to analyze the exonic sequences of 275 cancer-associated genes in a large cohort of human cancers. DNA was isolated from formalin fixed paraffin embedded whole tissue sections containing at least 20% tumor nuclei. Genes of interest were selected using a solution-phase Agilent SureSelect hybrid capture kit, and massively parallel sequencing was performed with an Illumina HiSeq 2500 sequencer. Lung tumors were analyzed for NKX2-1 loss of function mutations. Tumor morphology was characterized according to the International Association for the Study of Lung Cancer proposed criteria.

Results: 473 total lung cancers were analyzed for NKX2-1 mutations. Of these, 33 cases were diagnosed as mucinous adenocarcinomas, while an additional 20 cases had mucinous features on histology. Five cases of lung adenocarcinoma were identified that harbored NKX2-1 frameshift mutations predicted to cause NKX2-1 loss of function. All cases had a concurrent KRAS codon 12 mutation. Histological review showed that four of the cases were pure invasive mucinous adenocarcinoma, and one case was a mixed mucinous and non-mucinous adenocarcinoma. Of four cases with available NKX2-1 immunohistochemistry, three cases were negative for NKX2-1, and one case exhibited focal staining. NKX2-1 frameshift mutations were not identified in non-mucinous lung adenocarcinomas and carcinomas of gastrointestinal origin.

Conclusions: We report the first observation of recurrent somatic loss of function mutations involving NKX2-1 in lung adenocarcinoma. These neoplasms have distinct features, including mucinous differentiation and concurrent mutations in KRAS. This association supports a role of NKX2-1 as a putative tumor suppressor gene in the pathogenesis of human mucinous lung adenocarcinoma. Detection of NKX2-1 mutations may be helpful to distinguish a primary lung adenocarcinoma from metastasis in the context of ambiguous immunohistochemical results.

1919 Global Mutational Profiling and Comparative Analysis With Histomorphologic Features in Female Never-Smoker Lung Adenocarcinoma

Soo Hyun Hwang, Sang Yun Ha, Jhingook Kim, Yoon-La Choi. Samsung Medical Center, Seoul, Republic of Korea.

Background: The aim of this study was to determine the distribution of known oncogenic driver mutations in female never-smoker Asian patients with lung adenocarcinoma.

Design: We analyzed 214 mutations across 26 lung cancer-associated genes and three fusion genes using the MassARRAY® LungCarta Panel and *ALK*, *ROS1*, and *RET* fusion assay in 198 consecutively resected lung adenocarcinomas from never-smoker females at a single institution.

Results: *EGFR* mutation was the most frequent driver gene mutation and was found in 124 (63%) cases. Mutation of *ALK, KRAS*, *PIK3CA*, *TP53*, *ERBB2, BRAF, ROS1,* and *RET* was observed in *7%,* 4%, 2.5%, 2%, 1.5%, 1%, 1%, and 1%, respectively. Thus, 79% of lung adenocarcinomas from never-smoker females were found to harbor well-known oncogenic mutations. Mucinous adenocarcinoma had a tendency towards a lower frequency of known driver gene mutations compared with other histologic subtypes. *EGFR* mutation was positively correlated with older age and acinar-predominant pattern. *ALK* rearrangement was associated with younger age and solid predominant pattern.

Conclusions: Lung cancer in never-smoker Asian females is a distinct entity, with the majority of these cancers developing from oncogenic mutations. Prospective studies of driver mutation status in this subpopulation will be helpful in devising targeted therapies that will benefit many lung cancer patients.

1920 Immunohistochemistry Analysis of PTEN, p53, c-Met, ALK1, ROS1, and MDM2 in 84 Thymomas and Thymic Carcinomas

Martin Hyrcza, Allen Gown, Rola Ali, Nevin Murray, Diana Ionescu. University of British Columbia, Vancouver, BC, Canada; PhenoPath Laboratories, Seattle, WA; BC Cancer Agency, Vancouver, BC, Canada; Faculty of Medicine, Health Sciences Center, Kuwait University, Safat, Kuwait.

Background: Thymoma pathogenesis is poorly understood. To-date, no specific oncogene or tumor suppressor mutations have been identified in these tumors. We investigated the role of some well-known oncogenes and transcription factors by using immunohistochemistry to determine the expression levels of known oncogenes (MDM2, ROS, ALK1, and c-Met) and tumor suppressors (PTEN, p53).

Design: Review of British Columbia Cancer Agency files from 1995 to 2008 identified 174 thymomas and thymic carcinomas. Blocks were available for eighty three surgical specimens. One case represents a recurrence. Tissue microarray (TMA) was constructed using duplicate 1.0 cm cores from representative areas of each tumor. Among the 83 cases, there were 6 WHO class A tumours, 9 AB tumors, 18 B1 tumors, 31 B2 tumors, 15 B3 tumors and 5 thymic carcinomas. One case had separate areas of B2 thymoma and adenosquamous thymic carcinoma, both of which were included, for a total of 84 samples. The TMA was stained with monoclonal antibodies to PTEN, p53, c-Met, ALK1, ROS1, MDM2, as well as control stains with pankeratin cocktail (composed of AE1/AE3, MNF116, 5D3, and CAM5.2) and hematoxylin and eosin.

Results: None of the thymomas and thymic carcinomas showed any staining for ALK1, ROS1, or MDM2. PTEN loss was seen in 8 tumors. p53 showed wild type staining in 70 of 84 tumors, with one thymoma showing diffuse positivity, seven showing complete loss of staining and four being uninterpretable. No tumors showed diffuse, complete, circumferential, membranous c-Met staining (3+), but 7 thymomas (four B2 and three B3) and three thymic carcinomas showed strong but incomplete membranous (2+) staining. Further 10 tumors showed partial positivity (1+). Correlation with treatment and survival data is in progress.

WHO Class	Total	p53	PTEN	C-Met	Alk1	Ros1	Mdm2
A	6	1	1	0	0	0	0
AB	9	3	3	0	0	0	0
B1	18	2	0	0	0	0	0
B2	31	2	2	4	0	0	0
B3	15	2	1	4	0	0	0
C	5	0	1	4	0	0	0
Total	84	9	8	10	0	0	0

Conclusions: ALK1, ROS1, and MDM2 are not expressed in thymomas or thymic carcinomas. Minority of B2 and B3 thymomas and majority of thymic carcinomas show 2+ c-Met staining. PTEN and p53 loss and diffuse p53 positivity are all infrequent.

1921 Monoclonal PAX-8 Antibody Does Not Stain Thymomas or Thymic Carcinomas

Martin Hyrcza, Allen Gown, Rola Ali, Nevin Murray, Diana Ionescu. University of British Columbia, Vancouver, BC, Canada; PhenoPath Laboratories, Seattle, WA; BC Cancer Agency, Vancouver, BC, Canada; Faculty of Medicine, Health Sciences Center, Kuwait University, Safat, Kuwait.

Background: PAX-8 transcription factor is normally expressed in the kidney, thyroid and cervix. Multiple previous studies have described PAX-8 positivity in thymomas and the PAX-8 immunohistochemistry has been proposed and used as an adjunct marker of thymomas. However, with the advent of monoclonal PAX-8 antibodies it became apparent that many of the previous reports of PAX-8 positivity in other epithelial tumours were due to a cross-reactivity of the polyclonal antibodies to PAX-8 with the N-terminal regions of PAX-5 and / or PAX-6. We have therefore decided to retest PAX-8 immunohistochemistry in thymomas using a new monoclonal PAX-8 antibody.

Design: Review of British Columbia Cancer Agency files from 1995 to 2008 identified 174 thymomas and thymic carcinomas. Blocks were available for eighty three surgical specimens. One case represents a recurrence. Tissue microarray (TMA) was constructed using duplicate 1.0 cm cores from the representative areas of each tumor. Among the 83 cases, there were 6 WHO class A tumours, 9 AB tumors, 18 B1 tumors, 31 B2 tumors, 15 B3 tumors and 5 thymic carcinomas. One case had separate areas of B2 thymoma and adenosquamous thymic carcinoma, both of which were included, for a total of 84 samples. The TMA was stained with PAX-8 mouse monoclonal antibody (BC-12, Biocare Medical), PAX-5 mouse monoclonal (24, Cell Marque), PAX-6 mouse monoclonal (SC-81649, Santa Cruz), as well as control stains with pankeratin cocktail (composed of AE1/AE3, MNF116, 5D3, and CAM5.2) and hematoxylin and eosin. Staining was graded as 0 (staining in < 1% of tumor cells), 1+ (1-25%), 2+ (26-50%), 3+ (51-75%), and 4+ (76-100%).

Results: None of the eighty four thymomas and thymic carcinomas showed any detectable PAX-8 staining. Positive PAX-5 staining (1+ to 4+) was detected in 5 of 84 tumors (6%). Positive PAX-6 staining (1+ to 4+) was detected in 15 tumors (18%), however only 5 tumors (6%) showed staining in more than 25% of cells (2+ or higher). Three of those five tumours also had PAX-5 positivity. All samples showed pankeratin cocktail positivity.

Conclusions: Thymomas and thymic carcinomas do not express PAX-8. Previous reports of PAX-8 positivity in thymomas may be the result of cross-reactivity of the polyclonal PAX-8 antibodies with either PAX-5 or PAX-6. Therefore PAX-8 should no longer be used in the identification of thymomas and thymic carcinoma in clinical practice.

1922 Expression of Met in Circulating Tumor Cells Correlates With Tumor Tissue in NSCLC Patients

Marius Ilie, Edith Szafer-Glusman, Veronique Hofman, Elodie Long-Mira, Catherine Butori, Salome Lalvee, Julien Fayada, Eric Selva, Charles Hugo Marquette, Elizabeth Punnoose, Paul Hofman. Pasteur Hospital, Nice, France; Genentech, South San Francisco, CA.

Background: Overexpression of Met receptor tyrosine kinase is frequent in lung cancers and is associated with poor prognosis. Recent clinical studies of Met targeted therapies have used immunohistochemistry (IHC) in tissue biopsies to quantify Met protein expression, demonstrating benefit in patients that expressed high Met. Non-invasive methods for biomarker assessment, for example, analysis of circulating tumor cells (CTCs) present in a blood-draw, represent a promising approach for real-time measurement of tumor-associated markers. To investigate the utility of CTCs for Met status assessment, we evaluated Met expression in CTCs and matched bronchial biopsies in a prospective cohort of NSCLC patients.

Design: Specimens from 80 patients with advanced-stage IIIb/IV lung adenocarcinoma and positive for CTCs were evaluated in the study. CTCs were isolated on filters (ISET technology). Immunochemistry on CTCs and FFPE tissue sections were performed using the SP44 c-Met antibody from Roche Ventana (Tucson, AZ, USA). Met expression was quantified in tumor tissue and CTCs using two methods 1) the onartuzumab scoring algorithm, or 2) H-scores. Results from matched materials were blinded until study completion.

Results: CTC counts ranged from 7 to 256 CTCs/ml in the initial 30 patient cohort. Clusters of CTCs were observed in 93% of patients, exhibiting between 1 to 23-clusters/ml blood. The Met assay on CTCs was positive in 23 of 29 (79%) patients, and the Met assay on tissue was positive in 20 of 30 (67%) patients using the onartuzumab IHC scoring algorithm, with 89% concordance between tissue and CTCs. Quantification of Met expression using H-scores showed 92.3% concordance between Met expression in tissue and CTCs (Spearmann *correlation*:0.965).

Conclusions: Met status in CTCs isolated from blood samples in advance NSCLC patients correlated strongly with Met status in tumor tissue biopsies, illustrating the potential for using CTCs as a non-invasive, real-time biopsy to determine Met status of patients entering clinical trials. We are now expanding the CTC analysis to other biomarkers with relevance for lung therapeutics.

1923 Differentiating Lung Acute Cellular Rejection From Bronchus-Associated Lymphoid Tissue Using CD21+ To Identify Follicular Dendritic Cells

Marina Ivanovic, Husain Sattar, Mario Moric, Aliya Husain. University of Iowa, Iowa City, IA; University of Chicago, Chicago, IL; Rush University Medical Center, Chicago, IL.

Background: Transbronchial lung transplant biopsies are routinely evaluated for acute and chronic rejection. Acute rejection is defined as characteristic perivascular mixed inflammatory cell infiltrate (graded from A0-A4), and/or lymphocytic bronchiolitis (graded from B0-B4, 1996 grading scheme). The grading system is based on presence or absence of inflammatory infiltrate and its intensity and localization. While most cases of acute rejection can be easily recognized, occasionally it may be difficult to distinguish perivascular/peribronchiolar infiltrate from bronchus-associated lymphoid tissue (BALT). BALT is part of the lung immune system that consists of well-circumscribed, small aggregates of lymphoid cells in the submucosa/wall of the airways and along the lymphatic routes. BALT is usually composed of a central vessel with prominent epithelioid endothelial cells surrounded by mixture of follicular center cells with small lymphocytes and plasma cells at the periphery of the aggregate.

Design: The goal of the study was to determine if the presence of CD21 positive follicular dendritic cells could distinguish acute rejection from BALT. 75 cases of transbronchial lung transplant biopsies containing rejection and/or one or more BALTs were selected. CD21 antibody was used to evaluate 20 rejections and 63 BALTs for

presence or absence of follicular dendritic cells. To evaluate statistical significance the categorical data was analyzed using a Fisher's exact test due to uneven contingency table distribution. Significance was defined as P-Value < 0.05.

Results: All 20 biopsies with acute rejection were negative for CD21 (0% positive) while 46 of 63 BALTs (73%) were positive for CD21, a significant difference (P-value<0.0001) and 17 were negative (27%).

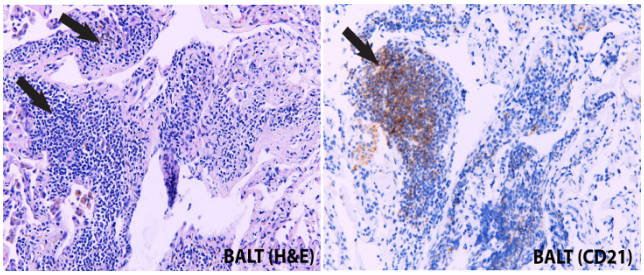

Conclusions: In lung transplant biopsies in which the perivascular/peribronchiolar inflammatory infiltrate is difficult to distinguish from the BALT, CD21 antibody may be helpful as it detects follicular dendritic cells in 3/4 of BALTs.

1924 Spread Through Alveolar Spaces: A Novel Pattern of Invasion Associated With Poor Prognosis in 411 Small (≤ 2cm) Stage I Lung Adenocarcinomas (LAdc)

Kyuichi Kadota, Jun-ichi Nitadori, Camelia Sima, David Jones, William Travis, Prasad Adusumilli. Memorial Sloan Kettering Cancer Center, New York, NY.

Background: Invasion in lung cancer is traditionally defined by tumor growing into stroma, pleura or blood vessels. We have identified a novel pattern of invasion in LAdc where tumor cells spread through alveolar spaces (STAS). This is a pattern not seen in other organ systems because of the unique anatomy of the airspaces in the lung. We investigated whether STAS correlated with a risk of recurrence according to types of surgery (limited and anatomical resection) and locations of recurrence (locoregional and distant).

Design: We reviewed resected small (≤ 2cm) stage I LAdc (n = 411; 1995-2006). Tumor STAS was defined as isolated tumor cells within alveolar spaces separate from the main tumor, and was composed of 3 morphological patterns: micropapillary structures, solid nests, and single cells. Differences in recurrence-free probability (RFP) between groups were examined using logrank test. Multivariate analyses were performed using Cox proportional hazards regression.

Results: STAS was observed in 155 cases (38%). In limited resection group (n = 120), the RFP for any recurrence of patients with STAS-positive tumors was significantly lower than STAS-negative tumors (5-year RFP, 52% vs. 88%; $P < 0.001$; Fig.1A); and STAS significantly correlated with a risk of distant ($P = 0.011$; Fig.1B) and locoregional recurrence ($P < 0.001$; Fig.1C). By contrast, in anatomical resection group (n = 291), STAS was not associated with any ($P = 0.48$) or distant recurrence ($P = 0.65$). On multivariate analysis, STAS independently correlated with a risk of recurrence (HR, 3.34; $P = 0.005$) after adjusting for tumor size (HR, 4.28; $P = 0.051$) and vascular invasion (HR, 2.16; $P = 0.053$) in limited resection group.

Figure 1 Recurrence-free probability by STAS in limited resection group

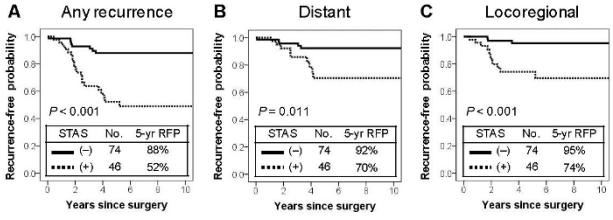

Conclusions: STAS is a significant risk factor for recurrence in small LAdc treated with limited resection. It is an under-recognized pattern of invasion with adverse prognostic significance. It may be appropriate to consider reporting STAS along with vascular invasion and visceral pleural invasion in LAdc resection synoptic reports. It may help clinicians make clinical decisions on postoperative therapies, such as adjuvant chemotherapy and completion of anatomical resection among patients treated with limited resection.

1925 Thymic Carcinomas Associated With Epstein-Barr Virus: A Clinicopathologic Study

Nooshin Karamzadeh Dashti, Marie Christine Aubry, Eunhee Yi, Daniel Visscher, Yolanda Garces, Stephen Cassivi, Julian Molina, Anja Roden. Mayo Clinic, Rochester, MN.

Background: Epstein-Barr virus (EBV)-associated thymic carcinomas (TCa), considered a subset of lymphoepithelioma-like carcinomas, are rare and usually have a poor prognosis. Because their chemotherapeutic protocol differs from other TCa, its distinction is important. We systematically reviewed our TCa to identify clinical, morphologic and immunophenotypic features that might prompt the consideration of the diagnosis.

Design: Medical records and slides from pts treated for TCa at Mayo Clinic Rochester (1953-2014) were re-reviewed. 28 cases were previously reported (Roden et al. 2013). Tumors, classified according to WHO and staged using TNM, were stained with CK5/6 and/or p40 antibodies. EBV-encoded DNA was detected by in situ hybridization (ISH).

Results: Findings of 37 pts with TCa are summarized in Table 1. EBV-ISH was positive in 3 cases (8.1%) who presented with chest pain (n=3), shortness of breath (n=2), weight loss (n=1), cough (n=1) and/or back pain since childbirth (n=1). The tumors were of moderate (n=1) or poorly (n=2) differentiated morphology. All underwent neoadjuvant and/or adjuvant therapy.

TCa	EBV+ (n=3)	EBV- (n=34) a
Age,median (range)	22 (19-31)	52 (30-81)
Male:Female	2	1.4
RacebCaucasian Asian African AmericanUnknown	2 (66.7) 1 (33.3) 00	22 (64.7) 1 (2.9) 2 (5.8) 9 (26.5)
Tumor size,cm,median (range)	14 (10-16.6)	6.7 (2.5-23)
Complete resectionb	2 (66.7)	18 (56)
StagebIIIIIIIV	0003 (100)	04 (11.7) 13 (38.2) 17 (50)
Lymphocyticinfiltrateba) Surroundingtumor cell nestsNoneMildModerateSevereb) Median% lymphocytes within tumor cell nests (range) CK5/6+and/or p40+bGranulomabNecrosisb	003 (100) 045 (20-65) 3 (100) 1 (33.3) 0	17 (51.5) 12 (36.4) 4 (12.1) 03 (0-30) 27 (81.8) 010 (30.3)
Follow up time,years (range)	3.3 (0.8-4.2)	2.3 (0.2-11.5)
Recurrence/metastasisb	3 (100)	17 (51.5)
Deathb	0	21 (63.6)

[a]Nohistory in N=1;[b]N(%cases)

Conclusions: We show that EBV+ TCa comprise 8% of TCa and are commonly of higher stage at time of diagnosis. Although these tumors have a moderate peritumoral and usually higher intratumoral lymphocytic infiltrate, these features overlap with other TCa. Therefore, suspicion for EBV+ TCa should be low in young pts with large TCa that express CK5/6 and/or p40 and have a moderate lymphocytic tumor infiltrate.

1926 Patterns of Parenchymal Fibrosis in Post-Transplant Transbronchial Lung Biopsies From Patients With Restrictive Allograft Syndrome

Shirin Karimi, Masaaki Sato, Heidi C Roberts, Cecilia Chaparro, Lianne Singer, Thomas Waddell, Shaf Keshavjee, David Hwang. University Health Network, Toronto, ON, Canada.

Background: Restrictive Allograft Syndrome (RAS) has recently been described as a specific from of chronic lung allograft dysfunction (CLAD), characterized functionally by restrictive ventilatory deficits, and histologically by a constellation of features including pleuroparenchymal fibroelastosis and interstitial fibrosis. RAS is commonly preceded by acute lung injury, which may often be seen in post-transplant transbronchial lung biopsies (PTxTBLB) of patients developing RAS. However, the frequency with which features diagnostic of RAS may be identified in PTxTBLB is not known. We therefore reviewed PTxTBLB of patients with RAS, to characterize the presence of parenchymal fibroelastosis and other forms of fibrosis in these samples.

Design: We retrospectively reviewed PTxTBLB specimens from 13 patients with histologically confirmed RAS, transplanted at our institution between March 2003 and June 2011. Thirty-eight controls PTxTBLB matched for time post-transplant were also reviewed. The H&E and elastic trichrome slides of all specimens were assessed for histologic patterns of lung parenchymal fibrosis. All slides were reviewed by two pathologists with pulmonary expertise.

Results: A total of 41 PTxTBLB from 13 RAS patients were available for review. Of these, 5 cases from 5 patients demonstrated features of parenchymal fibroelastosis, characterized by patchy but confluent deposition of hypocellular collagen with marked thickening alveolar septae. Nine cases demonstrated focal intra-alveolar organizing fibrosis, and 9 cases demonstrated interstitial/septal fibrosis with a non-specific appearance and 6 cases demonstrating both patterns of fibrosis. The majority of PTxTBLB (29/41) showed at least one pattern of fibrosis. We found no parenchymal fibrosis in the controls but two control cases showed focal peribronchial fibrosis with features suggestive of previous biopsy sites.

Conclusions: Features of pleuroparenchymal fibroelastosis and lung parenchymal fibrosis are frequently present in the PTxTBLB of patients who develop RAS. Further studies to assess the significance of fibrosis in PTxTBLB are warranted.

1927 Potential for Next Generation Sequencing To Identify Therapeutic Targets in EGFR Mutation/ALK Rearrangement-Negative Lung Cancer

Matthew Keeney, Anup Tilak, Ramakrishna Sompallae, Natalya Guseva, Aaron Bossler. University of Iowa, Iowa City, IA.

Background: Next generation sequencing (NGS) is a sensitive, rapid method for detecting mutations in many genes simultaneously. The goal of this study was to identify potential genomic signatures involving genes other than *EGFR* and *ALK* in patients with lung cancer which could be used as therapeutic targets or prognostic markers. In addition, we sought to correlate the mutational profiling results of lung cancer tumors with clinical history, survival and response to therapy.

Design: Formalin-fixed paraffin-embedded tissue specimens from patients diagnosed with lung cancer which did not have *EGFR* mutations or *ALK* rearrangements identified by Sanger sequencing or fluorescence in situ hybridization, respectively, had DNA sequencing targeting a 50 gene mutation panel (PGM, Ion Torrent/Thermo Fisher).

Clinical and pathological data including stage at time of diagnosis, survival, histologic subtype, age, smoking status and therapy were retrieved from the electronic medical record and tabulated.

Results: A total of 40 patient samples from 20 men and 20 women, 50-90 years of age (average 66.5 years) were analyzed. Of these 40 patients, 22 are deceased with survival times ranging from 0.5-21 months (average 5.5 months) and three were lost to follow-up. All but one patient had a smoking history with reported pack-years ranging from 5 to 105 (median 40 pack-years). Exon mutations were identified in *TP53* (18), *KRAS* (13), *MET* (9), *STK11* (6), *APC* (4), *SMAD4* (4), *RB1* (4), *RET* (3), *NRAS* (2), *PIK3CA* (2), *GNAQ* (2), *ATM* (2) and one each in *ERBB2*, *ABL1*, *AKT1*, *ALK*, *BRAF*, *CTNNB1*, *ERBB4*, *FGFR3*, *FLT3*, *IDH2*, *PTPN11*, *SMARCB1* and *VHL*. Of the 82 mutations identified, 24 conferred potential eligibility for open clinical trials (as identified on clinicaltrials.gov on 9/18/14), four were found in potential therapeutic targets based on preclinical trials, seven were negative prognostic indicators and one could have been included in a clinical trial which was terminated in 2013 due to lack of accrual.

Conclusions: Molecular-based therapies are limited to a minority of patients with adenocarcinoma of the lung who often present with late-stage disease and have a very poor survival.

A plethora of mutations can be identified in lung cancer cases with normal *EGFR* and *ALK* genes, many of which add clinically relevant data including valuable prognostic information and the potential eligibility of some patients for clinical trials.

NGS is a valuable tool in the management of patients with lung cancer.

1928 Giant Cell Interstitial Pneumonia (GIP) Is Not Specific for Hard Metal Lung Disease

Andras Khoor, Anja Roden, Francisco Alvarez, David Erasmus, Jorge Mallea, Cesar Keller. Mayo Clinic, Jacksonville, FL; Mayo Clinic, Rochester, MN.

Background: Although rare cases with no apparent hard metal or cobalt dust exposure have been reported, GIP is currently considered pathognomonic for hard metal lung disease by most experts.

Design: The aim of this study was to further explore the association between GIP and hard metal lung disease. Our surgical pathology files were searched for explanted lungs with the histologic diagnosis of GIP. After confirmation of the histologic diagnosis, the clinical history was reviewed and mass spectrometry and analytical scanning electron microscopy (SEM) data were obtained on the lung tissue.

Results: Between 2001 and 2014, 443 lung transplants were performed at our institution. Out of the 443 cases, 3 met histologic criteria for GIP. These cases showed bronchiolocentric chronic interstitial pneumonia with fibrosis, alveolar macrophage accumulation, and numerous intraalveolar multinucleated giant cells with emperipolesis. Multinucleated giant cells of Type II pneumocyte origin, as confirmed by immunohistochemistry for TTF-1, were also present. The occupational history and analytical data are summarized in the table.

Case	Age	Sex	Occupational history	Mass spectrometry	SEM
1	36	Male	Firefighter	Undetectable cobalt and tungsten	No cobalt or tungsten particles
2	58	Male	Welder	Elevated cobalt, undetectable tungsten	No cobalt or tungsten particles
3	45	Male	Environmental inspector	Undetectable cobalt and tungsten	Pending

All three patients are alive 33, 31 and 3 months after transplant, respectively. Interestingly, repeated post-transplant biopsies showed recurrence of GIP in patient 1.

Conclusions: All three patients had relatively nonspecific occupational histories and only one patient had a detectable cobalt level in the lung tissue. These findings suggest that GIP is not limited to patients with hard metal exposure and other environmental exposures may lead to the same histologic pattern.

1929 Architectural Differences Between Typical and Atypical Carcinoids of the Lung and Their Prognostic Significance

Ihab Lamzabi, Lauren Rosen, Richa Jain, Aparna Harbhajanka, Sahr Syed, Vijaya Reddy, Paolo Gattuso. Rush University Medical Center, Chicago, IL.

Background: Well differentiated pulmonary neuroendocrine tumors (NETs) consist of typical (TC) and atypical carcinoid (AC). They are subdivided by World Health Organization (WHO) based on mitoses and necrosis into grade 1 (TC) and grade 2 (AC). However, 10 to 20% of patients with TC die of disease within 5 years and literature regarding the histologic characteristics of these "high-risk" well-differentiated NETs is limited. To improve our recognition of higher risk subgroups of TC and AC, we therefore investigated a cohort of cases using objective and thorough histologic criteria.

Design: We searched our electronic surgical pathology records to identify cases of TC and AC. Only resection specimens, tumors larger than 0.5 cm and cases with available H&E slides were included. The H&E slides were blindly reviewed separately by 2 pathologists for an exhaustive list of histologic features.Tumor grade was also reassessed according to the most recent WHO classification. Statistical analysis was performed with Spearman correlation (SPSS software). Architectural findings are reported in this abstract.

Results: Fifty cases including 35 TC and 15 AC were blindly reviewed. Compared to TC, AC were more likely to show nested growth pattern (p=0.001), and have more infiltrative outlines (p=0.01), and prominent permeation of adjacent lung (p=0.002). Typical carcinoid were more likely to show with capsule (p=0.02) and have a trabecular growth pattern (p=0.004).

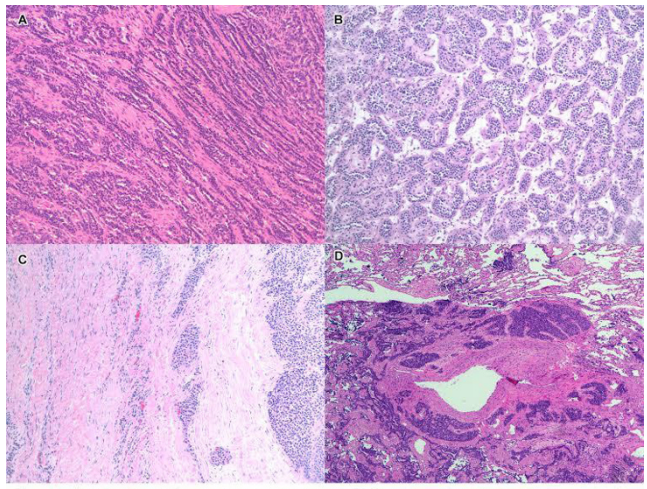

Figure 1. A) Trabecular growth pattern in a typical carcinoid, B) Nested growth pattern in atypical carcinoid, C) Infiltrative margin in atypical carcinoid, D) Permiative margin in atypical carcinoid.

Lymph node metastasis correlated with number of mitoses (p=0.01), presence of necrosis (p=0.008), permeation of adjacent lung (p=0.007). Distant metastases correlated with mitoses (p<0.001), necrosis (p<0.001), and nested growth pattern (p=0.001).

Conclusions: AC seems to show distinct architectural features with prominent nested pattern, and permeation of adjacent lung. These architectural characteristic correlated with lymph node and distant metastasis and may help stratify patients with either TC or AC into low and high risk categories.

1930 EGFR, C-Met and Axl Expressions as Predictive Factors of Tyrosine Kinase Inhibitor Response in EGFR Mutated Lung Adenocarcinomas

Sylvie Lantuejoul, Julie Gervasoni, Anne McLeer, Frederic Fina, Linda Sakhri, Florence de Fraipont, Helene Nagy-Mignotte, Denis Moro-Sibilot, Elisabeth Brambilla. CHU, Grenoble, France; Genetics and Molecular Plateform INCa, Grenoble, France; Thoracic Oncology, CHU, Grenoble, France; INSERM U823/UJF, Grenoble, France; APHM, Marseille, France.

Background: Adenocarcinoma is the most common lung cancer and nearly 10% present EGFR mutations, the most common being exon 21 mutation and exon 19 deletion. These EGFR mutations are correlated with response to tyrosine kinase inhibitors (TKI) and are detected by DNA sequencing, immunohistochemistry showing a variable sensitivity. Mechanisms of acquired or *de novo* resistance to TKI mainly involve T790M mutation, C-Met amplification or AXL activation. Objective of this study is to evaluate the sensitivity and specificity of antibodies targeting specifically EGFR mutations, and to determine if T790M mutation, C-Met or AXL overexpressions before treatment could predict TKI response or resistance.

Design: EGFR, C-Met and AXL expressions were compared by immunohistochemistry in 40 tumors exon 19 deleted and in 29 tumors mutated exon 21, with 48 adenocarcinomas EGFR wild-type. For EGFR antibodies, tumors were considered as positive when more than 10% of the cells were positive. For C-Met and AXL, high scores (≥ 50% positive cells 2 and 3 + intensity) were considered as positive. Mutations were detected by pyrosequencing.

Results: Sensitivities of the EGFR exon 19 mutant–specific antibody and EGFR exon 21 mutant specific antibody were 75% and 86%, respectively; both specificities were of 93.5%. High levels of C-Met expression were observed in 35% of exon 21 mutated EGFR cases (10/29), and in 25% of exon 19 EGFR deleted cases (10/40); the frequency of AXL high expression was the same in both groups (31% and 32%). Among the 23 patients TKI treated, for one patient with complete response, no T790M mutation, C-Met hyperexpression or AXL expression was observed; for 5 patients with stable diseases, a high AXL expression was observed in 2 tumors; in contrast, for patients with partial response (n=11) or progression (n=6), T790M mutation was observed in 5 cases, C-Met overexpression in 5 cases and high AXL expression in 5 cases. Overall, T790M mutation, C-Met hyperexpression or AXL expressions were observed in 71% patients with partial response or progression, and were mutually exclusive except for 2 patients.

Conclusions: EGFR antibodies offer a good specificity but a low sensitivity, and cannot serve as a routine diagnostic tool. In contrast, *de novo* T790M mutation, or high levels of C-Met or AXL expression can contribute to predict a partial TKI response or progression.

1931 Malignant Pleural Mesothelioma in Children and Young Adults: A Clinicopathological Study of 47 Cases

Sylvie Lantuejoul, Christelle Combaz-Lair, Nolwenn Le Stang, Anabelle Gilg-Soit-Ilg, Francoise Galateau-Salle. Grenoble University Hospital, Grenoble, France; CHU Côte de Nacre, Caen, France; Institut de Veille Sanitaire (InVS), Saint Maurice, France.

Background: Malignant pleural mesothelioma (MPM) is a rare tumour with a poor prognosis, mainly occurring in adults older than 60 years and asbestos exposed. MPM in childhood has an incidence closed to 0, and MPM in young adults has never been studied in large series with an age-specific mortality rate 0.04 per 100,000 PY in France for the years 2000-2010. The aim of our study was to evaluate the clinicopathological particularities of MPM arising in patients under 40 years, in comparison with a standard population.

Design: 47 patients, including 18 women and 29 men from 13 to 40 years, have been selected from the CNR MESOPATH/MESOBANK database- Pr F. Galateau-Caen,

France. They have been compared to a control population of 423 patients older than 60, randomly selected from the same database between 1998 and 2013. Clinical data (gender, age, risk factors such as asbestos and radiation exposure, medical histories, clinical symptoms, imaging and survival), as well as histological type (Epithelioid, Sarcomatoid, Biphasic or Desmoplastic), and immunohistochemical data were recorded and compared to the reference population. Histologic patterns, cytological features and mitotic count were also noticed in the young patients' group.

Results: There was a slight female predominance in the young population in comparison with older patients' population (38% vs 25%; p=0.05) ; young patients were less frequently asbestos exposed (58% vs 77%; p=0.01) but more often irradiated for lymphomas/leukemias and breast cancers (16% vs 6%; p=0.07); they presented less frequently with pleural effusion (77% vs 97%; p<0.0001), but more often with pleural nodules (39% vs 15%; p=0.0008). The median survival was better for younger patients (24 months vs 14 months; p=0.01). However, the distribution of the histological types was comparable in the two populations (Epithelioid; 81%, Biphasic; 10-15%, Sarcomatoid; 2-6%, Desmoplastic; 2-3%), as well as immunophenotypes. Interestingly, 14% of the tumors in young patients harboured rhabdoid features, very rarely reported in MPM.

Conclusions: MPM in young adults and children affects more often females, asbestos exposed (58%) or with a past history of irradiation for hematological or breast malignancies (16%). The overall survival appears better than for other MPM. There is no histological or immunohistochemical particularities, but rhabdoid features, rarely reported in MPM, were not infrequent.

1932 Pulmonary Myoepithelial Tumors (MT): A Pathologic and Molecular Study

Charles Leduc, Lei Zhang, Junya Fukuoka, William Travis, Cristina Antonescu. Memorial Sloan Kettering Cancer Center, New York, NY; Nagasaki University Hospital, Nagasaki, Japan.

Background: MTs of the lung (LMTs) are rare tumors which have not been well characterized morphologically and genetically. Recent studies identified *EWSR1* or *FUS* gene fusions in soft tissue MTs, and *HMGA2* or *PLAG1* rearrangements or amplifications in salivary gland MT. We investigated the pathologic and genetic features in a series of LMTs.

Design: Twelve primary LMTs were selected with myoepithelial differentiation by morphology and immunoprofile. Histologic features, including mitotic activity, cellular atypia and necrosis were recorded. Fluorescence in situ hybridization (FISH) for *EWSR1* and *FUS* was carried out on formalin fixed paraffin embedded sections. Negative cases were then tested for *PLAG1* and *HMGA2*. *EWSR1* or *FUS* rearranged cases were further tested for fusion partners *POU5F1, ZNF444, PBX1, ATF1,* and *CREB1*.

Results: Mean age was 55 years (15 to 80), with 7 females and 5 males. Four LMTs arose in large airways and 8 in the parenchyma. Histologic subtyping yielded 8 myoepitheliomas (MEs), 3 myoepithelial carcinomas (MCs), and 1 combined myoepithelial carcinoma and adenocarcinoma (MCAC). None of the tumors were encapsulated and all MCs had at least moderate nuclear atypia and focal necrosis. Mitotic counts were >5/2 mm^2 (5.6-8) in 3 of 4 MCs, and one MC had 0-1/2 mm^2, while MEs ranged from 0-2.3/2 mm^2. Genetic changes were found in 5 (42%) of cases. *EWSR1* rearrangements were seen in 3 cases (25%, 2 MCs and 1 ME). *EWSR1-ZNF444* and *EWSR1-PBX1* fusion genes were identified in the 2 MCs. An *FUS* rearrangement was identified in one ME (8.3%). The one case of MCAC showed *HMGA2* amplification, while no *PLAG1* abnormalities were detected.

Conclusions: LMTs show a wide histologic spectrum and frequently have characteristic genetic features. While elevated mitotic activity might be an indicator of high grade lesions, cytologic atypia and necrosis appear to be more reliable predictors of malignancy. Similar to soft tissue, LMTs lack encapsulation and, of the 42% of cases with molecular aberrations, the majority had *EWSR1* and *FUS* abnormalities. The only case with *HMGA2* amplification, typically associated with salivary gland origin, occurred in combination with adenocarcinoma, which might represent a histologically and molecularly distinct type of LMTs. While the clinical significance of these molecular signatures has yet to be determined, they are novel ancillary markers in the challenging diagnosis of LMT.

1933 Quantification of Architectural Patterns in Lung Adenocarcinoma: Interobserver Reproducibility in Consecutive Clinical Cases

Charles Leduc, Yuan Li, Kyuichi Kadota, Andre Moreira, William Travis, Natasha Rekhtman. Memorial Sloan Kettering Cancer Center, New York, NY.

Background: Histologic subtyping of lung adenocarcinoma, particularly identification of a predominant pattern, is currently recommended. Reproducibility has been previously comprehensively studied using photomicrographic images (Thunnissen E et al, Mod Pathol 2012), however there are still only limited data on reproducibility in complete clinical cases consisting of multiple slides (Warth A et al, Eur Respir J 2012; *Wells JM et al, Mod Pathol suppl 2012*).

Design: All tumor slides (average 5, range 2-10) from 20 consecutive prospectively-encountered resected adenocarcinomas were reviewed by 6 pathologists with experience in lung pathology. For each case, reviewers assigned a percentage, in increments of 5%, of the following 6 patterns: lepidic, acinar, papillary, micropapillary, cribriform, and solid, and selected a single predominant pattern.

Results: The number of patterns identified per case averaged 3.9 (range 2-6). Complete agreement among 6 reviewers on a predominant pattern was achieved in 4/20 (20%) cases, and 5 of 6 reviewers agreed in 10/20 (50%) cases. In pairwise comparison, agreement on predominant pattern between 2 reviewers ranged from 35-75%. On average, predominant pattern exceeded other patterns by 29%, but in 30% of scores this difference was ≤10%. In cases with complete agreement, the amount of predominant pattern exceeded other patterns by an average of 46%, compared to an average of 25% in cases without complete agreement (P<0.0001). There was no difference in the average number of slides for cases with or without complete agreement (5.5 vs 5.6, respectively; P=0.865). Overall, there was greater variability in quantitation of acinar, papillary and micropapillary than lepidic, cribriform and solid patterns (P=0.0007).

Conclusions: Lung adenocarcinomas are highly heterogeneous histologically, as reflected by the high number of patterns identified per case. We find that close co-dominance of more than one pattern may occur in up to one third of cases, and this feature correlates with low reproducibility in selecting a single predominant pattern among reviewers. On the other hand, the wide range of agreement in pairwise comparison and the variability in quantifying patterns suggests that further refining the morphologic definitions and group training sessions could improve reproducibility.

1934 Organizing Pneumonia in Wedge Biopsies of the Lung: Does Bronchiolocentric or Interstitial Location Correlate With Clinical Findings?

Teklu Legesse, Jennifer Collins, Ellen Marciniak, Nevins Todd, Seth Kligerman, Allen Burke. University of Maryland Medical center, Baltimore, MD.

Background: Organizing pneumonia (OP) has many causes, and may plug bronchioles (bronchiolitis obliterans organizing pneumonia, BOOP) or have no apparent association with airways. The use of the terms "BOOP," "idiopathic BOOP," "OP," and "cryptogenic organizing pneumonia" (COP) is not completely standardized. We undertook a retrospective study to determine the frequency of bronchiolocentric v. interstitial organizing pneumonia with emphasis on underlying associations.

Design: 40 open biopsies over a 12-year period with the diagnosis of "organizing pneumonia" were retrospectively reviewed. Clinical data, including pulmonary function tests, follow-up, serologic tests, and thoracic computed tomographic imaging were collected, resulting in 3 clinical groups: idiopathic (cryptogenic) organizing pneumonia (I-OP), organizing pneumonia associated with autoimmune diseases (A-OP), and presumed post-infections organizing pneumonia (P-OP). Independently, the numbers of loose fibroblastic nodules, distribution of OP (interstitial only, predominantly interstitial, and predominantly bronchiolocentric with luminal plugs), and extent of bronchiolar inflammation were semiquantitated without knowledge of clinical grouping.

Results: There were 15 cases of I-OP, 14 cases of A-OP, and 11 cases of post-infectious OP. Autoimmune diseases included undifferentiated connective tissue disease (n=6), rheumatoid arthritis (n=2), dermatomyositis (n=3), granulomatous polyangiitis (n=1), scleroderma / polymyositis (n=1), Crohn's disease (n=1). 17 patients were women and 23 men, with a mean age of 54; A-OP and post-infectious OP were younger than I-OP patients (p=0.04). There were 15 biopsies with only interstitial OP, 22 with predominantly interstitial OP, and 3 with predominant bronchiolar plugs. There was no significant difference in the numbers of nodules across groups. There was a positive association between bronchiolar location and patients with autoimmune disease (p=.01). Bronchiolitis and peribronchiolar metaplasia were more extensive in A-OP than I-OP and post-infectious OP (p=0.02).

Conclusions: Bronchiolocentric OP and bronchiolar inflammation is relatively extensive in OP associated with autoimmune disease. It may be useful to maintaining separate designations for "BOOP" and "OP" as the rate of underlying diseases differs.

1935 A New EGFR L858R Specific Rabbit Monoclonal Antibody for Immunohistochemical Application

Aihua Li, Yuekai Zhang, Hongyang Pan, Jackie Chan, Shyh-Chang Chen, John Wang, Chi-Kuan Chen, Johan Chien, Daniel Lin, Taiying Chen. Epitomics – an Abcam Company, Burlingame, CA; Taichung Veterans General Hospital, Taichung, Taiwan; Mackay Memorial Hospital, Taipei, Taiwan; Hong Jing Biotechnology Inc (FemtoPath), Taipei, Taiwan.

Background: Determining EGFR mutation status is valuable for lung cancer patients in selecting treatment regimens. However, genetic testing remains costly and time-consuming. Due to the challenging nature of developing mutation specific antibodies, only a few EGFR L858R monoclonal antibodies exist for immunohistochemical (IHC) testing. Here we report a new EGFR L858R RabMAb developed by utilizing the RabMAb® technology, designated as clone EP344. The concordance of the IHC staining results with EGFR L858R mutation status was analyzed.

Design: Rabbits were immunized with EGFR L858R peptide. Sera collected from immunized rabbits were screened by ELISA, WB and IHC. Hybridoma was generated by fusing splenocytes with the fusion partner cell line (240E-W2). Antibody from final hybridoma cell line was further characterized by extensive IHC testing using formalin fixed paraffin embedded (FFPE) human normal, tumor and EGFR L858R mutant tumor tissues. EGFR L858R gene mutation was detected by FemtoPath (Patent No. P2708-TW) or Sanger dideoxy sequencing (ABI 3730) mutation analysis. The concordance of EP344 IHC staining results with mutation status was analyzed and compared against EGFR L858R rabbit monoclones SP125 and 43B2.

Results: A 175 KDa EGFR L858R protein was detected by WB in EGFR L858R mutant H1975 cells, but not in wild type cells. IHC analysis of EP344, SP125 and 43B2 on human tissue microarray (TMA) comprising 16 types of normal tissues showed that all 3 antibodies stained negatively in all normal cells. In two tumor TMAs comprise of 16 types of tumors showed that 3 in 16 lung adenocarcinomas and 2 in 21 lung squamous carcinomas are positive with all 3 antibodies. EP344 is negative in all other tumors, while SP125 and 43B2 positive staining was found in breast carcinoma with EGFR wild type. Furthermore, a separate group of 13 lung carcinomas with EGFR L858R mutation was stained with all antibodies. We found that the concordance of EP344, SP125 and 43B2 staining results with mutation status was 92.3%, 77% and 23% respectively.

Conclusions: RabMAbs anti-EGFR L858R, clone EP344 is specific and sensitive in the detection of target mutant proteins by IHC in FFPE tissues. EP344 is highly concordant with EGFR L858R mutation status. Comparing to current EGFR L858R antibodies, EP344 may be a potentially better tool for predicting EGFR L858R mutation status by IHC testing.

1936 PHLDA2 Is a Key Oncogene-Induced Negative Feedback Inhibitor of EGFR/ErbB2 Signaling Via Interference With AKT Signaling

Guangyuan Li, Xiaoqi Wang, Sanjay Koul, Rieko Ohki, Matthew Maurer, Alain Borczuk, Balazs Halmos. University Hospitals of Case Medical Center, Cleveland, OH; Herbert Irving Comprehensive Cancer Center, New York, NY; Columbia University Medical Center, New York, NY; National Cancer Center Research Institute, Tokyo, Japan.

Background: EGFR and ErbB2 are two key oncogenic members of the HER family involved in multiple different cancers. The major downstream pathways governing modulation of EGFR/ErbB2 oncogenic pathways remain partially understood. Via several transcriptional profiling studies we identified a key group of early EGFR/ErbB2 target genes including PHLDA2 which is capable of binding phosphatidyl inositol signaling intermediates and thereby might directly modulate AKT signaling.

Design: To validate that PHLDA2 is immediately regulated by EGFR/ErbB2 inhibition, quantitative RT-PCR and Western blotting analysis were performed. The level of PHLDA2 and AKT activation via IHC for p-AKT were analyzed in 117 annotated primary NSCLC tissue sections and 11 normal lung samples to serve as controls represented in 3 TMAs. Association of PHLDA2 expression and AKT activation was determined.

Results: We showed that PHLDA2 as a robustly induced, novel downstream target of oncogenic EGFR/ErbB2 signaling. The level of PHLDA2 protein expression correlates positively with AKT activation in human lung cancers (correlation coefficient=0.336, p=0.0002) corroborating our data that PHLDA2 is induced upon oncogenic activation and might serve as a biomarker for AKT pathway activation. We also showed that PHLDA2 overexpression inhibits AKT phosphorylation while decreased PHLDA2 expression mediated by siRNA interference increases AKT activity. In further studies we find that PHLDA2 competes with the PH domain of AKT for binding of membrane lipids, thereby directly inhibiting AKT translocation to the cellular membrane and subsequent activation. Indeed, PHLDA2 overexpression suppresses anchorage-independent cell growth and decreased PHLDA2 expression results in increased cell proliferation and reduced sensitivity to targeted agents of EGFR/ErbB2-driven cancers demonstrating functional relevance for this interaction.

Conclusions: PHLDA2 expression is immediately and strongly regulated by EGFR/ErbB2 signaling and inhibits cell proliferation via repressing AKT activation in lung cancers in a negative feedback loop. Our studies demonstrate a novel action for PHLDA2 as an AKT inhibitor with translational implications and highlight PHLDA2 expression as a potential biomarker for AKT pathway activation.

1937 Psammoma Bodies in Lung Adenocarcinoma: Incidence and Association With ALK/ROS1/RET Fusions

Yuan Li, Xuxia Shen, Rui Wang, Haichuan Hu, Haiquan Chen, Sanjay Mukhopadhyay. Fudan University Shanghai Cancer Center, Shanghai, China; Cleveland Clinic, Cleveland, OH.

Background: The incidence and significance of psammoma bodies in lung adenocarcinomas is unknown. Recent studies have reported a high incidence of psammoma bodies in tumors with ALK, ROS1 or RET fusions. The aim of this study was to determine the incidence of psammoma bodies in lung adenocarcinomas, and examine their association with histologic patterns and oncogenic drivers.

Design: Comprehensive histologic subtyping of 648 resected lung adenocarcinomas (United States 364, China 284) was performed. The presence of psammoma bodies was noted, and the predominant histologic pattern was recorded. All cases from China had been tested for EGFR, ALK, KRAS, ROS1 and RET. They included 48 fusion-positive (23 ALK-pos, 9 ROS1-pos, 16 RET-pos) tumors and 230 fusion-negative tumors (27 EGFR-pos, 20 KRAS-pos, 183 pan-negative). The incidence of psammoma bodies in fusion-positive and fusion-negative adenocarcinomas was compared.

Results: The incidence of psammoma bodies in resected lung adenocarcinoma was 7% in the US cases (27/366) and 17% in China (46/278). In the 27 US cases with psammoma bodies, the predominant histologic patterns were acinar (13), micropapillary (12), solid (1) and lepidic (1). Most (25/27) had a micropapillary component. In the 46 Chinese cases with psammoma bodies, the predominant histologic patterns were acinar (23), micropapillary (9), mucinous (6), solid (5), papillary (2) and lepidic (1); most (38/46) had a micropapillary component. Psammoma bodies were more common in tumors with any micropapillary component than in tumors lacking a micropapillary component ($p<0.001$). In the Chinese cases, psammoma bodies were found in tumors positive for ALK (13/23, 57%), ROS1 (3/9, 33%), RET (8/16, 50%), EGFR (5/27, 19%) and KRAS (1/20, 5%), and were uncommon in pan-negative tumors (16/183, 9%). Lung adenocarcinomas with psammoma bodies were significantly more likely to contain a mutation or fusion ($p<0.0001$), and significantly more likely to be fusion-positive (ALK-pos/ROS1-pos/RET-pos) than fusion negative (EGFR-pos/KRAS-pos/pan-neg) ($p<0.001$).

Conclusions: The incidence of psammoma bodies in lung adenocarcinomas is 7-17%, and is higher in China than the United States. Most lung adenocarcinomas with psammoma bodies have a micropapillary component, and are likely to harbor an oncogenic driver mutation or translocation. There is a strong association between psammoma bodies and oncogenic fusions (ALK/ROS1/RET).

1938 Distribution of p40 and TTF-1 Expression in Lung Adenocarcinomas With Solid Growth Patterns: Implication for Diagnosis on Small Biopsy Samples

Sandy Liu, Borislav Alexiev, Allen Burke. University of Maryland, Baltimore, MD.

Background: Poorly differentiated carcinomas are difficult to subclassify on small biopsy samples. For conservation of tissue, a minimum of immunohistochemical stains, limited to p40 and TTF-1, has been recommended. The role of sampling in small biopsy samples may be especially important if focal staining for either antigen is present. Because adenocarcinomas may express both TTF-1 and p40, discordant patterns of staining may represent a potential pitfall in diagnosis due to tumor heterogeneity.

Design: 41 solid adenocarcinomas were stained with TTF-1 and p40, with determination of staining distribution and extent for both antibodies. Tumors were sub-classified into adenocarcinoma with focal cribriform areas (diagnosis based on architecture, group A); adenocarcinoma with scattered mucin vacuoles without cribriform growth (group B); and solid adenocarcinoma without cribriform areas or mucin vacuoles, with TTF-1 expression (group C). Potential misdiagnosis on limited sampling was determined if there were significant areas of discordance of TTF-1 and p40 expression.

Results: There were 19 group A, 12 group B, and 10 group C tumors. Of group C tumors, 4 showed squamoid features, 2 had prominent desmoplasia, 2 rhabdoid features, and 2 prominent nested pattern. The mean percentages of TTF-1 positive cells in group A, B, and C were 81.8%, 32.1%, and 60.5% respectively ($p=0.0026$, ANOVA). 31 tumors were negative for p40 (85%); of these, 12 (29%) showed TTF-1 staining in ≤ 50% of tumor cells. Of these 12, diagnosis of adenocarcinoma was made on focal TTF-1 staining in 5, and focal mucin vacuoles in 7; none showed cribriform growth. 6 tumors expressed p40; of these, 2 showed discordant staining, with approximate equal staining of both antigen; 2 showed very focal p40 staining, and 2 showed concordant TTF-1 and p40 staining.

Conclusions: Based on extent of TTF-1 and p 40 staining, 5 tumors in this series may have been diagnosed on biopsy as non-small cell, NOS, because of focal TTF-1 stainin, and 2 may have been misdiagnosed as squamous based on sampling of p40 positive and TTF-1 negative areas. Therefore, the rate of imprecise diagnosis of non-small cell carcinomas could have been as high as 12% (missing TTF-1 positive areas) and incorrect diagnosis of squamous carcinoma in up to 5% (discordant staining). 17% would have required the finding of intracytoplasmic mucin vacuoles. These findings suggest a low rate of misdiagnosis (5%) if p40, TTF-1 and mucin staining is performed on small biopsy samples of lung carcinomas with solid growth.

1939 Programmed Death Ligand1 (PD-L1) Expression in a Cohort of 65 Pleural Malignant Mesotheliomas (MMs), Lymphohistiocytioid MMs Compared To Conventional MMs

Celine Lize-Dufranc, Nolwenn Le Stang, Julien Pontoizeau, CNR MESOPATH Panel, Anabelle Gilg Soit Ilg, Francoise Galateau-Salle. CHU, Caen, Normandy, France; French National Health Institute, Saint Maurice, Ile de France, France.

Background: Malignant mesotheliomas (MMs) have dismal prognosis and no effective treatment to date.

Immuno-therapeutic approaches targeting PD-1 or its primary ligand, PD-L1, and their predictive biomarkers, such as tumor PD-L1expression are of great interest. Previous human studies and mouse model data suggest a high expression of PD-L1 in MMs. In addition, it is suggested that PD-L1 expression could be linked to the quantity of tumor infiltrative lymphocytes (TILs).

Herein we investigated PD-L1 expression in a series of lymphohistiocytioid malignant mesotheliomas (LHMMs) compared to conventional malignant mesothelioma types(CMMs), and its relationship with the number of TILs and their PD-1 expression.

Design: 64 formalin-fixed paraffin-embedded (FFPE) pleural MMs were retrieved from the MESOPATH files. Twenty nine LHMMs and 35 CMMs (28 epithelioid, 6 biphasic, and 1 Sarcomatoid) were strictly ascertained according to the French standardized certification. PD-L1 (3F2.1) and PD-1 (NAT) expressions were evaluated immunohistochemically. According to previous studies PD-L1 positivity was considered when ≥5% membrane cell staining was observed. PD1 expression in TILs was evaluated by percent of cytoplasmic positive staining on lymphocytes within the tumor. TILs quantity was scored from 0 to 3 by quarters of 25% of cells within the tumor.

Results: A total of 69% (44/64) cases were positive for PD-L1. LHMMs tended to be less PD-L1 positive (17/29; 59%) than CMMs (27/35; 77%) ($p=0.11$). Surprisingly, PDL1 positive MMs had a better overall survival at 2 years, confirmed in multivariate analysis (adjusted for histologic type, age, and necrosis) with 2 times less risks of death for PD-L1 positive patients (RR adjusted =0.4; IC [0.212-0.769]). PD-L1 had a tendency to be less expressed in TILs rich tumors. PD-1 was more expressed in PD-L1 positive tumors ($p=0,005$) with a negative predictive value of PD-L1 for PD-1 of 100% (9/9), and a positive predictive value of 54% (14/26).

Conclusions: MMs have a high rate of PD-L1 expression (69%). Unexpectedly, LHMMs are less often positive for PD-L1 than CMMs (59% vs 77%). Moreover, in our series, PDL1 positive MMs have a better survival at 2 years, both in uni and multivariate analysis (RR adjusted=0.4; $p=0.0058$). Consequently, additional studies are mandatory for a better understanding of the PD-1/PD-L1 and TILs mechanisms in MMs and their type and subtypes. Whatever MMs could be of great interest for anti PD-1/PD-L1 therapies.

1940 Expression of Programmed Death Ligand-1 (PD-L1) and T-Cell Populations in Neoplastic and Non-Neoplastic Thymus

Alberto Marchevsky, Beatrice Knudsen, Steven Swartwood, Ann Walts. Cedars-Sinai Medical Center, Los Angeles, CA.

Background: PD-L1 inhibits activated T-cells by binding to its receptor, PD-1, on the surface of activated T-cells. The ability of tumor cells to express ligands for programmed cell death protein-1, primarily PD-L1, downregulates immunoregulation helping tumors avoid detection and allowing for tumor growth, progression, and/or metastases. Therapeutic antibodies that block the PD-1 immune checkpoint promote immune responses against tumors. Expression of PD-L1 has not been previously reported in neoplastic and non-neoplastic thymus.

Design: 12 non-neoplastic thymus, 7 thymomas (classified per WHO as 1 AB, 3 B2, 3 B3), and 3 thymic squamous carcinomas were selected from our pathology database. Selected slides were immunostained using PD-L1 antibody (clone E1L3N; Cell Signaling, Danvers MA). 17 of the 22 cases were stained by multiplex

immunohistochemistry using antibodies directed against PD-L1, CD4, and CD8 (SP35 and SP57, respectively; Ventana, Tucson AZ). Any immunoreactivity was recorded as positive. The percentage of cases positive for each antibody was recorded.
Results: PD-L1 immunoreactivity was observed in 3 (25%) of 12 non-neoplastic thymus, 5 of 7 thymomas, and 3 of 3 (100%) thymic squamous carcinomas. Non-neoplastic thymus showed a predominance of CD4+ T-cells in the cortex and predominance of CD8+ T-cells in medullary areas. In 4 of the 5 PD-L1-positive thymomas and all 3 PD-L1-positive carcinomas a predominance of CD4+ T-cells was observed. One AB thymoma showed a predominance of CD8+ T-cells in the spindle cell component.
Conclusions: - PD-L1 is expressed in 25% non-neoplastic thymus.
- PD-L1 is expressed in >70% of thymomas and thymic squamous carcinomas.
-Additional studies quantifying expression of PD-L1, PD-1 and T-cell subsets in these neoplasms by digital image analysis are needed to determine whether the PD-L1/PD-1 pathway is a potential therapeutic target for the treatment of advanced thymic neoplasms.

1941 Pathological Role of Fibroblastic Foci and Bronchiolar Epithelial Proliferation in Idiopathic Pulmonary Fibrosis (IPF)/Usual Interstitial Pneumonia (UIP)

Osamu Matsubara, Yuichi Ishikawa, Yukio Nakatani, Eugene Mark. The Cancer Institute, Tokyo, Japan; Hiratsuka Kyosai Hospital, Hiratsuka, Japan; Chiba University, Chiba, Japan; Massachusetts General Hospital and Harvard Medical School, Boston, MA.
Background: Characteristic features of IPF / UIP on histology include patchy interstitial fibrosis, active fibroblastic foci (FF), and surrounding bronchiolar epithelial proliferation (BEP). FF consist of a loose myxoid stroma and active fibroblasts and myofibroblasts which open nuclei and covered by pneumocytes or respiratory epithelial cells, and would seem to be as the sites where fibrotic responses and acute exacerbation events are initiated. Previous studies suggest that increased FF signify a worse prognosis and faster disease progression.
Design: We investigated the cellular and molecular profile of FF and bronchiolar epithelial proliferation in 27 video-assisted thoracoscopic biopsies (VATS) of IPF/UIP with 5 patients who had acute exacerbation later and a variety of control lung samples, focusing on the immunohistochemical expression of the molecules involved in FF and cellular proliferation, namely alpha-SMA, vimentin, desmin, TGF-beta1, CTGF, VEGF, E-cadherin, beta-catenin, TTF-1, napsin A, Ki-67, PCNA, cyclin D1, MMPs and TIMPs. We used a standard indirect avidin-biotin horseradish peroxidase method with various antigen retrievals. Apoptotic DNA strand break by nick end-labeling technique (TUNEL) was also examined.
Results: The spindle cells in FF expressed alpha-SMA, vimentin, as well as TGF-beta 1, CTGF and VEGF, but only faintly MMPs and TIMPs. The covering epithelium expressed TGF-beta 1 and CTGF and partially TTF-1 but had diminished expression of E-cadherin and beta-catenin. There was increased staining of Ki-67, PCNA and cyclin D1 in fibrotic cells, pneumocytes and bronchiolar cells. Apoptotic cells were not detected. There were no significant differences in the frequency of FF and the degree of BEP between the patients with and without later acute exacerbation, but more extensive accumulation of alveolar macrophages was seen in the patients with later acute exacerbation.
Conclusions: Up-regulation of markers of cell proliferation in both mesenchymal and epithelial cells at sites of FF is consistent with remodeling of lung in UIP/IPF at these sites. Overexpression of various growth factors may cause the exaggerated and proliferative character of the fibroblasts/myofibroblasts and bronchiolar epithelium that leads to architectural simplification and honeycomb fibrosis. Acute exacerbation initiation might not be related to FF lesions.

1942 BAP1 Loss Portends Improved Prognosis in Malignant Pleural Mesothelioma Due To Frequent Association With Epithelioid Morphology

Stephanie McGregor, Ryan Dunning, Duraid Hadi, Wickii Vigneswaran, Aliya Husain, Thomas Krausz. University of Chicago Hospitals, Chicago, IL.
Background: BAP1 (BRCA-associated protein 1) is a tumor suppressor that is frequently inactivated either by allelic loss or mutation in both familial and sporadic malignant pleural mesothelioma (MPM). Reports of BAP1 alteration in MPM are varied, and it is currently unclear if BAP1 inactivation occurs more commonly in any particular histologic subtype or if such loss of BAP1 carries prognostic significance. The potential for BAP1 analysis as a diagnostic tool also remains unknown.
Design: We constructed a tissue microarray (TMA) consisting of 115 MPM cases (57 epithelioid, 48 biphasic and 10 sarcomatoid; 112 surgical and 3 autopsy). H&E and immunohistochemical staining for BAP1 were performed on the TMA and 26 reactive mesothelial controls. BAP1 nuclear staining was scored as positive or negative. Fibroblasts and lymphocytes served as internal positive controls. Survival data was obtained by chart review and statistical analysis was performed using MedCalc; autopsy cases were excluded from survival analysis.
Results: BAP1 positive staining was identified in all 26 reactive mesothelial controls (100%). In contrast, staining for BAP1 was negative in 47 of 57 epithelioid (82%), 24 of 48 biphasic (50%) and 0 of 10 sarcomatoid (0%) MPM cases. Kaplan-Meier analysis demonstrated an increase in overall survival (OR 2.0433) in patients with loss of BAP1 staining (c2=9.6635, p=0.0019, 95% CI=1.1874-3.5161). However, when histological subtype was included in a Cox proportional-hazards regression analysis, BAP1 loss was no longer significant prognostically (histology: c2=13.805, p=0.0002, 95% CI=1.4569-3.0886). When only epithelioid cases were analyzed, there was a trend toward improved prognosis with loss of Bap1 that was not significant (c2=3.4619, p=0.0628, 95% CI=0.7222-6.2562).
Conclusions: BAP1 staining is reliably positive in reactive mesothelial proliferations but is frequently lost in MPM, particularly in epithelioid cases. Therefore, loss of BAP1 staining likely has utility in distinguishing malignant from benign epithelioid mesothelial cells. However, while loss of BAP1 staining is associated with a relatively favorable prognosis compared to cases with retained staining, the association does not appear to be independent of histologic subtype.

1943 Morphologic Characteristics Predictive of Outcome in Patients With Sarcomatoid Carcinoma of the Lung: A Clinicopathologic Study of 40 Cases

Mitra Mehrad, Danielle Carpenter. Washington University, St. Louis, MO.
Background: Pulmonary sarcomatoid carcinomas (SC) are a rare group of non-small cell lung carcinomas, representing a spectrum of epithelial and mesenchymal differentiation. Studies have shown that these tumors are associated with a poor prognosis independent of stage at presentation. Our goal was to evaluate the clinicopathologic features and prognostic factors of this tumor.
Design: We retrospectively retrieved consecutive patients with surgically treated SC from 1999 to 2012. Two study pathologists reviewed cases to confirm the diagnoses and to evaluate morphologic findings. Various histologic subtypes of the tumor were quantified. Clinical and survival data were obtained by chart review.
Results: A total of 40 cases were reviewed. The mean age at presentation was 71.6 years with a median of 73.5. The majority (60%) of the patients were male. The overall survival rates at 1, 2, 3 and 5 years were 56.4%, 38.4%, 30.7% and 12.8%, respectively. Based on morphologic features, the different tumor components in order of frequency included spindle cell, glandular, squamous, giant cell, large cell, rhabdoid and true sarcoma. At univariate analyses, tumor size greater than 3 cm (p value: 0.01), stage IV disease (p value 0.004) and any amount of rhabdoid component (p value: 0.003) were strongly associated with poor patient outcome. Necrosis, vascular or pleural invasion, and histologic subtypes other than rhabdoid features did not correlate with survival.
Conclusions: Although tumor necrosis and lymphvascular and pleural space invasion are important pathologic findings, they may not as significantly predict survival as stage at diagnosis and tumor size in SC of the lung, an already aggressive tumor. However, our data suggests that rhabdoid features in SC is predictive of an even more aggressive outcome in these patients and therefore need to be recognized.

1944 Pulmonary Vascular Abnormalities in Neurofibromatosis Type 1 Patients: An Autopsy Study of 8 Cases

Wadad Mneimneh, Eunhee Yi, Jay Ryu, Anja Roden. Mayo Clinic, Rochester, MN.
Background: Pulmonary abnormalities in neurofibromatosis type 1 (NF1) patients reported in the literature are relatively sparse and mainly based on clinical and radiographic findings. Although vascular changes have been reported in association with NF1, pulmonary vascular abnormalities in this setting are not well documented. Moreover, pulmonary fibrosis associated with NF1 has been debated. We systematically reviewed the histologic features in the lung tissue obtained from the NF-1 patients who underwent autopsy at our institution.
Design: Autopsy files of Mayo Clinic Rochester (1995-2014) were searched for NF-1. One case was excluded due to concurrent hemoglobin S-beta thalassemia causing extensive thromboembolic vascular disease involving the lung as well as other sites. Hematoxylin-&-eosin and Movat pentachrome stained sections of both lungs were re-reviewed in all cases. Histopathologic features of interstitial, vascular, airway and pleural changes were recorded.
Results: Eight patients (3 men) with NF-1 died at a median age of 53.5 years (range, 33-79) from sepsis (n=3), air embolism, pulmonary hypertension (PHT), dilated cardiomyopathy, massive internal hemorrhage due to post-operative dilutional coagulopathy, and malignant peripheral nerve sheath tumor (n=1, each), respectively. Two of these patients had a clinically documented PHT. Histologic findings are summarized in table 1.

Histologic Findings	Number of Patients (n=8)
Vascular changes	5
Pulmonary arteries Intimal thickening Plexiform lesions Thromboembolic lesions Medial hypertrophy	4403 (2 fresh, 1 recanalized)2
Pulmonary veinsIntimal thickeningPerivenular inflammation, patchy	554
Capillary proliferation	2
Chronic bronchiolitis, mild	3
Emphysema, minimal to mild	4
Acute bronchopneumonia	2
Malignant peripheral nerve sheath tumor	2
Silicotic nodules	1
Subpleural fibroelastosis	1

Conclusions: Our study included a limited number of cases. However, pulmonary vascular changes were the most prevalent pathologic findings (5/8 cases) identified in our systematic review of autopsy cases in patients with NF1. These showed intimal thickening in pulmonary venules. Most of these cases presented with concurrent arterial lesions characterized by myo-intimal thickening and thromboembolic disease with no plexiform lesions. No patient showed significant cellular or fibrosing interstitial lung disease.

1945 Antibody Mediated Rejection in Lung Allograft: Morphological Changes in Cryobiopsies and in One Autopsy

MAngeles Montero, Tina Osadolor, Alexandra Rice, Andrew Nicholson, Berta Saez, Cristina Berastegui, Victor Monforte. Royal Brompton and Harefield NHS Trust Foundation, London, United Kingdom; University Hospital Vall d'Hebron, Barcelona, Spain; Imperial College London, London, United Kingdom.

Background: Diagnostic criteria of antibody mediated rejection (AMR) in kidney and heart allografts are well established, however morphological criteria for AMR in lung allografts have not been agreed. The aim of this study is to present morphological changes in biopsies of patients who fulfill clinical and morphological criteria of AMR: positive donor specific antibodies, clinical and morphological lung dysfunction, and variable expression of C4D.

Design: 207 lung transplants were performed between 2009 and 2012 in University Hospital Vall d'Hebron, Barcelona, Spain. 7 out of 207 (3,4%) patients fulfilled criteria for AMR. Transbronchial cryobiopsies and one autopsy were reviewed and histopathological features were described.

Results: Diffuse and intense C4D staining was seen in 3 patients, which comprise biopsies with neutrophilic capillaritis, fibrin and interstitial haemorrhage. Interstitial and intravascular histiocytosis, thrombosis, haemorrhage and fibrin in cryobiopsies and marked arteritis and venulitis in the autopsy were noted in one patient. Negative C4D was seen in 4 patients with non-specific interstitial increase of lymphocytes and no evidence of capillaritis. Two patients with non-specific interstitial lymphocytosis evolved to restrictive allograft syndrome, one to bronchiolitis obliterans, 3 died after several episodes of AMR and 1 patient is well and alive.

Conclusions: Histological AMR in lung allograft comprises a morphological spectrum of changes inconsistently associated with immunohistochemical expression of C4D. Positive C4D staining is more frequently seen in patients with capillaritis, however damage of the capillary meshwork might be related to the loss of C4D staining.

1946 Interstitial Lymphocytic Pneumonitis as a Histological Feature in Patients With Lung Antibody Mediated Rejection

M Angeles Montero-Fernandez, Tina Osadolor, Andrew Nicholson, Berta Saez, Cristina Berastegui, Victor Monforte. Royal Brompton and Harefield NHS Trust Foundation, London, United Kingdom; University Hospital Vall d´Hebron, Barcelona, Spain; Imperial College London, London, United Kingdom.

Background: Capillaritis defined as intense septal infiltration by neutrophils and karyorrhesis, is the main histological feature of antibody mediated rejection (AMR). However, some patients with donor specific antibodies and organ dysfunction show an increase in interstitial lymphocytes in transbronchial biopsies. Our aim is to highlight this histological feature.

Design: 207 lung transplants were performed between 2009 and 2012 in University Hospital Vall d'Hebron, Barcelona, Spain. 7 out of 207 (3,4%) patients fulfilled criteria for AMR (Am J Transplantation 2004;4:1033-1041), and 4 showed interstitial lymphocytosis. Transbronchial cryobiopsies were reviewed and histopathological features were described.

Results: 4 out of 7 patients with donor specific antibodies were negative on immunohistochemistry for C4d and cryobiopsies showed a non-specific interstitial increase of lymphocytes. There was no evidence of capillaritis or histological criteria of acute cellular rejection. Infection was clinically excluded. Two patients with non-specific interstitial lymphocytosis evolved to bronchiolitis obliterans, one to restrictive allograft syndrome, and 1 died after several episodes of AMR.

Conclusions: Non-specific increase of lymphocytes in the alveolar septa is seen in patients with donor specific antibodies and allograft dysfunction. Immunohistochemistry for C4d was negative in all cases. Despite treatment, patients evolved to chronic allograft dysfunction and death in one case.

	HLA	C4d	treatment	evolution
1	Pos 20 locus	Neg	Steroids, total lymphoid irradiation (TLI)	RAS
2	Pos 3 locus	Neg	Steroids, Thymoglobulin, Basilisimab, TLI	BOS, Cellular Rejection
3	Pos 4 locus	Neg	No treatment	BOS
4	Pos 5 locus	Neg	Steroids, Bortezomib	Death

1947 Diagnostic Value of Immunohistochemical ROS1 Expression in ROS1-Lung Cancer

Noriko Motoi, Yosuke Matsuura, Hironori Ninomiya, Hiroko Nagano, Tomoyo Kakita, Sakae Okumura, Yuichi Ishikawa. The Cancer Institute, Japanese Foundation for Cancer Research, Tokyo, Japan; The Cancer Institute Hospital, Japanese Foundation for Cancer Research, Tokyo, Japan.

Background: Concerning clinical assessment of lung cancer, it is necessary to build a proper screening system for target oncogene mutations, especially for rare events, such as ALK, ROS1 and RET. This study is conducted to evaluate a diagnostic value of immunohistochemistry (IHC) for a screening of ROS1-altered lung cancer (ROS1-LC) and compared to fluorescence *in situ* hybridization (FISH).

Design: Formalin-fixed paraffin-embedded specimens of surgically resected 354 primary lung cancers; 256 adenocarcinoma (Ad, including 15 genetically confirmed ROS1-positive cases) and 98 squamous cell carcinoma (Sq), were examined by IHC using anti-ROS1 antibody (D4D6). IHC results were scored in 0,1,2, based on the combination of cytoplasmic intensity and proportion. Score 0; negative, score 1; weak intensity in any percentqge or strong intensity in less than 10% of tumor cells, score 2; strong intensity in more than 10% of tumor cells. Twenty-four IHC-positive cases (score 1 and 2) and three IHC-negative cases (score 0) were simultaneously evaluated by FISH using dual-color berak-apart style ROS1 probes. Ratio of split-positive cells were calculated by counting in 50 nuclei per case. The gene rearrangement was defined as positive when the ratio was over 30%.

Results: Score 2 of ROS1-IHC was observed in 38/0 (14.8/0%) of Ad/Sq, respectively, which included all previously confirmed ROS1-positive cases. Score 1 was observed in 102/7 (39.8/7.1%) of Ad/Sq, respectively. The score 2 positivity was not only restricted to the cancer cells, but also observed in the non-neoplastic cells. Out of 27 cases examined by FISH, three cases (11.1%) were positive, which were exclusively score 2 by IHC. The majority of IHC score 2 cases did not carry ROS1 rearrangement. Sensitivity, specificity, positive predictive value and negative predictive value of IHC in this study condition were calculated as 100/100/100/13.0%, respectively.

Conclusions: Our data suggested that ROS1-IHC could be used for a screening of ROS1-positive lung cancer. However, it should be mentioned that ROS1-rearrangement-negative lung cancer could exhibit overexpression of ROS1 protein by IHC. Further confirmation by another methods, such as FISH or sequencing, should be mandatory due to relatively high nonspecific positivity rate for a diagnostic application.

1948 Metastases To the Lung From Non-Pulmonary Carcinomas After Recurrence-Free Intervals of Greater Than 5 Years

Sanjay Mukhopadhyay, Andres A Roma. Cleveland Clinic, Cleveland, OH.

Background: A 5-year recurrence-free interval after resection for carcinoma is generally considered curative. Hence, a metastasis is thought to be unlikely if a lung mass develops after 5 recurrence-free years following resection of a non-pulmonary carcinoma. The aim of this study was to determine whether non-pulmonary carcinomas can metastasize to the lung after a 5-year recurrence-free interval, and if so, to determine the incidence and characteristics of such tumors.

Design: Our archives (2008-2014) were searched for metastatic carcinomas to the lung from non-pulmonary sites. The interval between resection and lung metastasis was determined by reviewing clinical and pathologic records. Cases were included in the study if: (1) the site of origin could be confidently determined on histologic grounds by immunohistochemistry and/or comparison of the lung metastasis with the primary tumor, (2) the recurrence-free interval between resection of the extra-pulmonary primary and subsequent lung metastasis was >5 years, and (3) there was no evidence of distant metastases at the time of initial diagnosis. Radiology reports were reviewed to determine the number of lung nodules at the time of lung metastasis.

Results: We identified 187 cases of metastatic carcinoma to the lung from non-pulmonary sites. Of these, 17 (17/187, 9%) metastasized to the lung after a recurrence-free interval of ≥5 years following definitive resection of the primary cancer. These included 4 renal cell carcinomas [interval between resection and lung metastasis in parentheses] (8-33y), 4 endometrial carcinomas (8-10y), 2 colon carcinomas (9y,13y), 2 breast carcinomas (8y,12y) and one carcinoma each of the thyroid (10y), epiglottis (12y), esophagus (8y), ovary (15y) and prostate (12y). The recurrence-free interval was greater than 10 years in 7 cases (7/187, 4%). Most (12) patients had no interval chest imaging, 4 had negative interval surveillance chest X-rays and 1 had a negative chest CT. At the time of metastasis, lung nodules were multiple in 10 and solitary in 7 (2 endometrium, 1 kidney, 1 esophagus, 1 colon, 1 epiglottis, 1 breast).

Conclusions: The possibility of metastatic carcinoma must be considered in patients with lung nodule(s) and a history of carcinoma of a non-pulmonary site, even after a recurrence-free interval of greater than 5 years. Although late metastases to the lung are uncommon, they may occur as long as 33 years after definitive resection of the non-pulmonary primary, and can present as a solitary lung mass. The most common culprits are carcinomas of the kidney and endometrium.

1949 PHGDH and TRIM29 as Novel Diagnostic Markers for Malignant Pleural Mesothelioma: An Exploring Approach From FFPE Tissue-Based Gene Expression Profiling of a Synchronous Thoracic Tumor

Tomoaki Naka, Yutaka Hatanaka, Hiromi Kanno, Kanako Hatanaka, Tomoko Mitsuhashi, Yoshihiro Matsuno. Hokkaido University Hospital, Sapporo, Japan.

Background: Despite the routine application of immunohistochemical markers in diagnostic practice, very effective ones that clearly distinguish malignant pleural mesothelioma (MPM) from primary pulmonary adenocarcinoma (PAC) or from other malignancy are still lacking. On the other hand, gene expression profiling is now feasible for the analysis on formalin-fixed paraffin-embedded (FFPE) tissues to explore novel diagnostic markers. A unique case of synchronous collision tumor consisting of MPM and PAC, with the identical genetic background, would be an excellent model for comparative gene expression analysis, hunting for novel differential markers.

Design: FFPE tissues of MPM and PAC lesions surgically resected from a 77-year-old man with a history of long-term smoking and the asbestos exposure were used. Each of these MPM and PAC lesions exhibited a typical immunophenotype and genomic alteration (calretinin+/D2-40+/9q21 loss and TTF-1+/BerEP4+, respectively). DNA microarray analysis was performed using the 3D-Gene human Oligo chip 25k (Toray) with RNA extracts from each lesion. Cell lines originated from MPM and PAC lesions were used for validation. Immunohistochemical studies were evaluated by 14 MPM (10 epithelioid type and 4 sarcomatoid type) and 15 PAC cases.

Results: According to the gene expression profiling, 54 genes indicating higher expression in MPM lesion than in PAC lesion were extracted, and we finally identified two novel MPM marker genes, *phosphoglycerate dehydrogenase (PHGDH)* and *TRIM29*. Validation assay using qRT-PCR method showed that enhanced *PHGDH* and *TRIM29* expressions were much higher in the MPM cell lines compared to the PAC cell lines. In immunohistochemical analysis with 14 MPM and 15 PAC cases, PHGDH showed higher sensitivity than calretinin (78.6% vs 71.4%). TRIM29 was equivalent to calretinin in specificity (93.3% vs 100.0%). In sarcomatoid type of MPM, much more tumors were PHGDH positive than calretinin (50.0% vs 0.0%).

Conclusions: A comparative gene expression analysis between quite different lesions with the identical genetic background allowed the exploration of novel marker molecules even from FFPE tissue. PHGDH and TRIM29 may serve as diagnostic markers for differentiating MPM from PAC, and from other malignancy.

1950 CD74-NRG1 Gene Rearrangements Appears To Be Rarer Than Reported in Cohort of Pulmonary Mucinous Adenocarcinoma

Carlos Pagan, Navneet Narula, Shivakumar Subramaniyan. Weill Cornell Medical College and New York Presbyterian Hospital, New York, NY.

Background: Pulmonary mucinous adenocarcinoma (PMA) is a subtype of lung adenocarcinomas characterized by tall columnar cells with basal nuclei and pale cytoplasm with varying amounts of mucin. Various driver mutations and oncogenic gene fusions of potential therapeutic targets have been identified in lung adenocarcinomas. The recently discovered *CD74* and neuregulin-1 (*NRG1*) gene fusion has been shown to have a higher incidence in PMA. 10 cases with *CD74-NRG1* gene fusions have been described in the literature. A majority of patients with *CD74-NRG1* are women, never smokers, with no *KRAS* mutation, and with histological features of PMA. The present study was primarily undertaken to see the frequency of CD74-NRG1 gene fusion in our cohort of PMA.

Design: 131 patients with a diagnosis of PMA from 2001 to 2013 were identified at our institution. FFPE tissue samples were available in 62 cases (22/M, 40/F, age range 50-87 yrs, mean 70.7 yrs, median 71 yrs) and were included in this study. FISH analysis was performed on tissue micro array slides using CD74-NRG1 dual color dual fusion and NRG1 and ALK dual color break apart probes. Results of mutational analysis for *EGFR, KRAS,* and *BRAF* genes were obtained from the hospital records.

Results: Of the 62 cases a rearrangement of CD74-NRG1 or NRG1 gene rearrangement were not observed in the TMA cores suggesting the rarity of *CD74-NRG1* translocations in lung adenocarcinomas. However, rearrangement of *ALK* gene was observed in 2/53 (3.8%) patients studied. These patients were also negative for *KRAS* and *EGFR* gene mutations. Interestingly, a high frequency of *KRAS* mutations were found in 19/28 (68%) patients. *KRAS* mutations were present in codon 12 (G->T – 15 cases and G->A – 4 cases) of the gene. Transversion mutations (G->T) were commonly observed in smokers (12 cases) when compared to non-smokers (3 cases). *EGFR* mutations were found in 2/30 (7%) patients. Both cases showed deletions in exon 19 and these cases did not show either rearrangement of *ALK* or *KRAS* mutation. *BRAF* mutational analysis was performed on two patients: one patient was positive for p.G12C mutation in the *BRAF* gene. This patient also had p.G12C (c.34G>T) mutation in codon 12 of the *KRAS* gene.

Conclusions: *CD74-NRG1* fusions represent a likely therapeutic opportunity for PMA. The rarity of the mutation may limit its potential as a therapeutic option. Studies on large series of lung adenocarcinomas are under way to determine the frequency of *CD74-NRG1* gene fusions in our patient population.

1951 Determination of PTEN and c-MET Status for Lung Adenocarcinoma Is Variable in Biopsy and Concurrent Excisional Specimens

Dimple Pandya, Achim Jungbluth, Natasha Rekhtman, Andre Moreira. Memorial Sloan Kettering Cancer Center, New York, NY.

Background: Targeted therapy in lung cancer is an expanding field. Molecular alterations in phosphatase and tensin homolog (PTEN) and c-MET (mesenchymal epithelial transition protooncogene) are potential therapeutic targets. Loss of PTEN expression has been associated with activation of *PIK3CA/AKT/mTOR* pathway and is associated with sensitivity to mTOR inhibitors. Amplification or overexpression of c-MET is associated with resistance to tyrosine kinase inhibitors and/or poor prognosis. Both PTEN and c-MET can be detected by immunohistochemistry. In this study we evaluated the concordance rate of both antibodies in biopsy material and subsequent excision of the same tumor.

Design: Pathology database was queried for concurrent biopsy and surgical specimens from 12/2013-7/2014. Concurrent biopsy and surgical specimens from 21 patients were reviewed to evaluate tumor histology and specimen cellularity. Immunohistochemistry with PTEN antibody clone (138G6) and c-MET antibody (clone sp44) were performed according to manufactures' instruction following a rigorous validation using positive and negative controls. PTEN staining was evaluated for complete loss of expression or retention (any cytoplasmic or nuclear stain). c-MET staining was evaluated for the intensity and extent of the staining. Positivity is defined as a strong membranous staining (2-3+) in more than 50% of the tumor cells.

Results: There was a 90% (19/21) concordance for PTEN expression between biopsy and resection (k=0.76). 6 cases showed loss of expression in the biopsy, among these cases 2 were classified as retained PTEN in the excision. In both cases the excision specimen had partial loss of PTEN. Partial loss of PTEN was seen in 3 other cases with retained PTEN in biopsy. There is a 95.2% (20/21) concordance in c-MET staining (k=0.89). In the discrepant case, the biopsy was deemed positive (2+ > 50% of tumor cells), with a negative excision (1+ >70% of tumor cells).

Conclusions: Despite a good correlation between biopsy and resection for both markers, our results show there is a greater possibility of discrepant results for PTEN than c-MET because of geographic heterogenetic of expression and scoring criteria. Therefore evaluation of PTEN and c-MET staining in biopsy material should be interpreted with caution, especially when designing clinical trials for potential therapy.

1952 Frequency of Microsatellite Instability in Mucinous Adenocarcinomas of the Lung

Kyung Park, Shivakumar Subramaniyam, Jose Jessurun, Navneet Narula. Weill Cornell Medical College, New York, NY.

Background: Microsatellite instability (MSI) occurs in about 15% of colonic adenocarcinomas. Several morphologic features have been associated with MSI including a mucinous phenotype. MSI has previously been shown to be present in approximately half of small cell lung carcinomas and about 20% of non-small cell lung carcinomas. This study was designed to investigate whether the frequency of MSI is overrepresented in mucinous adenocarcinomas of the lung (MAC).

Design: A tissue microarray (TMA) was constructed from formalin-fixed paraffin-embedded tissue blocks from fifty-eight lung resection specimens from patients with MAC. The TMA was composed of two representative cores of each tumor. Immunohistochemistry using antibodies against MLH1, PMS2, MSH2, and MSH6 was performed. Any detectable nuclear staining was considered positive and indicative of microsatellite stability. MSI deficient tumors were identified by absence of immunoreactivity.

Results: Fifty-eight patients with MAC were analyzed, 20 (34%) males and 38 (66%) females with a median age at diagnosis of 71 years (range 58-87). Concurrent loss of MSH2 and MSH6 expression was present in two (3%) patients; loss of MSH6 alone was seen in five (9%) patients. All tumors expressed MLH1 and PMS2. Six of seven (85%) patients with MSI were females. Overall the frequency of MSI in our cohort of MAC is 12%.

Conclusions: MSI as determined by immunohistochemistry is observed in 12% of MAC. A noticeable difference with colonic adenocarcinoma is universal expression of MLH1 and PMS2 in these tumors. Molecular testing will be performed to see if the loss of MSH2 and MSH6 expression is due to germline mutations or chromosomal loss (loss of heterozygosity). In addition, it remains to be determined whether MSI is predictive of a better prognosis and response to chemotherapy as is the case for colonic adenocarcinomas.

1953 Nuclear Features Predict Outcome in Pulmonary Adenocarcinomas

Adina Paulk, Sandy Liu, Borislav Alexiev, Allen Burke. University of Maryland, Baltimore, MD.

Background: The grading of lung adenocarcinomas is generally based on architectural features, such as extent of growth patterns that are associated with poor prognosis, such as micropapillary, cribriform and solid areas. The role of cytologic features has been relatively less extensively studied.

Design: We performed a retrospective study of 207 lung adenocarcinomas resected between 2003 and 2009. The tumor size, percent poor prognostic growth (solid/cribriform and micropapillary), lymph-vascular invasion, mitotic rate, and nuclear pleomorphism (based on nucleolar size) were recorded independent of knowledge of follow-up data. Overall survival and disease-specific survival (mean 66 months) were retrospectively determined by chart review, and development of lymph node or distant metastases. A grading system incorporating % poor prognostic growth, mitotic activity, and nuclear pleomorphism was designed on a three-point scale.

Results: By univariate analysis, nuclear pleomorphism (p<.0001), % poor prognostic growth (p<.0001), and mitotic rate (p=.007) correlated positively with lymph-vascular invasion. Nuclear pleomorphism was associated with distant metastasis (p=.006) and nodal disease (p= .0004) as was % poor prognostic growth (p=.02). Survival data by univariate analysis showed an inverse correlation between tumor grade and nuclear pleomorphism and disease specific survival (p<.001), with a lesser effect of % poor prognostic growth (p=.04). By multivariate analysis, nuclear grade was associated with overall survival independent of age, gender, and tumor size (p=.02).

Conclusions: Grading systems for lung adenocarcinomas should include cytologic features, especially nuclear pleomorphism, as well as growth patterns.

1954 Prognostic Significance of "Spread Through Alveolar Spaces" in Mucinous Adenocarcinomas of the Lung

Adina Paulk, Sandy Liu, Borislav Alexiev, Allen Burke. University of Maryland Medical Center, Baltimore, MD.

Background: The recently revised WHO classification of pulmonary adenocarcinomas replaces "mucinous bronchioloalveolar carcinoma" with "mucinous adenocarcinoma," and adds tumor spread through alveolar spaces (STAS), also known as "small cluster invasion", as a type of invasion. Although micropapillary patterns of non-mucinous pulmonary adenocarcinomas can overlap histologically with STAS, the former has been associated with negative prognostic factors while the clinical significance of STAS, particularly in the mucinous subset, has not been extensively studied.

Design: We retrospectively reclassified mucinous adenocarcinomas resected over a ten-year period by the WHO criteria, and correlated histologic findings, type and extent of invasion, mucin staining, and TTF-1 expression with recurrence and metastatic disease.

Results: There were 30 resections (9% of all adenocarcinomas), with a 1.3:1 female predominance. Mean age was greater in men (71 years) than in women (63 years, p=0.02). There were 2 colloid carcinomas and 28 invasive mucinous adenocarcinomas (IMA), of which 7 were entirely lepidic or minimally (< 5 mm) invasive, but classified as invasive based on size > 3 cm (n=2) or the presence of STAS (n=3). STAS was present as a combination of single cells, solid clusters, or tubules in 15 tumors, and as micropapillary structures in 7. 8 IMAs had little or no in situ component, 7 of which showed cystic (> 2mm) acinar invasive pattern. Other invasive patterns were solid / cribriform (n=11, 3 with signet ring cells), and acinar (n=13). The predominant mucin cell type was columnar with clear cytoplasm (n=14) and columnar with eosinophilic cytoplasm and intermixed goblet cells (n=16). TTF-1 was positive 13 tumors (43%), often weakly, was more frequently positive in cuboidal than in columnar cells (p<.001)

and was inversely correlated with percent of mucin positive cells (p<.001). There was no correlation between mucin cell type or TTF-1 expression and type of invasion or frequency of metastasis. STAS of all types was weakly associated with distant metastasis (p=0.07) and recurrence (p=0.08), whereas micropapillary STAS was significantly associated with distant metastasis (p=.04) and recurrence (p=.03). Tumor size was associated with lymph node metastasis (p=.03), and size of solid component with distant metastasis. (p=.01)

Conclusions: STAS is common in mucinous adenocarcinomas. The micropapillary type of STAS, as well as the size of the solid invasive component has prognostic significance in terms of metastasis and recurrence.

1955 Targeted Next Generation Sequencing of Cancer Genes Dissects the Mutation Profiles of Pulmonary Large Cell Carcinoma, Supporting the Immunohistochemistry Axiom "No p40, No Squamous"

Giuseppe Pelosi, Mauro Papotti, Giulio Rossi, Alberto Cavazza, Ugo Pastorino. Fondazione IRCCS Istituto Nazionale dei Tumori, Milan, Italy; Università degli Studi, Torino, Italy; Azienda Ospedaliero-Universitaria Pisana, Policlinico di Modena, Modena, Italy; IRCCS Azienda Arcispedale S. Maria Nuova, Reggio Emilia, Italy.

Background: Little is known about targeted next generation sequencing (NGS) and its clinico-pathologic implications in large cell carcinoma (LCC), an undifferentiated subtype of lung cancer.

Design: Thirty LCC were dissected by unsupervised targeted NGS analysis according to IonTorrent AmpliSeq™ Hotspot Cancer Panel v2, which identifies selected regions of 50 frequently cancer-associated oncogenes and tumor suppressor genes. Cell differentiation lineages of LCC were investigated by means of thyroid transcription factor-1 (TTF1) immunohistochemistry (IHC) for adenocarcinoma (ADC) and DNp63/p40 for squamous cell carcinoma (SQC), dichotomizing TTF1 as negative or positive (whatever extent) and p40 as negative, positive or focal if there were ≤5% reactive tumor cells.

Results: While 3 LCC were wild type (all TTF1+/p40-), the remaining 27 LCC showed at least one gene mutation, whose distribution closely mirrored IHC profiles. In particular, 7 cases with TTF1+/p40- or p40± phenotype corresponding to ADC exhibited *ATM*, *ERBB4*, *FLT3, KRAS, BRAF, NRAS, TP53* or *FBXW7* mutations, and 3 cases with TTF1-/p40+ phenotype pointing to SQC showed *TP53* mutations only, whereas 17 cases with null (TTF1-/p40-) or unclear (TTF1-/p40±) phenotype presented *ATM, BRAF, CDKN2A, EGFR, FBXW7, KRAS, PIK3CA, PTPN11, RET, SMAD4, SMO, STK11 or TP53* mutations. Frequency of mutated allelic DNA ranged from 6% (*RET*) to 76% (*ATM*). Single, double, triple, quadruple and quintuple mutations occurred in 16, 6, 2, 2 and 1 patient, respectively, with *BRAF, ERBB4* and *CDKN2A* being mutually exclusive mutations. Tumor patients expressing ^{3}3 mutations experienced shorter OS (p=0.001) and DFS (p=0.007), independent of tumor stage. In turn, IHC categorization did not affect survival.

Conclusions: NGS analysis identified a plethora of gene mutations in LCC with close genotypic-phenotypic correlations, where TTF1/p40 null and unclear phenotypes basically corresponded to undifferentiated ADC thereby confirming on molecular grounds the IHC axiom "no p40, no squamous".

1956 Thymic Neuroendocrine Neoplasms (T-NENs) With CTNNB1 (Beta-Catenin) Gene Mutation Show Components of Well-Differentiated Tumor and Poor-Differentiated Carcinoma, Challenging the Concept of Secondary High-Grade Neuroendocrine Carcinoma

Giuseppe Pelosi, Manuela Bimbatti, Alessandra Fabbri, Paolo Bidoli, Stefania Canova, Ugo Pastorino. Fondazione IRCCS Istituto Nazionale dei Tumori, Milan, Italy; San Gerardo Hospital, Monza, Italy.

Background: Little is known about the molecular pathogenesis of neuroendocrine neoplasms primary to the thymus, which account for 2-5% of all tumors arising in this organ.

Design: Nine T-NENs accounting for different histologic variants according to the current WHO classification, including 5 atypical carcinoid (AC), 3 large cell neuroendocrine carcinoma (LCNEC) and one small cell carcinoma (SCC), were investigated by immunohistochemistry (IHC) for Ki-67 labeling index and beta-catenin, the latter acting as a pivotal player of the cell adhesion system at adherens junctions and main transducer of the Wnt signaling pathway to the nucleus where it activates transcription of several reporter genes. Two of these tumors also underwent unsupervised targeted next generation sequencing (T-NGS) analysis for 50 cancer-associated oncogenes and tumor suppressor genes (IonTorrent AmpliSeq™ Hotspot Cancer Panel v2).

Results: There were 8 males and 1 female, ranging from 20 to 73 years. Three out of 9 T-NENs (all LCNEC) showed cytoplasmic to nuclear decoration for beta-catenin and an intra-tumor heterogeneity of Ki-67 labeling index consistent with either spatially separated or admixed morphologic components of well-differentiated tumor (Ki-67: 10-15%) and poor-differentiated carcinoma (Ki-67: 45-75%). At variance, the remaining 6 tumors (5 AC and one SCC) presented predominantly with membrane labeling and a more homogeneous distribution of Ki-67 labeling index inside tumor mass (ranging from 10 to 90% according to histology). Exon 3 CTNNB1 gene mutations were found in the 2 LCNEC thus far analyzed by T-NGS with cytoplasmic/nuclear beta-catenin accumulation, one of which was developed as a metachronous LCNEC 17 years after a previous thymic AC harboring the same gene mutation.

Conclusions: Activation of the Wnt signaling pathway by CTNNB1 gene mutation may contribute to the development of a subset of T-NENs featuring simultaneous well-differentiated tumor and poor-differentiated carcinoma, as either synchronous or metachronous lesion. These findings challenge the concept of secondary high-grade neuroendocrine carcinoma in the thymus.

1957 Lung Cancer Ethnic Disparities: Co-Morbidity or Tumorigenicity?

Saraswati Pokharel, Umesh Sharma. Roswell Park Cancer Institute, Buffalo, NY; University at Buffalo, Buffalo, NY.

Background: Lung cancer is the leading cause of cancer related death in the United States. The incidence rate is highest among African American (AA) males followed by non-Hispanic-Whites (NHW). Earlier reports suggested that life expectancy in lung cancer patients varies between different ethnic groups. The underlying reasons for these survival disparities are not clearly known. We aim to investigate the health-related behavioral factors, tumor-types and tumor-grades to explain lung cancer survival discrepancies between non-Hispanic Whites, African Americans, and American Indians, treated in our minority-serving and NCI-designated cancer center.

Design: Systematic review of the Roswell Park Cancer Institute's lung cancer registry from January 1996 to September 2009 was performed. Patient demographics, tumor-types, tumor-grades, smoking habits, patient survival status and the cause of death were analyzed.

Results: Of the 2828 gender-matched patient cohort, 2600 (92%) were non-Hispanic whites (NHW), 204 (7%) were African Americans (AA), and 24 (1%) were American Indians (AI). More than 70% of patients of all three ethnic categories had non-small cell lung cancer- mostly grade II-III. The smoking history was positive in 92% of NHW, 89% of AA and 100% of the AI patients. Five-year survival rate was highest among NHW (18%) and lowest among AI (8%). Analysis for the cause of death revealed that 15% of AA died of the causes other than lung cancer as opposed to 21% of NHW and 25% of AI. More importantly, 70% of AA died of recurrent or persistent lung cancer in contrast to 60% NHW, and 66% of AI (P<0.05).

Conclusions: Our comprehensive registry data show significant lung cancer survival disparities among three major ethnic groups. Despite comparable tumor-types and tumor-grades, mortality due to lung cancer itself is higher among AA and AI. Whether this is related to limited access to health care or due to the susceptibility for cancer recurrence- needs to be further studied.

1958 Malignant Mesothelioma Mutation Profile – OncoPanel Results From Tumor Profiling Study

Emilian Racila, Lynette Sholl, Neal Lindeman, William Richards, Raphael Bueno, Lucian Chirieac. Brigham & Women's Hospital, Boston, MA.

Background: With the recent development of new high throughput technologies, there is increased interest of investigating the molecular heterogeneity of malignant mesothelioma.

Design: We tested 49 MM specimens in an institutional tumor profiling initiative, using targeted next-generation sequencing (NGS) of the entire exon sequence of 275 genes and selected intron coverage of 30 additional genes. The mutation profile was examined for the overall number and type of nucleotide substitutions and mutational frequency (MF) was determined. Copy number variation analysis (CNV) was also performed. The mutations were divided into four major tiers (T), T1 to T4, based on the clinical relevance for targeted therapy or prognosis of that particular mutation, with most clinically relevant mutations in T1 and T2, potentially therapeutically-targetable alterations in T3, and alterations of unknown significance in T4.

Results: The specimens were collected from 38 (78%) men and 11 (22%) women with MM. The average age was 71 years and 58 years for male and female patients, respectively. In the male group, there were 20 (53%) epithelioid, 4 (11%) sarcomatoid and 14 (36%) biphasic types of MM. The female group consisted of 8 epithelioid (73%), 1 (9%) sarcomatoid and 2 (18%) biphasic MM. The overall mutational frequency was higher in the female group (4.64) compared to the male group (3.5). Analysis of mutational frequency by type of MM showed that the highest number of mutations are recorded in the sarcomatoid type (4.6), followed by biphasic (3.88) and epithelioid (3.54) types of MM. Among genetic mesothelioma factors the following combinations are observed: Bap1 only - 6 cases (12%); 22q loss only - 1 case (2%); 9p loss only - 6 cases (12%); 22q and 9p loss - 2 cases (4%); Bap1 and 9p loss - 8 cases (16%); Bap1, 9p and 22q loss - 3 cases (6%). CNV analysis showed that 19 of the 38 male patients (50%) and 6 of the 11 female patients (55%) have CDKN2A or CDKN2B deletions, this alteration being the most frequent change in chromosomal copy number observed in this study group.

Conclusions: Mutational frequency differences are observed between epithelioid, sarcomatoid and biphasic types of MM that may impact on tumor behaviour. The most frequent alteration in chromosomal copy number in MM involves the CDKN2A and CDKN2B regions. A study is in progress to determine if NGS can be used to identify specific mutational patterns for asbestos-related or asbestos-independent etiology of MM.

1959 Squamous Cell Carcinoma Mutation Profile as a Tool To Distinguish Metastatic From Primary Lung Cancer

Emilian Racila, Frank Kuo, Lynette Sholl. Brigham & Women's Hospital, Boston, MA.

Background: Squamous cell carcinoma (SCC) of lung is difficult or impossible to distinguish from metastatic SCC from other sites based on morphology or immunophenotype. We hypothesized that mutational profiles as derived from next-generation sequencing (NGS) can be used to help distinguish these events.

Design: We tested 80 SCC specimens (among 1000 total tumors) in an institutional tumor profiling initiative, using targeted NGS of entire exon sequence of 275 genes and selected intron coverage of 30 additional genes. This cohort includes 7 skin cases, 4 gynecologic (GYN) cases, 45 head and neck (H&N) cases, 1 esophageal, 3 mediastinal and 20 lung cases. The mutation profile was examined for the overall number and type of nucleotide substitutions. Mutational signatures (MUTSIG) were evaluated in all tumors with 10 or more mutations. MUTSIG were defined by the substitution type and sequence context immediately 3' and 5' to the mutated base.

Results: The highest mutational frequency (MF), 32.6, was seen in SCC cases from skin with MUTSIG being consistent with UV-related changes in the majority of the cases, followed by significantly lower MF in GYN, H&N and lung tumors with an average number of 4.8, 7.6 and 10.3 mutations, respectively.

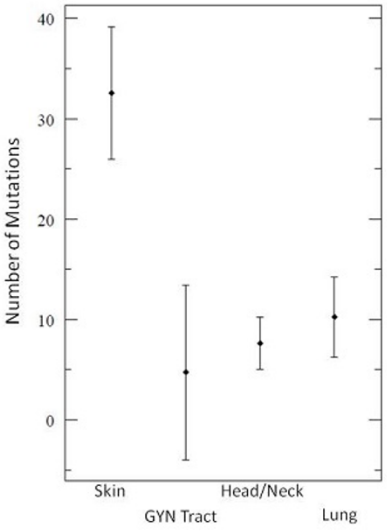

Among thoracic SCC cases, MUTSIG were evaluated in 11 (9 lung, 2 mediastinal) tumors. Four primary lung tumors had a C>A/G>T transversion signature characteristic of smoking-related mutagenesis. Two lung cases, had numerous dipyrimidine substitutions consistent with UV-related mutagenesis; on review of the clinical history, both patients had prior histories of cutaneous SCC. In the remaining 3 lung cases the MUTSIG was equivocal. On the other hand, both anterior mediastinal tumors, initially classified as thymic SCC, showed smoking-related MUTSIG.

Conclusions: NGS can be used to distinguish lung SCC from metastatic SCC arising from cutaneous primaries using a NGS approach and an algorithm to identify mutational patterns. In this small cohort of presumed thoracic SCC, characteristic MUTSIG triggered the clinical and pathologic reclassification of 17% of tumors, including two cases of presumed lung origin reclassified as metastases from the skin and two cases of possible thymic origin reclassified as probable lung origin.

1960 PiwiRNA Expression Is Related To Prognosis of Non-Small Cell Lung Carcinoma

Jose Ramirez, Rut Tejero, Anna Cordeiro, Ramon Marrades, Nuria Vinolas, Adela Saco, Mariano Monzo, Alfons Navarro. Hospital Clínic, IDIBAPS, University of Barcelona, Barcelona, Spain; University of Barcelona, Barcelona, Spain.

Background: PiwiRNAs (piRNAs) are a recently discovered class of small RNAs (24-32nt). To date, more than 23,000 piRNAs have been discovered. Until recently, their expression was believed to be limited to germinal stem cells. However, piRNA expression has now been identified in somatic cells and especially in tumor cells. We aim to explore the relationship between the activation of the piRNA pathway and the prognosis of non-small cell lung carcinoma (NSCLC).

Design: We studied prospectively 71 surgically resected NSCLC patients from 2007 to 2011. We assessed the expression of the four PIWI proteins: PIWIL1-4; both in normal and tumor tissue by RT-PCR (frozen tissue) and also by immunohistochemical techniques (FFPE tissue). The expression levels were correlated with patient outcome: disease free survival (DFS) and the overall survival (OS).

Results: The median follow up was 49 months (range 2 to 80 months). Forty patients were stage I, 17 stage II and 10 stage III. Nineteen patients received adjuvant treatment after surgery. The tumors were classified as Adenocarcinoma (n=40) or Squamous Cell Carcinoma (n=31). The quantification of the mRNA levels of the four PIWI proteins showed first that PIWIL1 where not expressed in any normal tissue, but its expression was detected in 11 tumor samples. Interestingly, the prognosis analysis showed that the 11 patients expressing PIWIL1 had worse DFS (20 vs 50 months; p=0.0078) and shorter OS (32 vs 61 months; p=0.0076). These results were validated by immunochemistry, with a faintly cytoplasmic reactivity in the positive cases. Second, PIWIL3 were not expressed neither in normal lung tissue nor tumor tissue. Third, PIWIL2 and PIWIL4 were detected in all the samples. However, both were downregulated in tumor tissue in comparison to the paired normal tissue (p<0.001, Figure 1). Of note, the patients with lower levels of PIWIL4 had worse prognosis for DFS (28 vs 51 months; p=0.034) and OS (36 vs 62 months; p=0.033).

Conclusions: PIWIL1 is related to the primary processing pathway of piRNAs while PIWIL4 is related with the secondary pathway. Little is known about the functions of the primary pathway, which we observed inactivated in somatic lung tissue and its re-expression in the tumor was associated with worst prognosis. On the other side, the secondary pathway was active in somatic cells.

Supported by: AECC-Catalunya 2013.

1961 Lung Cancer in Patients With Systemic Sclerosis: Foci of Atypical Adenomatous Hyperplasia Progressing Into Lepidic and Acinar Predominant Adenocarcinoma

Kirtee Raparia, Jane Dematte, Rishi Agrawal, Jeremy Katzen. Northwestern University, Chicago, IL.

Background: Chronic diffuse fibrotic lung diseases can often show areas of epithelial proliferations including honeycomb changes, peribronchiolar and squamous metaplasia with and without atypia. These changes have been postulated as an underlying mechanism for the development of lung cancer in patients with connective tissue related interstitial lung disease such as Systemic Sclerosis (SSc).

Design: A single center review of all cases of lung cancer in patients with SSc was performed. Clinical, radiological, histopathological and molecular characteristics of these patients were studied.

Results: 18 cases of lung cancer in SSc were identified. Majority of these patients were females (83%). 12 patients were former or current smokers with 10 to 80 pack year's history. Thirteen cases had radiographic evidence of SSc lung involvement, with nonspecific interstitial pneumonia (NSIP) being the most common pattern. The tumors comprised of 15 adenocarcinoma, 1 adenosquamous carcinoma, 1 small cell carcinoma and 1 large cell neuroendocrine carcinoma. Adenocarcinoma with either lepidic or acinar predominant pattern was the most common type of lung cancer in these patients (9/15). 7 of the adenocarcinomas had mucinous features. Five cases of resected adenocarcinoma showed multiple foci of atypical adenomatous hyperplasia (AAH) closely associated with areas of microscopic honeycombing, and transitioning into areas of lepidic and acinar predominat adenocarcinoma. 9 of these tumors stained positive with TTF-1 immunostaining. Of the ten tumors which underwent molecular mutational profiling, 2 had KRAS mutation and 1 had EGFR mutation. Usual interstitial pneumonia (UIP) and desquamative interstitial pneumonia (DIP) like areas were the common pathologic patterns seen in the background lung parenchyma.

Conclusions: Adenocarcinoma is the most common type of lung cancer seen in patients with SSc. The high proportion of lepidic and acinar adenocarcinomas with multiple foci of AAH, seen in our study suggests that the atypical epithelial proliferations in fibrotic lungs are the underlying pathogenetic mechanism of lung cancer development in these patients. Although these tumors are well differentiated, the tumor foci can be multiple, and hence these patients can present at higher stage disease with poor prognosis.

1962 Histopathologic and Cytogenetic Features of Pulmonary Adenoid Cystic Carcinoma

Anja Roden, Patricia Greipp, Darlene Knutson, Sara Kloft-Nelson, Randolph Marks, Marie Christine Aubry, Joaquin Garcia. Mayo Clinic, Rochester, MN.

Background: In adenoid cystic carcinoma (ACC) of the head and neck, a t(6;9)(q22-23;p23-24) translocation that results in a fusion of the *MYB* oncogene and the transcription factor gene *NFIB*, has been demonstrated. The MYB-NFIB fusion oncoprotein activates transcription of MYB-mediated pathways that impact cell cycle control, DNA repair and apoptosis. This translocation appears highly specific for ACC. Moreover, therapies targeting MYB or MYB-activated pathways to treat ACCs are being explored. Pulmonary ACC (PACC) has not been studied for rearrangements of the *MYB* gene.

Design: Institutional files (1972-2011) were searched for PACC. 35 of 40 cases were previously reported (Macarenco et al. 2008). All cases were re-reviewed and classified according to the predominant histologic pattern (cribriform, solid, tubular). Fluorescence in situ hybridization (FISH) was employed using a break-apart strategy to detect *MYB* rearrangement (at 6q23.3). A Mayo laboratory-developed probe set was comprised of 5'*MYB* DNA labeled with SpectrumOrange dUTP (Abbott Molecular/Vysis Products) and 3'*MYB* DNA labeled with SpectrumGreen dUTP (Abbott Molecular/Vysis Products). 100 interphase tumor cell nuclei were evaluated per case. Medical records were studied.

Results: The histologic patterns and clinical findings of 40 PACC are summarized in Table 1.

	All Cases	MYB Rearranged	MYB not Rearranged
Number of patients	40	12	17
Age years (range)	56.6 (21.6-73.4)	53.1 (29.7-72.6)	53.9 (21.6-70.9)
Male : Female	0.67	0.71	0.7
Predominant histologic pattern (%) CribriformSolidTubular	77.57.515.0	75.08.316.6	82.311.85.9
ResectionResection status known (n) Complete (%)Incomplete (%)Biopsy (%)	15531333	560040	8502525
Positive lymph nodes (% cases)a	22	50	0
Adjuvant therapy (% cases)	32.5	33.3	47.1
Follow up, years (range)	4.7 (0-34.3)	6.0 (0-25.2)	4.6 (0-20.6)
% patient died	72.5	83.3	64.7
% patient died of disease	30	41.7	35.3
% patients with metastasis/recurrence	57.5	58.3	64.7
a Information available in 9 cases			

Tissue blocks for FISH studies were available in 35 cases. Disruption of the MYB gene region was observed in 12 cases whereas 17 showed no evidence of rearrangement. Six cases failed to hybridize. Follow up was available in all patients.

Conclusions: 41% of PACC harbor a *MYB* rearrangement. FISH studies for *MYB* may be of diagnostic utility in PACC, particularly on small biopsy specimens. *MYB* rearrangement in PACC did not appear to be associated with clinical features or prognosis.

1963 Beyond Mitosis and Necrosis: Additional Histo-Cytologic Differences Between Typical and Atypical Carcinoids of the Lung and Their Prognostic Significance

Lauren Rosen, Ihab Lamzabi, Vijaya Reddy, Paolo Gattuso. Rush University Medical Center, Chicago, IL.

Background: Well differentiated pulmonary neuroendocrine tumors (NETs) consist of typical (TC) and atypical carcinoid (AC). They are subdivided by The World Health Organization (WHO) based on mitoses and necrosis into grade 1 (TC) and grade 2 (AC). However, 10 to 20% of patients with TC die of disease within 5 years and literature regarding the histologic characteristics of these "high-risk" well-differentiated NETs is limited. To improve our recognition of higher risk subgroups of TC and AC, we investigated a cohort of cases using objective and thorough histologic criteria.

Design: We searched our electronic surgical pathology records to identify cases of TC and AC. Only resection specimens, tumors larger than 0.5 cm and cases with available H&E slides were included. The H&E slides were blindly reviewed separately by 2 pathologists for an exhaustive list of histologic features.

Histo-cytologic Features			
Cytologic	Architectural	Microscopic Behavioral	Microenvironment
Nuclear-cytoplasmic ratio	Growth pattern	Infiltrative margin	Intratumoral vascularity
Nuclear size	Indian filing	Permiation of adjacent lung	Intratumoral lymphocytes
Nuclear pleomorphism		Lymphatic vascular invasion	
Presence of nucleoli		Perineural invasion	
Nuclear contours			
Cytoplasmic granularity			
Nuclear shape			

Tumor grade was reassessed according to the most recent WHO classification. Statistical analysis was performed with Spearman correlation (SPSS software).

Results: Fifty cases including 35 TC and 15 AC were reviewed. Compared to TC, AC had larger nuclear size (p=0.005), showed more nuclear pleomorphism (p=0.03), more prominent nucleoli (p=0.02), and a predominantly nested pattern (p=0.001). Lymph node (LN) metastasis correlated with mitoses (p=0.01), necrosis (p=0.008), multinucleation (p=0.004), and high nuclear to cytoplasmic (NC) ratio (p=0.01). Distant metastases correlated with mitoses (p<0.001), necrosis (p<0.001), larger nuclear size (p=0.01), presence of smudged chromatin (p=0.001) and nested growth pattern (p=0.001).

Conclusions: AC show distinct histologic features from TC. Furthermore, in addition to mitoses and necrosis, we identified other morphologic features including nested growth pattern, larger nuclear size, high NC ration, and smudged chromatin that are associated with LN and distant metastases and may help stratify patients with either TC or AC into low and high risk categories.

1964 Characterization of ROS1-Rearrangements in a Cohort of Spanish Patients Diagnosed of NSCLC

Marta Salido, Sergi Clave, Javier Gimeno, Lara Pijuan, Joana Vidal, Marta Lorenzo, Silvia Menendez, Alvaro Taus, Ana Munoz-Marmol, Enric Carcereny, Noemi Reguart, Jose Luis Mate, Joan Albanell, Sergi Serrano, Edurne Arriola, Blanca Espinet. Hospital del Mar, Barcelona, Spain; Institut Hospital del Mar d'Investigacions Mèdiques (IMIM), Barcelona, Spain; Hospital Germans Trias i Pujol, Badalona, Spain; Hospital Clínic, Barcelona, Spain.

Background: Recently, ROS proto-oncogene 1, receptor tyrosine kinase (*ROS1*, 6q22) has been identified as a driver oncogene in NSCLC. Patients carrying *ROS1* rearrangements are candidates to targeted therapy with Crizotinib. We aimed to determine the prevalence of ROS1-rearranged cases, their pattern and their fusion partners in a cohort of patients with NSCLC and to characterize *ROS1* copy number alterations (CNAs) by fluorescence *in-situ* hybridization (FISH).

Design: A total of 216 NSCLC patients (median age 64.1 years, 66.5% males, 72.0% smokers, 81.2% with ADC histology, 37.1% in clinical stage IV) were analyzed, 49 of them included in a tissue microarray (TMA). *ROS1* abnormalities were tested first using a break-apart FISH probe (Zytovision) and immunohistochemistry (IHC) with *ROS1* D4D6 antibody (Cell Signalling Technology) was also performed in TMA and *ROS1*-rearranged cases. To characterize *ROS1*-rearranged partners, clones from Human 32K BAC Re-Array Library were used to develop *CD74*, *EZR* and *SLC34A2* probes. Correlation with clinico-pathologic information was investigated.

Results: Twenty-seven samples were non-assessable due to assay failure. Four out of the 189 samples were *ROS1*-rearranged (2.1%): three showed deletion of the non-rearranged allele and one had a 5'*ROS1* deletion. All rearranged cases were positive for *ROS1* IHC staining, three with a cytoplasmic predominant pattern and one with membranous predominant pattern. Negative IHC staining was detected in all non-rearranged cases. Regarding to *ROS1* rearrangement partners, one case harbored a *SLC34A2-ROS1* fusion and another case a *CD74-ROS1* fusion. No fusion partner was identified in the other two samples. All *ROS1*-rearranged tumors were ADC and *wild-type* for *EGFR*, *KRAS* and *ALK*. We observed an association with non-smoking habit (p=0.036). Regarding CNAs in *ROS1* non-rearranged cases, 49.7% presented gains (3-6 copies), 30.2% deletions and 2.1% amplifications (›6 copies in >10% of tumor cells).

Conclusions: We confirm the low prevalence described of *ROS1*-rearranged NSCLC cases in the Spanish population. Moreover, our study reveals a significant frequency of *ROS1* deletions as a potentially relevant cytogenetic aberration, also detected in *ROS1*-rearranged cases.

1965 EGFR and ALK Testing in NSCLC: Clinical and Cost Implications of Universal Versus Advanced-Stage Only Testing

Jennifer Sauter, Kelly Butnor. Mayo Clinic, Rochester, MN; The University of Vermont Medical Center, Burlington, VT.

Background: Targeted agents have been shown to benefit patients with locally advanced or metastatic (stages III and IV) non-small cell lung carcinoma (NSCLC) whose tumors harbor specific genetic alterations. The College of American Pathologists/International Association for the Study of Lung Cancer/Association for Molecular Pathology jointly recommends all advanced-stage NSCLC patients in whom an adenocarcinoma component cannot completely be excluded undergo EGFR mutation testing and ALK rearrangement testing. While no targeted agents have been approved for patients with early-stage (stages I and II) NSCLC, many institutions perform molecular testing at the time of initial diagnosis, regardless of stage. This is the first study to examine the cost and clinical impact of EGFR and ALK testing in patients with non-advanced-stage NSCLC.

Design: All NSCLC patients whose initial diagnosis was made on a non-resection sample (pleural fluid, bronchoscopic or image-guided aspiration/biopsy) at the University of Vermont Medical Center during 2012 were identified and stage at presentation, treatment, and follow-up data were recorded. Charges billed to our institution by the reference laboratory utilized to perform EGFR and ALK testing were used to compare the relative costs of universal testing with testing only advanced-stage patients.

Results: Of a total of 133 patients, 47 were early-stage (stage I or II) and 86 had advanced or metastatic (stage III or IV) disease at presentation. The cost of testing all newly diagnosed NSCLC patients at our institution for EGFR mutations and ALK rearrangements is estimated to be an additional $75,200 per year compared to testing only advanced-stage patients. Eight (17%) non-advanced-stage patients progressed or recurred during the 18-30 month follow-up period, 75% of whom had pathologic confirmation of progression/recurrence.

Conclusions: The cost of universal EGFR and ALK testing in NSCLC patients is substantial. The clinical impact of testing early-stage NSCLC patients at the time of initial diagnosis appears negligible. Most early-stage NSCLC patients do not recur. Those that do typically are biopsied to confirm recurrence, providing a tissue source that may be more desirable for testing that the original sample. The findings in this study call into question the practice of universal molecular testing of NSCLC patients at the time of initial diagnosis.

1966 BAP1 Immunohistochemistry and p16 FISH To Separate Benign From Malignant Mesothelial Proliferations

Brandon Sheffield, Harry Hwang, Anna Lee, Allen Gown, Andrew Churg. Vancouver General Hospital, Vancouver, BC, Canada; PhenoPath Laboratories, Seattle, WA; Children's and Women's Health Centre of British Columbia, Vancouver, BC, Canada.

Background: The separation of malignant from benign is crucial to patient care, but is often a difficult problem for the pathologist. A variety of immunohistochemical (IHC) stains have been proposed to mark either benign or malignant mesothelial proliferations but each lacks the specificity required for clinical use. Homozygous deletions of 9p21, resulting in loss of the p16 tumor suppressor (*CDKN2A*) is a good marker of mesotheliomas, but lacks sensitivity. Recent reports indicate that some mesotheliomas are associated with loss of *BRCA-associated protein 1*(*BAP1*) expression. The frequency and specificity of loss have not been reported. Here we investigate *BAP1* and *CDKN2A* as potential markers of malignancy and compare test characteristics to previously proposed markers.

Design: A previously well-characterized tissue microarray (TMA) containing both benign and malignant mesothelial proliferations was used. BAP1 protein was interrogated by IHC. The *CDKN2A* locus was examined by fluorescent *in situ* hybridization (FISH) directed towards chromosome 9p21. EMA and p53 were examined by IHC and results combined with previous IHC data for IMP3 and GLUT1 on the same TMA for comparison.

Results: Loss of BAP1 was identified in 7/26 mesotheliomas and 0/49 benign proliferations. Loss of *CDKN2A* was identified in 14/27 mesotheliomas and 0/40 benign proliferations, yielding 100% specificity and positive predictive value for each marker. Three cases showed loss of both *CDKN2A* and BAP1. Together, BAP1 IHC and *CDKN2A* FISH were 58% sensitive for detecting malignancy. Combinations of p53, EMA, IMP3 and GLUT1 showed inferior test characteristics.

Panel	BAP1 IHCor p16 FISH	p53 or EMA IHC	IMP3 and GLUT1 IHC	EMA and IMP3 and GLUT1 IHC
Number of cases	61	76	78	76
Sensitivity(95% CI)	58%(46-71%)	64%(54%-75%)	43%(32%-54%)	20%(11%-29%)
Specificity(95% CI)	100%(100%-100%)	50%(39%-61%)	96%(91%-100%)	98%(95%-100%)

Conclusions: The combined approach of BAP1 IHC and *CDKN2A* FISH, although not sensitive, is very specific for diagnosing malignant mesotheliomas. The test characteristics of previously proposed markers EMA, p53, GLUT-1, IMP-3, suggest that, even in combination, these markers are not practical tools in this clinical setting.

1967 Expression of PAK1 and PAK2 Is Associated With Grade of Pulmonary Neuroendocrine Tumors

Stephen Smith, Adam Bissonnette, David Cohen, Cynthia Timmers, Jin Jen, Junya Fukuoka, Teri Franks, William Travis, David Carbone, Konstantin Shilo. Ohio State University, Columbus, OH; Mayo Clinic, Rochester, MN; Nagasaki University, Nagasaki, Japan; Joint Pathology Center, Silver Spring, MD; Memorial Sloan Kettering Cancer Center, New York, NY.

Background: Cytoskeletal dynamics, cell survival and proliferation are regulated in part by a family of GTPases termed p21-activated kinases (PAKs). Expression of both PAK1 and PAK2 with subsequent activation of NFKB has been shown in recurrent respiratory papillomas, documenting an alternative to COX-2 activation of these pathways. Expression of PAK1 has also been documented in squamous cell lung carcinomas. PAKs activate proliferative/anti-apoptotic pathways – including MEK, ras and BRAF. While PAK mutations are rare, their overexpression has been documented in cancers making them attractive therapeutic targets. Whether PAK1 or PAK2 has a role in tumorigenesis of pulmonary neuroendocrine tumors (NET) is unknown. This study investigates PAK1 and PAK2 expression in lung tumors and its correlation with clinicopathologic findings.

Design: Three hundred ninety-two lung tumors were evaluated for PAK1 (1:1200, clone EP795Y) and PAK2 (1:600, clone EP795Y) expression utilizing tissue microarray based samples. PAK1 and PAK2 expression was assessed in comparison to normal lung parenchyma as negative, low and high, and was correlated with clinicopathologic variables (SYSTAT, Chicago, IL).

Results: Twenty-nine of 46 (63.0%) typical carcinoid tumors (TC), 18 of 29 (62.1%) atypical carcinoid tumors (AC), 7 of 26 (26.9%) large cell neuroendocrine carcinomas (LCNEC), 8 of 59 (13.6%) small cell lung carcinomas (SCLC), 78 of 109 (71.6%) of adenocarcinomas (ADC) and 51 of 101 (50.5%) of squamous cell carcinomas (SQC) showed PAK1 expression. Twelve of 43 (27.9%) TC, 8 of 29 (27.6%) AC, 11 of 25 (44.0%) LCNEC, 34 of 56 (60.7%) SCLC, 87 of 109 (79.8%) of ADC and 63 of 101 (62.4%) SQC showed PAK2. Both markers were localized predominantly to cytoplasm. PAK1 expression was associated with grade and tumor size ($p < 0.05$) while PAK2 expression was associated with grade ($r < 0.05$) but not with other clinicopathologic variables. No statistically significant association between PAK1 and PAK2 expression and clinicopathological variables was identified in NSCLC.

Conclusions: Expression of PAK1 and PAK2 is seen with a significant frequency throughout a wide spectrum of lung tumors. PAK1 expression is associated with pulmonary carcinoid tumors, whereas PAK2 expression with high grade NET. Strong association of PAK2 expression with SCLC warrants its further investigation as a potential therapeutic target.

1968 TTF-1 [SPT24] Staining Specificity in Lung Adenocarcinoma versus Lung Squamous Cell Carcinoma Is Markedly Improved With Titer Optimization and Cut-Off Values

David Tacha, Ding Zhou. Biocare Medical, Concord, CA.

Background: Commercially available clones of thyroid transcription factor-1 (TTF-1) monoclonal antibodies 8G7G3/1 and SPT24 have been shown to have different sensitivities in lung adenocarcinomas (LADC) and in lung squamous cell carcinomas (SqCC). A study by Masai K, *et al*, demonstrated that SPT24 was much more sensitive than 8G7G3/1 in LADC (72.4% and 65.4% respectively). However, the study demonstrated that SPT24 stained a higher percentage of lung SqCC (16.8% vs. 1%). Higher expression of SPT24 in lung SqCC has also been shown to be heavily influenced by the sensitivity of different detections systems. These findings with clone SPT24 led us to investigate different dilution factors, cut-off values and screening antibodies that are highly specific for lung SqCC. In this study, we will screen all lung SqCC with a multiplex cocktail of Desmoglein 3 (DSG3)/p40 and Napsin A that has been shown to be highly specific and sensitive in the detection of lung SqCC versus LADC. The SPT24 titer will be optimized for LADC and cut-off values will be examined to improve overall staining specificity without compromising staining sensitivity.

Design: Formalin-fixed paraffin-embedded TMA lung SqCC (n = 137) and LADC (n = 60) were acquired. DSG3/p40 and Napsin A multiplex cocktail, TTF-1 [SPT24] and TTF-1 [8G7G3/1] antibodies were optimized for immunohistochemistry. SPT24 was optimally tittered so that normal liver was negative, unlike 8G7G3/1, which is highly expressed in normal liver.

Scoring Method

TTF-1 cases were considered positive if 10% or more of tumor cells were stained with a staining intensity of ≥ 1+. Cases with <10% staining and no focal areas of positive staining were scored as negative.

Results: TTF-1 [SPT24] stained 3.6% (5/137) of lung SqCC, however, all 5 cases of lung SqCC were also positive for DSG3 + p40 (Table 1). Napsin A was negative in all lung SqCC. In LADC, TTF1-1 [SPT24] stained 88% of cases compared to Napsin A (73.3%) and TTF-1 [8G7G3/1] (63.3%). Thus, SPT24 demonstrated high staining sensitivity (Table 2).

Table 1: Lung SqCC

DSG3/p40	Napsin A	TTF-1 [SPT24]
125/137 91.2%	0/137 0%	5/137 3.6%

Table 2: LADC

DSG3/p40	Napsin A	TTF-1 [SPT24]	TTF-1 [8G7G3/1]
1/60 1.7% (p40)	44/60 73.3%	53/60 88.3%	38/60 63.3%

Conclusions: TTF-1 [SPT24] specificity is improved with titer optimization and cut-off values. Antibodies DSG3 + p40 are highly specific for lung SqCC and, therefore, may be used as a pre-screener to rule out LADC.

1969 Gene Mutation Frequencies and Associations in Adenocarcinoma of the Lung

Farnoosh Tayyari, David Hwang, Suzanne Kamel-Reid, Ming-Sound Tsao. University Health Network, Toronto, ON, Canada.

Background: Recent years have seen a revolution in the treatment of lung cancer, resulting from the discovery of specific molecular alterations that render tumors with these abnormalities amenable to specific targeted therapies. In pulmonary adenocarcinomas, driver mutations in one of two genes, EGFR and KRAS, are typically present in over half of these tumors. However, the frequency of other less common, potentially targetable mutations has not been as well established in North American populations.

Design: We performed high-sensitivity mass spectrometry-based genotyping in 341 lung adenocarcinomas (resected at the Toronto General Hospital between 2003 and 2014), for over 200 potentially actionable mutations in 26 cancer-related genes (Sequenom MassARRAY platform). Pathology reports for all cases were reviewed to determine stage and dominant histologic pattern, for correlation with mutation profiles.

Results: In our set of 341 lung adenocarcinomas, KRAS was most frequently mutated (34% of cases), followed by EGFR (23%), BRAF (3%), and PIK3CA (2%). Mutations in several other genes were identified at a frequency of 1% or less, including MET, CTNNB1, ERBB2, JAK2, NRAS, STK11, NRF2, TP53, and HRAS. Double mutations were identified in 25 cases, including 13 cases with 2 EGFR mutations, 1 case with EGFR mutation in addition to a mutation in a different gene, and 11 cases with KRAS mutation with a mutation in a different gene. Stage I tumors less frequently harbored detectable mutations (106/184 tumors, or 58%) than higher stage tumors (stage II-IV; 88/117 tumors, or 75%) ($p=0.003$, Chi-square test). KRAS mutant tumors more frequently demonstrated mucinous morphology than KRAS wild-type tumors ($p=0.03$), while EGFR wild-type tumors more frequently demonstrated solid morphology than their EGFR-mutant counterparts ($p<0.001$).

Conclusions: Potentially actionable mutations are detectable in two-thirds of lung adenocarcinomas within a Canadian population of mixed ethnicity. EGFR and KRAS mutations comprised the majority of these, although almost 10% of cases harbored mutations in other genes. Double mutations may also occur infrequently. Our findings affirm previous reports of associations ofmutations with some histologic subtypes. Finally, our data suggest increased frequency of detectable mutations in higher stage, presumably biologically more aggressive tumors, but this finding needs to be further confirmed in larger studies.

1970 Molecular Characterization of Pulmonary Sarcomatoid Carcinoma – Analysis of 32 Cases

Simone Terra, Jin Jang, Lintao Bi, Jin Jen, Eunhee Yi, Jennifer Boland. Mayo Clinic, Rochester, MN.

Background: Several targetable genetic alterations including *ALK* rearrangements and *EGFR* mutations have been found in pulmonary adenocarcinomas, with FDA-approved therapies currently available. However, the molecular features and presence of targetable mutations in pulmonary sarcomatoid carcinomas (SCs) are largely unknown. Lung SCs are rare, aggressive, and poorly differentiated non-small cell lung carcinomas which contain at least 10% spindle cell morphology, tumor giant cells, and/or differentiated sarcoma. They account for 0.3-1.3% of all lung malignancies, tend to affect older males, and tobacco smoking is the most important risk factor. The aim of this study is to survey for potentially targetable mutations in 33 previously morphologically and immunohistochemically confirmed lung SCs.

Design: ALK1 immunohistochemistry was performed on formalin-fixed paraffin-embedded (FFPE) tumor sections. DNA was extracted from FFPE tumor samples, and applied to the Ion AmpliSeq™Cancer Hotspot Panel v2 to test for approximately 2,800 individual mutations in 50 oncogenes, including *EGFR, KRAS, NRAS, TP53, BRAF, ERBB2, JAK3, AKT1, ATM, MET, KIT,* and *PIK3CA*.

Results: All 33 lung SCs were negative for ALK1 immunohistochemistry. Mutational analysis was attempted in all 33 cases, but 1 case was excluded due to technical failure. Twenty-four of the 32 cases (75%) showed at least one detectable genetic alteration-19 cases (59%) had *TP53* mutations; 10 cases (31%) had *KRAS* mutations; mutations were found in *AKT1*, *JAK3*, *BRAF*, *NRAS*, and *PIK3CA* in one case each (3%). Six of the 19 cases (32%) with a mutation in *TP53* had simultaneous mutations in *KRAS.* The cases with mutations in *JAK3, BRAF*, and *NRAS* also had mutations in *TP53*. The case showing a mutation in *PIK3CA* also had a *KRAS* mutation. No *EGFR* mutations or mutations in the other tested genes were observed.

Conclusions: Mutations in the tumor suppressor gene *TP53* are the most common genetic alteration in pulmonary SCs. *KRAS* mutations were also frequent, and often occurred in conjunction with *TP53* mutations. In addition, occasional mutations were found in other genes involved in lung carcinogenesis, including *AKT1, JAK3, BRAF, NRAS,* and *PIK3CA*. The identified mutations have potential as future therapeutic targets to improve the poor outcome of pulmonary SC.

1971 Accuracy of the IASLC/ATS/ERS Histological Subtyping of Stage I Lung Adenocarcinoma on Intraoperative Frozen Sections

Humberto Trejo Bittar, Pimpin Incharoen, Andrew Althouse, Sanja Dacic. University of Pittsburgh Medical Center, Pittsburgh, PA; Magee-Womens Research Institute of the University of Pittsburgh, Pittsburgh, PA.

Background: Limited lung resection (LR) has been proposed as a treatment of choice for early stage lung adenocarcinoma (ADC); however, LR may not be appropriate in tumors with micropapillary (MP) pattern due to the risk of recurrence. The aim of this study was to determine diagnostic accuracy and interobserver variability in histological subtyping of lung ADC with intraoperative frozen sections (IFS).

Design: 112 cases of surgically resected stage IA/IB lung ADC were reviewed independently by three pathologists. Histological patterns (acinar, lepidic, papillary,

micropapillary,solid and mucinous) were recorded for each IFS and permanent sections. Kappa scores were calculated to evaluate agreement between pathologists' determination for each IFS versus the permanent section.
Results: Overall agreement between IFS and permanent section was fair for identification of primary pattern, with kappa scores ranging from 0.43-0.58, with more consistent agreement for stage IA tumors. Kappa scores for the secondary pattern ranged from 0.16-0.32. Acinar and solid patterns were most likely to be correctly identified as primary growth patterns. Pathologists identified MP pattern in only 11% to 55% of cases. The reasons for poor agreement were sampling errors and poor quality of IFS.
Conclusions: Our data suggest that is difficult to predict the primary ADC pattern on a single representative IFS. More extensive sampling of stage I lung ADC at the time of intraoperative consultation may be considered.

1972 Rocket Science Lung: Rare Aerospace Metals in Interstitial Lung Disease

Ramona Untanu, Ganesh Raghu, Jerrold Abraham. SUNY Upstate Medical University, Syracuse, NY; University of Washington, Seattle, WA.
Background: Interstitial lung disease can be caused by numerous occupational/environmental exposures. This unique case of interstitial fibrosis was associated with an unusual group of metal particles, including previously unreported Hafnium (Hf).
Design: A 75 year-old never smoking man developed progressive shortness of breath, dry cough, fatigue and radiological and physiological evidence of interstitial lung disease (ILD). He had worked 17 years at a facility producing nuclear, military and aerospace rare metal products. We examined transbronchial and surgical lung biopsy (SLB) specimens using bright field and polarized light microscopy and scanning electron microscopy with energy-dispersive x-ray spectroscopy (SEM/EDS).
Results: Transbronchial biopsy was insufficient for evaluation of interstitial disease but showed accumulation of fine opaque and birefringent particulates. The SLB showed areas of patchy and diffuse interstitial fibrosis with mononuclear inflammation, fibroblast foci and several small non-necrotizing granulomas, suggestive of hypersensitivity pneumonitis (HP). Rare intraalveolar 'cannibalistic' multinucleated giant cells were also noted, as seen in hard metal disease (HMD)/giant cell interstitial pneumonia. SEM/EDS analysis of 200 consecutive particles confirmed a range of metal particles not found in the general population. Most unusual was the finding of Hf. The metal particles, in decreasing frequency included zirconium (Zr), titanium (Ti), niobium (Nb), Hf, and some alloys such as NiTi. Fewer tantalum, aluminum, chromium and iron, as well as background aluminum silicate and silica particles were seen. Tungsten and cobalt (HMD metals) were not found. These metal particulates correlate well with the metals the patient had worked with over his career. The initial interpretation was usual interstitial pneumonia. However, diagnosis of 'idiopathic' pulmonary fibrosis (IPF) is not appropriate with a history and evidence of such occupational exposure. Although this complicated histopathology does not fit exactly with any standard pattern, it is most consistent with chronic HP.
Conclusions: It is essential to further analyze the lung tissues in patients whose diagnosis is unclear, especially when the exposure history raises the probability of ILD induced by metal or other particles. Based on his exposure history and the SEM/EDS findings, we attribute the etiology of his ILD (HP) to metal particles, some of which have been related to HP (Zr, Ti), but others previously unreported deserve further toxicologic study (Hf, Nb).

1973 Clinicopathologic and Genetic Characteristics of Young Patients With Pleural Diffuse Malignant Mesothelioma

Marina Vivero, William Richards, Raphael Bueno, Lucian Chirieac. Brigham & Women's Hospital, Boston, MA.
Background: Pleural diffuse malignant mesothelioma (PDMM) is an uncommon malignancy with poor median survival. PDMM typically presents during the seventh decade of life, and patients aged 35 or younger represent only 0.3% of all cases (SEER database). Therefore, the characteristics of PDMM in young patients are poorly understood and attributed to an unclear etiology possibly unrelated to asbestos exposure. This study examined the clinicopathologic and genetic characteristics of PDMM in young patients.
Design: We identified 36 consecutive patients aged 35 or less treated for PDMM between 1990 and 2013. We examined histologic type, predominant growth pattern, mitotic index (# mitoses per $2mm^2$), and nuclear atypia on H&E-stained slides, performed immunohistochemistry for BAP1, and recorded p16 and NF1 status by fluorescence in situ hybridization. Overall survival was compared to a cohort of 1,342 patients aged >35 treated for PDMM during the same time period.
Results: 19 (52%) men and 17 (48%) women with a mean age of 30 years (range 18 to 35) were identified. Pathologic stage was IB in 2 (6%) patients, II in 4 (11%), III in 25 (69%), and IV in 5 (14%). PDMM were epithelioid in 28 (78%), biphasic in 7 (20%), and sarcomatoid in one (3%) case. Predominant growth patterns were solid in 20 (55%) cases, tubulopapillary in 15 (42%) cases, and micropapillary in one (3%) case. The average mitotic index was 3.8 (range 1-13). Nuclear atypia was mild in 17 (47%), moderate in 12 (33%), and severe in 7 (20%) cases. BAP1 protein expression was lost in 8 (22%) cases. p16 was deleted in 4 (18%) and NF1 deleted in 15 (68%) of 22 tested cases. Personal or family history of other malignancies was present in 12 (33%) and 15 (42%) patients, respectively. 8 (22%) patients had a history of radiation for Hodgkin lymphoma. Young patients had a significantly longer overall survival than older patients (5-year overall survival rates 30.9% v 11.5%, p=0.012).
Conclusions: Young patients with PDMM have a higher rate of long term survival and lower rate of p16 deletion compared to older patients. Our data confirm local radiation as a common etiologic factor, equal sex distribution, and relatively indolent course as characteristics distinguishing PDMM in young patients. Stage distribution, histology, and BAP1 loss are similar in young and older patients. Our results indicate that certain clinicopathologic characteristics of young patients with PDMM are distinctive, suggesting unique biological behavior despite some similarities to PDMM in older patients, reflecting the biologic complexities of this disease.

1974 Complete Loss of PTEN Expression By Immunohistochemistry Predicts Deleterious PTEN Gene Alterations in Non-Small Cell Lung Carcinoma

Marina Vivero, Priyanka Shivdasani, Jason Hornick, Lynette Sholl. Brigham & Women's Hospital, Boston, MA.
Background: Phophatase and tensin homolog (PTEN) is a tumor suppressor gene and negative regulator of PI3K/AKT/mTOR pathways. PTEN loss of function is associated with response to inhibitors of these pathways. Deleterious gene-level *PTEN* alterations have been reported in up to 11% of squamous cell carcinomas (SqCC) and 2-3% of adenocarcinomas (ACA) in the lung. While immunohistochemical (IHC) detection of PTEN protein loss has been shown to correlate with gene alterations in endometrial and prostatic adenocarcinomas, it has not been well-characterized in non-small cell lung carcinoma (NSCLC). The aim of this study is to correlate PTEN IHC with gene-level changes in NSCLC.
Design: *PTEN* mutation and copy number were determined by targeted exon hybrid capture library preparation (Agilent) and next generation sequencing (NGS) using the Illumina HiSeq 2500. Mutation calls were generated using MuTect and GATK, copy number calls using VisCap Cancer, and large structural variants using BreakMer. PTEN IHC (Cell Signaling; clone 138G6) was performed on 4 micron formalin-fixed paraffin embedded tissue sections following pressure cooker antigen retrieval. Extent of staining was graded in 10% increments and intensity on a scale of 0-3 (from absent to strong relative to internal control) and multiplied to calculate an H-score. IHC was also graded by two pathologists to assess interobserver reproducibility.
Results: 152 tumors were tested, including 122 (80%) ACA, 22 (14%) SqCC, 7 (5%) unclassified NSCLC, and 1 (1%) atypical carcinoid. Overall, 11 (7%) patients had *PTEN* gene mutation or homozygous deletion, including 8 (6.5%) ACA and 3 (14%) SqCC. PTEN IHC expression was absent in 15 cases, 1-100 in 92, 101-200 in 41 and 201-300 in 4. Of tumors with gene-level *PTEN* alterations, 8 (73%) had absent PTEN expression and 3 (27%) had an H-score of 1-100. 7 (5%) patients without *PTEN* aberrations had absent expression. Interobserver agreement was good (Kappa coefficient 0.657). Absence of PTEN expression by IHC is 73% sensitive and 95% specific for a deleterious genetic event.
Conclusions: Complete loss of PTEN expression is highly specific for a deleterious gene-level alteration in *PTEN*. Alternative mechanisms of silencing such as DNA methylation may account for loss of expression in the absence of genetic alterations. Low level PTEN expression is frequent in NSCLC and does not specifically predict gene-level alterations.

1975 Genomic Drivers of Pleural Malignant Mesothelioma Determined By Comprehensive Genomic Profiling: Opportunities for Targeted Therapies

Olga Voronel, Kai Wang, Jie He, Tanguy Seiwert, Sahar Nozad, Christine Sheehan, Julia Elvin, Siraj Ali, Doron Lipson, Roman Yelensky, Juliann Chmielecki, Vincent Miller, Aliya Husain, Philip Stephens, Jeffrey Ross. Albany Medical College, Albany, NY; Foundation Medicine Inc, Cambridge, MA; University of Chicago, Chicago, IL.
Background: Malignant mesothelioma of the pleura (PMM) is an asbestos-associated malignancy that often presents at an advanced stage at diagnosis, is commonly unresponsive to chemotherapy and, consequently, carries a poor prognosis. We queried whether comprehensive genomic profiling (CGP) would uncover clinically relevant genomic alterations (CRGA) that could lead to targeted therapies for patients with this aggressive form of malignancy.
Design: DNA was extracted from 40 microns of FFPE sections from 127 PMM. CGP was performed on hybridization-captured, adaptor ligation based libraries to a mean coverage depth of 678X for 3,230 exons of 182 cancer-related genes plus 37 introns from 14 genes frequently rearranged in cancer. The results were evaluated for all classes of genomic alterations (GA). CRGA were defined as GA linked to drugs on the market or under evaluation in mechanism driven clinical trials.
Results: There were 89 male and 38 female patients with a mean age of 66.1 years. Samples used for CGP included pleural biopsies, metastasis biopsies and fluid cell blocks. Three (2%) of the MM were low grade and 124 (98%) high. 92 (72%) of PMM were epithelioid, 7 (6%) were sarcomatoid and 28 (22%) were biphasic. There were 41 (32%) stage III and 85 (67%) stage IV tumors at the time of sequencing. Staging data was unavailable for 1 sample. CGP revealed 366 total GA (2.9 GA/sample). 113 (89%) of PMM featured at least 1 CRGA with a total of 229 CRGA identified (1.8 CRGA/tumor). The most frequent CRGA included *BAP1* (51%), *CDKN2A* (43%), *NF2* (28%), *FBXW7* (6%) and *DNMT3A* (6%). Further, 53 (42%) of PMM featured GA in the PI3K/AKT/MTOR pathway genes including *AKT2*, *AKT3*, *FBXW7*, *NF1*, *NF2*, *PIK3CA*, *PIK3R1*, *PIK3R2*, *PTEN*, *RICTOR*, *STK11, TSC2*. Frequent non-CR GA identified included *CDKN2B* (39%), *TP53* (13%), *SETD2* (11%) and *PBRM1* (11%).
Conclusions: PMM features a high frequency of CRGA that can be readily detected in clinical samples including fluid cell blocks. The frequent CRGA in the BAP1 and *NF2* genes confirm previous results for PMM and suggest further evaluation of mechanism driven clinical trials of targeted therapies including histone deacetylase and PIKCA-AKT-MTOR inhibitors in MM appear warranted.

1976 Can Next Generation Sequencing Help Distinguish Multiple Primary Pulmonary Adenocarcinomas From Intrapulmonary Metastases?

Ann Walts, Andy Pao, Alberto Marchevsky, Jean Lopategui. Cedars-Sinai Medical Center, Los Angeles, CA.

Background: Distinguishing independent primary pulmonary adenocarcinomas (PA) from metastases impacts management and prognosis but can be difficult in practice. Previous next generation sequencing (NGS) studies have shown that metastatic tumors generally retain at least some of the same mutations as the primary lesions.

Design: Tumors from 7 patients (5 with synchronous bilateral PA resected within 6 months, one with synchronous PA and tumor in the small intestine, and 1 with metachronous contralateral PA resected 12 years apart) were selected from our pathology database for study. Only the patient with metachronous tumors received chemotherapy prior to NGS. DNA extracted from macrodissected formalin fixed paraffin embedded sections of the 15 tumors was analyzed for 2855 hotspot mutations (HSM) in 50 genes using the IonAmpliSeq™ Cancer Hotspot Panelv2 (Life Technologies Corp., Grand Island NY) per the manufacturer's recommendations. The laboratory's limit of detection (LOD) is 10% at 250X coverage. NGS results were compared per patient.

Results: Synchronous PA (n=11): 10 HSM (3 KRAS, 3 TP53, 2 EGFR, 2 BRAF) were identified in 9 of the 11 tumors from 5 patients with synchronous bilateral PA (1 patient with 3 synchronous PA). The HSM per tumor ranged from 0 to 2. HSM were different in the synchronous tumors from all 5 patients. These findings support the diagnosis of independent synchronous lesions in each of these patients.

Synchronous metastatic tumors (n=2): Both tumors from the patient with a PA and a synchronous intestinal tumor showed identical KRAS and APC-HSM, findings supporting the diagnosis of metastasis.

Metachronous PA (n=2): NGS identified 4 HSM (1 in each gene: KRAS, TP53, KIT, and CDKN2A) in the initial PA and a different TP53-HSM in the subsequent tumor. Although the 2 tumors exhibited morphologic similarities, the NGS findings support independent primaries or loss of 4 original HSM and gain of a new TP53 HSM as a result of therapy related mutation and/or branched evolution.

Conclusions: -NGS is a potentially useful tool for categorization of multiple pulmonary PA as either independent primaries or metastases.

-Bilateral PA with different and distinct mutations should probably be classified as independent primaries while tumors with identical mutations are probably metastatic.

-The findings are difficult to interpret in metachronous tumors especially after treatment.

-NGS studies with additional patients and clinical outcome are needed to determine if this categorization can be used for staging and management.

1977 Desmoglein-3 and P40 Immunoreactivity in Thymoma and Non-Neoplastic Thymus

Ann Walts, Alberto Marchevsky. Cedars-Sinai Medical Center, Los Angeles, CA.

Background: The distinction between thymoma and non-neoplastic thymic tissue (NNTT) can be difficult in selected cases, resulting in diagnostic and staging problems. The potential role of the squamous markers desmoglein-3 (DSM) and p40 in this differential diagnosis has not been investigated.

Design: Selected slides of 5 normal thymus, 5 hyperplastic thymus, and 57 thymomas including WHO type A (n=2), AB (n=16), B1 (n=15), B2 (n=16), and B3 (n=8) from our pathology files were immunostained using desmoglein-3 (BC11) and p40 antibodies (both from Biocare, Concord CA). The immunostained slides of 35 of the thymomas included adjacent NNTT. Cytoplasmic/membranous or nuclear staining in ≥ 10% of the neoplastic and/or NNTT was recorded as DSM-positive or p40-positive, respectively. Staining in <10% of the thymic epithelial cells was recorded as negative. DSM and p40 expression in each thymoma was compared with expression in NNTT, including normal and hyperplastic glands and thymic tissue adjacent to the thymoma.

Results: Thymic epithelial cells in all (100%) thymomas and NNTT were positive for p40 in a diffuse distribution pattern proportional to the density of thymic epithelial cells. The p40 immunostain did not help distinguish or delineate thymoma from NNTT. All (100%) NNTT expressed DSM in an "organotypic" distribution pattern with immunoreactivity observed in subcapsular, medullary, and only focal cortical epithelial cells and Hassall's corpuscles. Sheets of DSM-positive epithelial cells highlighted the presence of thymic hyperplasia. In contrast, only 35 (61.4%) of the thymomas were DSM-positive; the remaining 22 (38.6%) were DSM-negative. 18 of these 22 cases had adjacent NNTT and in each case the NNTT was DSM-positive, serving as an internal positive control for the immunostain.

Conclusions: Normal and hyperplastic thymus, and 61.4% of thymomas express DSM in an "organotypic" distribution pattern. Negative immunoreactivity for DSM in 38.6% of thymomas can be helpful to distinguish these neoplasms from NNTT and to delineate tumor extension. The presence of DSM-positive and -negative thymomas suggests that these tumors may originate from 2 different types of thymic epithelial cells. As DSM is expressed predominantly in medullary and subcapsular thymic epithelial cells, the possibility that DSM-positive thymomas arise from these cells rather than from cortical cells or Hassall's corpuscles warrants investigation.

1978 Anatomic Distritubion of Smoking-Related Interstitial Fibrosis (SRIF) in Lung Lobectomy/Pneumonectomy Specimens

Rebecca Waters, Mahmoud Eltorky, Gurinder Singh, Shawn Nishi. University of Texas Medical Branch, Galveston, TX.

Background: Smoking-related interstitial fibrosis (SRIF) is a common finding in smokers with distinct pathologic features from other chronic fibrosing lung diseases. The reported morphological features include a patchy, subpleural distribution of ropy, eosinophilic collagen within alveolar septae in the upper lobes of the lungs, often in a background of emphysema and respiratory bronchiolitis. Unlike other interstitial lung diseases (ILD), SRIF has a much more favorable prognosis. Therefore, it is important to classify SRIF as a distinct diagnosis. Our objective was to investigate the frequency of SRIF with regards to anatomic distribution in lung-resected specimens and its relation to pulmonary function tests (PFTs) and radiological findings.

Design: Non-neoplastic slides from patients with past lobectomies, pneumonectomies, smoking history, and primary lung cancer (2003-2014) were reviewed (n=90) for presence of SRIF. The following sets of data were recorded: Patient age, gender, smoking history, radiological findings, tumor location, pathological diagnosis, PFT results, history of collagen vascular disease, tumor stage, and follow up care. Carcinoid tumors from previous pneumonectomy specimens in patients without smoking history were reviewed and used as controls (n=5).

Results: SRIF was identified in 39% (n=35) of the cases. Sixty percent (n=21) were located in the upper lobe, 11% (n=4) were in the middle lobe, and 29% (n=10) were in the lower lobe. Seventy-one percent (n=25) were male and 29% (n=10) were female. The average age was 67 years. No cases (n=0) had a recorded history of collagen vascular disease. A review of PFTs revealed 49% (n=17) with obstructive disease, 11% (n=4) with normal spirometries, 3% (n=1) with obstructive and restrictive disease, and no (n=0) cases of restrictive disease. Thirty-seven percent (n=13) of patients had no PFTs. The possibility of amyloid deposition was eliminated by negative staining with Congo–red. The number of pneumocytes lining the restricted alveolar lining of SRIF was significantly lower when compared to adjacent normal alveoli by Thyroid Transcription Factor 1 (TTF1) immunohistochemical staining.

Conclusions: SRIF is a common entity in smokers affecting all lung lobes with minimal clinical presentation and must be recognized and separated from other forms of interstitial lung fibrosis.

1979 Expression of PD1 and Its Ligand PD-L1 in Thymic Epithelial Neoplasms: An Immunohistochemical Study of 100 Cases

Annikka Weissferdt, Neda Kalhor, Junya Fujimoto, Jaime Rodriguez Canales, Barbara Mino, Sayuri Nunomura, Edwin Parra Cuentas, Ignacio Wistuba, Cesar Moran. University of Texas MD Anderson Cancer Center, Houston, TX.

Background: Thymic epithelial neoplasms (TEN) are rare tumors which are incompletely understood and lack standardized treatment approaches. An emerging new strategy in cancer treatment is the blockade of immune checkpoints. Programmed death 1 (PD1) is a key immune checkpoint receptor expressed by activated T cells which mediates immunosuppression by binding to its ligand PD-L1 on the surface of tumor cells. Inhibition of this pathway using monoclonal antibodies against PD1 or PD-L1 is emerging as an effective treatment alternative. Overexpression of these molecules detectable by immunohistochemical methods is thought to be a potential biomarker for treatment response and durable drug effects have been demonstrated in some solid tumors and lymphomas. Here, immunohistochemical overexpression of PD1 and PD-L1 was investigated in 100 cases of TEN in order to evaluate the potential use of such treatment in these tumors.

Design: One hundred cases of TEN [26 thymic carcinomas, 25 spindle cell thymomas (WHO type A), 25 conventional thymomas (WHO B1/B2) and 24 atypical thymomas (WHO B3)] were reviewed and representative whole tissue sections from thymectomy specimens were selected for immunohistochemical studies using antibodies directed against PD1 and PD-L1. The percentage of positive tumor infiltrating T-cells and tumor cells, respectively, was evaluated and scored. Cases with strong membranous reactivity of the antibody on ≥5% of T-cells (PD1) or tumor cells (PD-L1) were considered positive.

Results: Overexpression of PD1 was detected in 10/26 thymic carcinomas (38%), 16/25 spindle cell thymomas (64%), 23/25 conventional thymomas (92%), and 14/24 atypical thymomas (58%). Positive PD-L1 cases included 14/26 thymic carcinomas (54%), 17/25 spindle cell thymomas (68%), 19/25 conventional thymomas (76%), and 19/24 atypical thymomas (79%). In combination, a total of 87 (87%) cases showed overexpression of PD1 and/or PD-L1 (thymic carcinoma: 16/26, 62%; spindle cell thymoma: 23/25, 92%; conventional thymoma: 25/25, 100%; atypical thymoma: 23/24, 96%).

Conclusions: PD1 and its ligand PD-L1 are immunohistochemically overexpressed in 87% of TEN and may be the cause of an immunosuppressive environment in these tumors. Our results suggest that TEN may be another group of tumors that should be considered for PD1/PD-L1-targeted therapies. Clinical trials to investigate the use of these immune-checkpoint inhibitors in patients with TEN may be indicated.

1980 Pulmonary Spindle Cell Carcinomas: A Clinicopathological and Immunohistochemical Study of 40 Cases

Annikka Weissferdt, Neda Kalhor, Hui Liu, Jaime Rodriguez Canales, Junya Fujimoto, Ignacio Wistuba, Cesar Moran. University of Texas MD Anderson Cancer Center, Houston, TX.

Background: Pulmonary spindle cell carcinoma (PSCC) is a rare tumor currently classified as a subtype of sarcomatoid carcinoma, a group of tumors with an aggressive clinical course. Their low incidence coupled with a lack in uniformity of terminology and diagnostic criteria has impaired the development of systematic treatment strategies for these tumors. We report the clinicopathological and immunohistochemical features of 40 PSCC.

Design: Sixty-five cases of resected sarcomatoid carcinomas of the lung were identified from our surgical pathology files. Forty cases fulfilling the criteria of PSCC (spindle cell component ≥90%) were analyzed for clinicopathological parameters. In 30 cases, immunohistochemical studies with antibodies directed against CAM5.2, CK5/6, p40, CK7, TTF-1, napsin A, calretinin and D2-40 were performed.

Results: The patients were 22 males and 18 females aged 42 to 86 years (mean 62.4). Main presenting symptoms included chest pain, shortness of breath and hemoptysis. Thirty-three patients had a smoking history. Histologically, the tumors were composed of malignant fusiform cells growing in interlacing fascicles. Twenty-seven cases were pure PSCC; 13 cases had an additional minor component (<10%) of conventional non-small cell carcinoma. Immunohistochemically, the spindle cells were characterized by

consistent reactivity for CAM5.2 (97%) and variable expression of CK5/6 (17%), p40 (13%), CK7 (80%), TTF-1 (37%), napsin A (10%), calretinin (13%) and D2-40 (7%). Twenty-six patients received chemoradiation therapy. Clinical follow-up showed that 28 patients had died 1 to 28 months after diagnosis (mean survival 10.9) and 8 patients were alive with a follow-up period from 17-165 months (mean 89).
Conclusions: PSCC primarily affect patients in the 7th decade with equal gender distribution and a strong association with smoking status. Although some authors consider pulmonary sarcomatoid carcinomas to be an independent clinicopathological entity, a significant number of our PSCC express immunohistochemical markers associated with the more common lung tumors. This not only supports the notion that these tumors may represent poorly differentiated non-small cell carcinomas but also raises the question if PSCC should be separated from the other tumors of the sarcomatoid carcinoma group. PSCC run an aggressive clinical course with a mean survival of only 10.9 months. Rigid pathological criteria and focused clinical studies are needed to guide future therapies and improve patient outcome.

1981 Computational Discovery of Prognostic Morphologic Features in Squamous Cell Carcinoma of the Lung

Daniel Xia, Ruben Casanova, Alex Soltermann, Andrew Beck. Beth Israel Deaconess Medical Center, Boston, MA; University Hospital of Zurich, Zurich, Switzerland.
Background: Microscopic examination of tissue histomorphology is critical for the appropriate classification of human malignancies into theranostic categories. In the western hemisphere, squamous cell carcinoma of the lung is the second most common histologic subtype of non-small cell lung cancer (NSCLC), accounting for approximately 30% of all NSCLC. In comparison to lung adenocarcinomas (as outlined in Travis et al.), relatively little is known about the histologic features that predict survival in squamous cell carcinomas. The goal of our study is to use a computational approach to identify prognostic histologic features in lung squamous cell carcinomas.
Design: Quantitative computational analysis was performed using the Definiens Tissue Studio software on digital tissue microarray (TMA) images. 1536 morphologic features (describing the nuclear, cytoplasmic, and global features of the cancer stroma and epithelium) were quantified for each of 468 TMA images from 234 patients with squamous cell carcinomas of the lung. Overall survival status, progression free survival status, and days to last follow-up were available for each patient. Significance of microarray (SAM) analysis was performed using R to identify features significantly associated with overall survival, after adjusting for multiple comparisons (cutoff is False Discovery Rate <0.05). For each feature significantly associated with survival, the 10 numerically highest and 10 lowest ranked images were selected for manual review by visual inspection.
Results: 4 morphologic features were significantly associated with overall survival (FDR < 5%). The manual review of images showing extreme values for the 4 features suggests that these features capture the presence or absence of stromal inflammatory cells and/or necrotic debris, which is associated with poor prognosis (see figure 1).
Conclusions: Quantitative computational analysis of digital pathology images may be an efficient "hypothesis generator" for morphologic discovery in human malignancies. Future studies will aim to validate our results on additional cohorts and to study the underlying molecular basis.

Figure 1. For each quantitative feature significantly associated with overall survival, images with the 10 highest and 10 lowest numerical values are examined by visual inspection. For example: the two images below are for the feature "Stroma.Nucleus.Std..Dev..Shape.index"; the image on the left is from a deceased patient with one of the 10 lowest values for the feature; the image on the right is from a living patient with one of the 10 highest values.

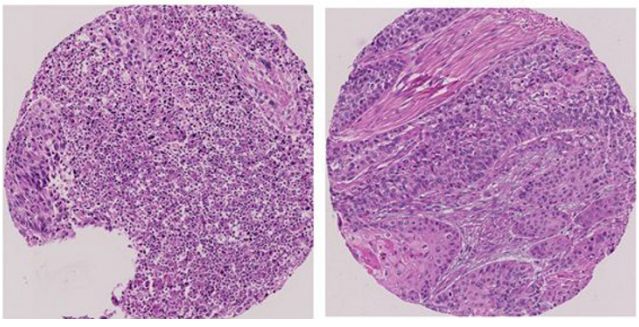

1982 Reliable Detection of ALK Gene Fusions in Lung Cancers By Hybrid Capture-Based Next-Generation Sequencing: High Concordance With ALK FISH and ALK IHC

Roman Yelensky, Amy Donahue, Zach Chalmers, Geoff Otto, Michelle Nahas, Jie He, Frank Juhn, Garrett Frampton, Juliann Chmielecki, Jeffrey Ross, Vincent Miller, Philip Stephens, Doron Lipson, Julianna Eng, Andre Moreira, Lu Wang, Ryma Benayed, Ahmet Zehir, Ronak Shah, Donavan Cheng, Michael Berger, Maureen Zakowski, Marc Ladanyi. Foundation Medicine Inc, Cambridge, MA; Albany Medical College, Albany, NY; Memorial Sloan Kettering Cancer Center, New York, NY.
Background: Hybrid capture-based (HCB) next-generation sequencing (NGS) assays have the potential to detect all classes of genomic alterations (missense and indel mutations, copy number alterations, select structural rearrangements) in multiple cancer genes in a single test. Here, we report the performance characteristics of two independent HCB NGS assays in detecting one of the most clinically significant gene fusions in solid cancers, *ALK* gene fusion in lung adenocarcinomas (LUAD).
Design: We evaluated fusion gene detection by FoundationONE, an HCB NGS test for all exons of 287 cancer genes, with deep sequencing of commonly rearranged introns in 19 (or, in alternative version, 31) genes. We created reference samples for sensitivity analyses by admixing 5 gene fusion-bearing cell lines (2 *ALK*, 1 *RET*, 1 *ROS1*, 1 *TMPRSS2*) into 22 different pools, such that each fusion was represented at simulated cellular fractions of 100%, 50%, 33%, 25%, and 20% at least once. Gene fusions were called if 5 or more chimeric reads were observed in a targeted intron. We tested 45 LUAD (22+/23-) FFPE clinical samples previously studied by *ALK* FISH (Abbott) or ALK IHC (antibody D5F3; Cell Signaling). In parallel, we optimized and validated a similar but independent assay, MSK-IMPACT, that interrogates 341 cancer genes and commonly rearranged introns in 14 cancer fusion genes.
Results: Of 32 tested gene fusion instances in the 22 cell line pools, all were detected by FoundationONE, down to 20% simulated tumor content, with no false positives. Among the clinical FFPE samples, of the 22 *ALK* FISH+ specimens (range of FISH+ nuclei: 17-86%; 9/9 also ALK IHC+), 20 were unequivocally + by FoundationONE, with the remaining 2 specimens showing marginal evidence of the events, while 22/23 FISH-negative specimens were also negative by FoundationONE, with the remaining specimen a possible false negative by FISH. The similarly designed MSK-IMPACT assay underwent preclinical optimization which showed that reliable detection of *ALK* fusions was achieved with approx. 500X coverage of *ALK* intron 19 (lower coverage, such as 100X, resulted in a high false negative rate). In prospective clinical testing using MSK-IMPACT, 4 EML4-ALK cases have been detected, all 4 also positive by ALK IHC (4/4) or *ALK* FISH (2/2).
Conclusions: HCB NGS assays that include baits for commonly rearranged introns can reliably detect clinically actionable gene fusions such as those involving ALK in LUAD.

1983 Insufficient Formalin Fixation Can Negatively Affect Detection of ALK Rearrangement in Lung Cancer By Fluorescence In Situ Hybridization (FISH)

Hong Yin, Shaobo Zhu, Michele Zelonis, Dana Snyder, Nefize Sertac Kip, Zongming Chen. Geisinger Medical Center, Danville, PA.
Background: The presence of EML4-ALK fusion as a consequence of ALK gene rearrangement is a useful biomarker to predict therapeutic responsiveness to anti-ALK agent such as Crizotinib in a subset of non-small cell lung cancer. The gold standard assay for detection of ALK rearrangement is by FISH analysis. Formalin fixation time is a known preanalytic variable that may interfere with FISH testing, we studied its effect on ALK testing in various types of clinical specimens.
Design: A total of 246 specimens including cytology cell block from fine needle aspiration and body cavity fluids, trans-brachial biopsy, frozen section, resection specimens for both primary and metastatic lesions were studied. Based on tissue fixation time in formalin before processing, the specimens were divided into two groups using 6 hours fixation time as an arbitrary cutoff. 169 cases had more than 6 hours formalin fixation while 77 cases had less than 6 hour fixation. FISH analysis was performed on all specimens using Vysis LSI ALK Break Apart Rearrangement probe (Abbott Molecular, Des Plaines, IL) according to the manufacturer recommended protocol. Signal patterns (patchy vs. diffuse) and repeat rates were compared between the two groups. Statistical analysis was performed using Fisher exact test.
Results: As shown in table 1, the repeat rates are significant increase in less than 6 hours fixation group (P<0.001). The signals are also very patchy in this group. Groups of tumor cells most at peripheral have some signals while groups of tumor cells most in the center have no signals or scattered signals. The specimens were repeated if signals were too patchy and not reliable. After modifying the protease digestion time, most cases resolved and results obtained. However, there are 4 cases which could not be scored due to too poor signal quality.

Table reveals variety of specimens in different fixation time.						
Fixation Time	Specimens				Repeat	P Value
	Transbronchial Biopsy	Cytology Core Biopsy	Cytology Cell Block	Resection		
>6 Hours	16	15	24	114	5%	
	25	23	29	0	65%	

Conclusions: Accurate assessment of ALK gene rearrangement by FISH is critical for identifying patients with NSCLC who may benefit from ALK inhibitor therapy. Our data indicate that insufficient formalin fixation time (<6 hrs) is an important preanalytical variable negatively affecting ALK FISH testing. Similar to HER2 testing in breast carcinomas, a guideline on minimal fixation time for ALK testing may be necessary.

1984 3D Pathology Construction Reveals Framework Structure of the Lung and Increase of Pores of Kohn as an Initial Event of Emphysema

Akira Yoshikawa, Tomonori Tanaka, Mikiko Hashisako, Yukio Kashima, Hiroki Karata, Kazuhiro Tabata, Junya Fukuoka. Nagasaki University Graduate School of Biomedical Sciences, Nagasaki, Japan.
Background: Construction of three dimensional (3D) image using series of two dimensional pictures is a common method for radiology. Observing 3D surfaces is efficient for providing easy understanding of the structure and detecting the unnoticeable tiny changes. To unveil pathogenic temporal sequential event of emphysema, we developed a method to observe lung specimen in 3D and compared normal-looking lung from patients with and without emphysema.
Design: 15 cases of lobectomy specimen each with and without emphysema were selected. One block for each case selected was cut for 300mm thick section, then

performed H&E staining (Figure a and b was from identical area). 5 areas of normal-looking lung parenchyma for each slide were randomly selected. The number of alveolar sac surrounded by string-like framework (FW) was counted.
Area ratios of Pores of Kohn to each alveolar sac membrane surrounded by framework (PK) were calculated with images from the spots of interest (Figure c). Image J was used for stack construction and measurement of images (Figure d). Clinical data including pulmonary function test of patients was collected. Comparison of clinical data was performed with t test. Multilevel linear mixed model was used to evaluate differences of FW and PK and associations with clinical data. P values <.05 were considered significant.

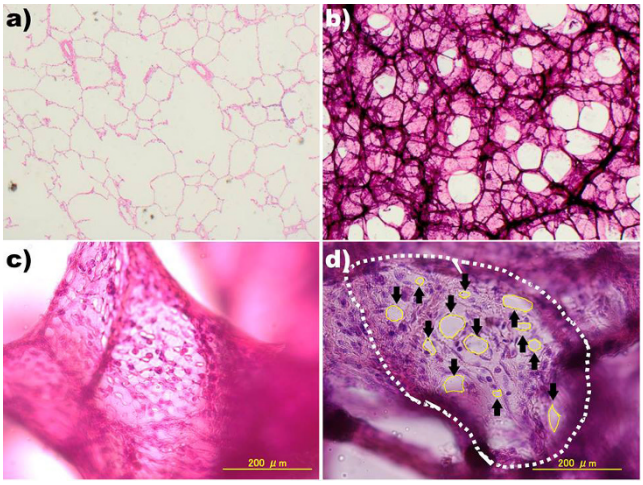

Results: Our approach revealed the structures that membrane-like alveolar sac is surrounded by thicker fibrous framework which spreads web-like structure throughout the lung parenchyma. Compared to lungs without emphysema, PK is higher (p=.04) and FW is lower (p=.02) in lungs with emphysema. Also, FW was influenced by %DLco (p=.04, r=.14), %FRC (p=.02, r=.11), FEV1% (p=.04, r=.28) and %DLco/VA (p<.01, r=.19), and PK was influenced by %DLco/VA (p<.01, r=-.011), CV (p=.04, r=.29) and %RV (p=.05, r=.01). Both did not show difference in %VC.
Conclusions: Histologically normal-looking lung from cases with emphysema had a higher area ratio of pores of Kohn/alveolar wall and a smaller number of alveolar sac. Presence of higher amount of pores of Kohn which associate with abnormal pulmonary function tests suggests that emphysema starts by increasing number of pores of Kohn.

1985 The Clinicopathological Characteristics of Lung Adenocarcinoma With Lgr5 Expression

Akihiko Yoshizawa. Kyoto University Hospital, Kyoto, Japan.
Background: The leucine-rich repeat-containing G-protein-coupled receptor 5 (Lgr5) has been identified as a promising gastrointestinal tract stem cell marker. There are only few published reports on the relationship between Lgr5 expression and clinicopathological features of patients with lung adenocarcinoma. RNAscope is a newly developed in situ RNA hybridization technique. The aim of this study was to detect expression of Lgr5 RNA in 349 consecutive surgically resected lung adenocarcinomas and to evaluate the relationship between expression of Lgr5 RNA and the clinicopathological parameters and prognosis of patients with lung cancer.
Design: In situ hybridization (ISH) for LGR5 was performed using the RNAscope Formalin-fixed, paraffin-embedded assay kit according to the manufacturer's instructions by using tissue microarray (TMA) slides. Based on the percentage of tumor cells that expressed LGR5, LGR5 staining was graded as: grade 0 (0%); grade 1 (1–5%); grade 2 (6–20%); grade 3 (21–100%). The results were grouped as positive (grade 3) or negative (grade 0 to 2). In addition, TTF-1, HNF4alpha, MUC2, Cdx2, MUC5AC, MUC5B, and MUC6 were immunohistochemically studied in the same TMAs. The associations between LGR5 expression and clinicopathological parameters/ other immunomarkers were evaluated. Kaplan-Meier survival analysis was used to estimate the effect of Lgr5 expression on survival.
Results: Lgr5 was detected in 20 tumors (5.7%). Lgr5 expression was significantly associated with vascular invasion (p = 0.015) and expression of Cdx2 (p = 0.017), MUC2 (p = 0.017), and HNF4alpha (p = 0.003), whereas it was not associated with age, sex, smoking history, tumor stage, tumor size, tumor grade, pleural invasion, lymphatic invasion, and expression of TTF-1, MUC5AC, MUC6, and MUC5B. Patients with Lgr5 expression showed significantly worse prognosis, with a 39.6% disease-free survival rate at 5 years compared to patients lacking expression of Lgr5 (5-year disease-free survival rate = 67.8%)(p = 0.008). However, the difference in overall survival rates between the two groups was not statistically significant.
Conclusions: The present study shows that tumors with Lgr5 RNA expression are a small subset of lung adenocarcinoma and are associated with expression of markers for colorectal cancer, HNF4alpha, and poorer prognosis. The results suggest that Lgr5-positive lung adenocarcinomas can be lineage of colorectal-type lung adenocarcinoma with poorer prognosis, although further studies are required to clarify the biological function of Lgr5 in lung adenocarcinoma.

1986 MASH1 Is Highly Specific for Neuroendocrine Carcinomas: An Immunohistochemical Evaluation in Normal and Various Neoplastic Tissues With Emphasis in Lung Cancer

Charlie Yu, David Tacha, Cristin Douglas, Faqian Li. Biocare Medical, Concord, CA; University of Rochester, Rochester, NY.
Background: Mammalian achaete-scute complex homolog-1 (MASH1) is a basic helix-loop-helix transcription factor crucial for neuroendocrine cell differentiation. High grade, poorly differentiated neuroendocrine carcinomas are classified by WHO (World Health Organization) as simply neuroendocrine carcinomas (NECs) and are distinguished from other neuroendocrine tumors (NETs). Neuroendocrine markers such as chromogranin and CD56 cannot distinguish NECs from NETs. Recent studies have shown MASH1 to stain a high percentage of small cell lung carcinomas (SCLCs) and large cell neuroendocrine carcinomas (LCNECs). Limited studies have shown MASH1 to be highly specific in various NECs versus other NETs. Our study will evaluate MASH1 on various normal and neoplastic tissues with emphasis on lung cancer.
Design: Formalin-fixed paraffin-embedded tissue microarrays (TMAs) were used consisting of normal tissues (n = 33), various neoplastic tissues (n = 751) and lung cancers (n = 250). MASH1 [24B72D11.1] titer was optimized at 1:200 and evaluated by IHC in all normal and neoplastic tissues. IHC of MASH1, chromogranin and CD56 was also compared in SCLC.
Results: In normal tissues, MASH1 was expressed (nuclear staining) in C-cells in thyroid and in neuroendocrine cells found in thymus. All other normal tissues were negative, including astrocytes and argentaffin cells found in the gastrointestinal tract. In lung cancers, MASH1 stained 1/91 squamous cells carcinomas and stained 1/87 lung adenocarcinoma, (Table 1). In SCLC, MASH1, chromogranin and CD56 stained 19/23, 18/23 and 21/23, respectively. In various cancers, MASH1 was expressed in thyroid medullary carcinomas (but not in thyroid papillary and follicular carcinomas), in thymic carcinomas, and in a small percentage of astrocytomas/glioblastomas and in pancreatic cancers. MASH1 was negative in all other cancer types.

Table 1: MASH1 Expression in Lung Cancer (n = 250)

Lung Cancers	MASH1	% Positive
Adenocarcinoma	1/87	1%
Squamous cell	1/91	1%
Classic large cell	0/30	0%
SCLC	19/23	83%
LCNEC	2/3	67%
Typical carcinoid	0/4	0%
A-typical carcinoid	5/11	42%

Conclusions: Although not organ specific, MASH1 is highly specific for NECs in lung cancers versus other lung phenotypes and may also be useful in discriminating NECs from other NETs in various types of cancers.

Quality Assurance

1987 Utility of Flow Cytometry in the Pathologic Evaluation of Tonsils and Adenoids

Omonigho Aisagbonhi, Amy Ly. Massachusetts General Hospital, Boston, MA.
Background: Tonsils and adenoids are often excised to treat infections and airway obstruction. In addition to histology, tonsils may be evaluated by flow cytometry, a study with significant financial cost. The added diagnostic value of flow cytometry in these specimens has not been addressed in literature. We examined our flow cytometry utilization pattern in tonsil/adenoid specimens and sought to identify clinical features where its application may be advantageous.
Design: Clinical, radiographic, and pathology findings were recorded for patients who underwent tonsil/adenoid excision or biopsy with concurrent flow cytometry analysis at Massachusetts General Hospital and Massachusetts Eye and Ear Institute from August 2011 to March 2014.
Results: The study included 154 patients (89 females, 65 males) averaging 27.4 years of age (range 2 to 87). 13 had malignancy histories: retinoblastoma (1), pediatric brain tumor NOS (1), Hodgkin lymphoma (1), pre B-ALL (2), lung adenocarcinoma (4), prostate adenocarcinoma (1), colon adenocarcinoma (1), breast carcinoma (1), melanoma (1) and lung small cell carcinoma (1).
Surgical removal/biopsy was prompted by adenotonsillar hypertrophy with tonsillitis and/or obstructive airway symptoms in 141 patients, discrete tonsillar masses in 10 patients, and PET-avid tonsillar lesions discovered during cancer staging scans in 3 patients.
In 148 cases, histology and flow cytometry findings were benign. Histology revealed malignancy in 6 of 154 (4%) patients: diffuse large B-cell lymphoma (2), small B-cell lymphoma (2), concomitant grade 3B follicular lymphoma and histocytic sarcoma (1), and extra-osseous plasmacytoma (1). Pre-operatively, 5 had unilateral tonsillar/neck masses, ranging from 1.5 to 7 cm in size. 1 had no definite mass, but had unilateral tonsillar fullness with cervical lymphadenopathy. All 6 patients were > 40 years old (range 42 – 87, mean 63.7). Only 1 patient had a history of malignancy (prostate adenocarcinoma).
Flow cytometry identified the 2 DLBCL and 2 small B-cell lymphomas; it failed to detect the follicular lymphoma/histiocytic sarcoma and plasmacytoma cases (67% sensitivity).
Conclusions: Flow cytometry is unnecessary for tonsil/adenoid specimens removed from patients without clinical/radiologic findings concerning for malignancy. Unilateral